



Effects of Water Mist System on a Controlled Fire

Report 5498, Lund 2015

Jasper Ho Hui Yang

International Master of Science in Fire Safety Engineering
(IMFSE)

Department of Fire Safety Engineering

Lund University, Sweden

Promoter: *Associate Professor Bjarne Paulsen Husted*

Spring 2015

This thesis is submitted in partial fulfillment of the requirements for the degree of *The International Master of Science in Fire Safety Engineering (IMFSE)*. This thesis has never been submitted for any degree or examination to any other University/programme. The author declares that this thesis is original work except where stated. This declaration constitutes an assertion that full and accurate references and citations have been included for all material, directly included and indirectly contributing to the thesis. The author gives permission to make this master thesis available for consultation and to copy parts of this master thesis for personal use. In the case of any other use, the limitations of the copyright have to be respected, in particular with regard to the obligation to state expressly the source when quoting results from this master thesis. The thesis supervisor must be informed when data or results are used.



Read and approved.
29th April 2015

Title: Effects of Water Mist System on a Controlled Fire

Author: Jasper Ho Hui Yang

Report 5498

ISSN: 1402-3504

ISRN: LUTVDG/TVBB—5498--SE

Number of pages: 114 (total), 67 (body)

Illustrations: The author's, (if not otherwise stated)

Keywords

Water mist, simulation, experiment, extinguishment.

Abstract

Current legislation regarding implementation of water mist system(s) requires full scale testing specific to its intended use which involves extensive funding that discourages potential users. This motivates the desire for accurate water mist simulation. The extent to this possibility is studied for a specific high pressure water mist system, "Danfoss 1910", and its effect on controlled fires of different heat release rates were studied. Concepts to accurately simulate the water mist system were also looked into, where the combined use of an additional air inlet, obstruction (turbulence) meshes and reduced initial particle velocity showed the best performance. A horizontal water mist orientation was adopted to reduce the direct interaction between water mist spray and buoyant plumes. The results attained from a quasi steady state extinguishment model, simulations and experimental data were compared and vast discrepancies were discovered. The quarter scale ISO room corner used was found to be too small which created high levels of circulation within the enclosure; hindering the proper assessment of extinguishing mechanisms such as gas phase cooling and oxygen depletion. One of the conclusions is the need to compile larger scale tests validation data to form a baseline reference.

© Copyright: Fire Safety Engineering, Lund University

Lund 200X.

Department of Fire Safety
Engineering

Lund University

P.O. Box 118

SE-221 00 Lund

Acknowledgements

Associate Professor Bjarne Paulsen Husted ***(Supervisor)***

A. Professor Husted helped immensely with provision of his doctorate thesis for reference, regular meetings to answer my queries, his invaluable inputs, the opportunity to present at the International Water Mist Association (IWMA) Scandinavian seminar, helping to source for the water mist equipment and the use simulation platforms (LUNARC and the Norwegian cluster at Stord/Haugesund University College).

Associate Professor Stefan Svensson ***(Laboratory in-Charge)***

A. Professor Svensson for his technical expertise and assistance on laboratory related issues.

Lasse S.Laustsen ***(Danfoss Country Manager)***

Mr Lausten for generously providing components of the water mist system; namely the appropriate connections, water mist nozzle, the high pressure hose and pipe.

Anders M.Lyhne ***(Danfoss Product Manager)***

Mr Lyhne for generously providing components of the water mist system; namely the high pressure pump system.

Daniel A.Martin ***(Fellow Thesis Student)***

Daniel for the fruitful discussions of our theses, his assistance for the experimental related issues, daily office companionship and *fika* breaks laughs.

Francisco J.Nieto and Caroline E.Lantz ***(Fellow Thesis Students)***

Francisco and Caroline for their willingness to discuss topics outside of their evacuation themed theses, office companionship and *fika* breaks laughs.

List of Abbreviations

(In order of appearance)

<i>IMFSE</i>	- International Master of Science in Fire Safety Engineering
<i>IWMA</i>	- International Water Mist Association
<i>IMO</i>	- International Maritime Organisation
<i>FDS</i>	- Fire Dynamic Simulator
<i>NFPA</i>	- National Fire Protection Association
<i>CFD</i>	- Computational Fluid Dynamics
<i>SHAR</i>	- Spray Heat Absorption Ratio
<i>REMP</i>	- Required Extinguishing Medium Portion
<i>LOC</i>	- Limiting Oxygen Concentration
<i>HRR</i>	- Heat Release Rate
<i>PDA</i>	- Phase Doppler Anemometry
<i>PIV</i>	- Particle Image Velocimetry
<i>ISO</i>	- International Organisation of Standardisation
<i>AMPUA</i>	- Accumulated Mass per Unit Area
<i>HRRPUA</i>	- Heat Release Rate per Unit Area
<i>DNS</i>	- Direct Numerical Simulation

List of Symbols

(In order of appearance)

Q_w = Rate of heat absorption by evaporation

Q_f = Heat release rate of fire

m'_e = Mass application of extinguishing agent

m'_g = Mass rate of fuel consumed

a = Empirical coefficient

σ = width of lognormal distribution

γ = Width of Rosin – Rammler distribution

$D_{v,0.5}$ = Median volumetric diameter

\dot{Q}_{Fire} = Fire's heat release rate

\dot{Q}_{Vent} = Energy lost due to exhaust gas

\dot{Q}_{Water} = Energy absorbed by water particles

$\dot{Q}_{H_2O\ vapour}$ = Energy required to vaporise water particles

CF_{Burner} = Correction factor for burner used

χ , Combustion efficiency ≈ 0.7

\dot{V}_f , Fuel volumetric flow rate = $\frac{\text{Fuel flow rate } [\frac{l}{min}]}{60 * 1000}$

ρ_f , Fuel density at ambient temperature (Propane) = $1.882 [\frac{kg}{m^3}]$

ΔH_c , Heat of combustion (Propane) = $46450 [\frac{kJ}{kg}]$

h_T , Overall heat transfer coefficient $\approx 30 [\frac{W}{m^2 K}]$

A = Internal surface area of enclosure [m^2]

ΔT , Temperature difference between steady state and ambient = $T_g - T_\infty$

T_g = Steady state gas temperature [K]

T_{∞} , Ambient temperature ≈ 293 [K]

\dot{m}_{gas} = Mass flow rate of exhaust gases $[\frac{kg}{s}]$

\dot{m}_{air} = Mass flow rate of ambient air into enclosure $[\frac{kg}{s}]$

C_{p_g} , Specific heat of hot gas ≈ 1 $[\frac{kJ}{kgK}]$

A_v = Vent opening area $[m^2]$

C_d , Discharge coefficient ≈ 0.7

ρ_{∞} , Density of ambient air ≈ 1.2 $[\frac{kg}{m^3}]$

g , Gravity ≈ 9.81 $[\frac{m}{s^2}]$

ρ_g , Density of hot gas = $\frac{353}{T_g}$ $[\frac{kg}{m^3}]$

H_v = Height of vent opening [m]

\dot{m}_{water} , Mass flow rate of water injection from nozzle $[\frac{kg}{s}] = \frac{0.42}{60} [\frac{l}{min}]$

C_{p_w} , Specific heat of water ≈ 4.181 $[\frac{kJ}{kgK}]$

$\gamma_{H_2O \text{ vapour}}$ = Mass fraction of water vapour in exhaust gas

L_v , Latent heat of vaporisation for water = 2260 $[\frac{kJ}{kg}]$

P_v , Partial pressure of water vapour [mm Hg]

P_{∞} , Atmospheric pressure = 760 [mm Hg]

$M_{W_{H_2O}}$, Molecular mass of water = 18 $[\frac{kg}{mol}]$

$M_{W_{air}}$, Molecular mass of air ≈ 28.97 $[\frac{kg}{mol}]$

$\Delta H_{R,O_2}$, Heat of reaction of oxygen $\approx 13,100$ $[\frac{kJ}{kg}]$

$\gamma_{O_2 \infty}$, Mass fraction of oxygen in **inflow** air ≈ 0.21

$\gamma_{O_2 \text{ dry}}$ = Mass fraction of oxygen in **outflow** air

$\gamma_{O_2 \text{ ss}}$ = Steady state oxygen concentration

$C_{O_2}(t)$, Oxygen concentration in enclosure at 't' secs [%]

$C_{O_2(\text{ss})}$, Steady state oxygen concentration [%]

\dot{v} = Volumetric flow rate of air/gas through the enclosure opening [$\frac{m^3}{s}$]

t = time of interest [sec]

v = Volume of enclosure [m^3]

D^* = Characteristic fire diameter

dx = Grid size [m]

I = Turbulence intensity

$Var(u)$ = Variance of velocity along x axis

$Var(v)$ = Variance of velocity along y axis

$Var(w)$ = Variance of velocity along z axis

\bar{u} = Mean velocity along x axis

\bar{v} = Mean velocity along y axis

\bar{w} = Mean velocity along z axis

mtr = Measure of turbulence resolution

k_{subgrid} = Kinetic energy within sub grid scales

k_{LES} = Kinetic energy resolved by "LES" software

KE = Kinetic Engery [J]

M = Mass [kg]

V = Velocity [$\frac{m}{s}$]

P_d = Pressure in duct [Pa]

ρ_d , Density of gas in duct = $\frac{353}{T_d [K]}$

$T_d = \text{Temperature in duct [K]}$

$V_d = \text{Velocity in duct } \left[\frac{m}{s}\right]$

$CF_d, \text{Correction factor for duct} = \frac{0.9}{1.08}$

$A_d = \text{Area of duct [m}^2\text{]}$

$C_{O_2(t)} = \text{Oxygen concentration at 't' seconds [\%]}$

$C_{O_2\infty} = \text{Ambient oxygen concentration [\%]}$

List of Figures

Figure 1. PIV particle velocity measurements [38,39]	9
Figure 2. Oxygen concentration behaviour	17
Figure 3. Theoretical trend between Extinguishment and HRR	18
Figure 4. Porosity test 2 results	20
Figure 5. Velocity profile comparison between FDS 4.07 performed by Husted [38] (left) and FDS 6.1.2 (right)	23
Figure 6. Particle insertion distance.....	23
Figure 7. Velocity Profile (with air inlet)	24
Figure 8. Vertical velocity slices of concepts.....	25
Figure 9. Velocity profile (with air inlet and turbulence mesh).....	26
Figure 10. Velocity profile (with best suited concept).....	27
Figure 11. Turbulence intensity	29
Figure 12. Turbulence resolution slices	31
Figure 13. Cups' grid format.....	32
Figure 14. Factors affecting water distribution	32
Figure 15. Water distribution analysis (example showing 11% of device measurements exceeding threshold value)	33
Figure 16. Study of maximum nozzle distance from opening.....	34
Figure 17. Mean and standard deviation analysis of water distribution (All simulations performed with original water mist concept except for 2 nd last where best suited concept was used).....	35
Figure 18. Cups' Position and Label	36
Figure 19. Experiment 1 setup	37
Figure 20. Experiment 2 setup	38
Figure 21. Experiment 3 setup	39
Figure 22. Experiment 4 and 5 setup	40
Figure 23. (Simulation) Scenario 1, Water Accumulated.....	42
Figure 24. (Simulation) Scenario 2, HRR	43
Figure 25. (Simulation) Scenario 2, Steady State Temperatures	43
Figure 26. (Simulation) Scenario 2, Temperatures	44
Figure 27. (Simulation) Scenario 3, HRR	45
Figure 28. (Simulation) Scenario 3, Temperatures	45
Figure 29. (Simulation) Scenario 4, HRR	46

Figure 30. (Simulation) Scenario 4, Temperatures	46
Figure 31. (Simulation) Scenario 5, HRR	47
Figure 32. (Simulation) Scenario 5, Temperatures	47
Figure 33. (Experiment) Scenario 1, Water accumulation	50
Figure 34. (Experiment) Scenario 2, HRR	51
Figure 35. (Experiment) Scenario 2, Steady State Temperatures	52
Figure 36. (Experiment) Scenario 2, Temperatures	52
Figure 37. (Experiment) Scenario 3, HRR	53
Figure 38. (Experiment) Scenario 3, Temperatures	53
Figure 39. (Experiment) Scenario 4, HRR	54
Figure 40. (Experiment) Scenario 4, Temperatures	54
Figure 41. (Experiment) Scenario, HRR	55
Figure 42. (Experiment) Scenario 5, Temperatures	55
Figure 43. (Simulation) Scenario 1, Measure of turbulence resolution slice at z=0.3m	57
Figure 44. (Simulation) Scenario 5, Oxygen volumetric concentration slice at x=0.3m	59
Figure 45. (Simulation) Scenario 5, Water density vector slice at x=0.3m	59
Figure 46. (Simulation) Scenario 5, V-Velocity slices at x=0.3m (top) and z=0.3m (bottom)	60

List of Tables

Table 1. Time to extinguishment for various heat release rates	17
Table 2. Grid size resolution study	21
Table 3. Initial particle velocity investigation	27
Table 4. Water distribution analysis (Higher percentage indicates better distribution)	33
Table 5. Scenario 1 comparison	56
Table 6. Scenario 2 comparison	56
Table 7. Scenarios 3-5 comparison	56

Table of Contents

Abstract.....	i
Acknowledgements.....	ii
List of Abbreviations	iii
List of Symbols	iv
List of Figures	viii
List of Tables	ix
1. Introduction	1
1.1. Objectives & Research Questions	1
1.2. Limitations.....	2
2. Literature Review.....	3
2.1. Suppression Mechanisms	3
2.2. Findings	6
2.3. Models	7
2.4. Simulation	7
2.5. Previous Work.....	8
3. Methodology.....	10
3.1. Quasi Steady State (Extinguishment) Model [2]	12
3.2. Overview of Steps	18
3.3. Material (PROMATECT H) Porosity Test (Step 1)	19
4. Simulation Setup.....	21
4.1. Grid Size Resolution	21
4.2. Replication of Previous Study’s Water Mist System Data (Step 2)	22
4.3. Concepts to Improve Simulation Accuracy (Step 3).....	24
4.4. Turbulence Intensity	28
4.5. Turbulence Resolution	30
4.6. Best Possible Distribution of Water Particles in Enclosure (Step 4 & 5).....	31
4.7. Scenarios’ Simulation (Steps 6-9).....	34
5. Experimental Setup / Details	36
6. Results.....	41
6.1. Simulations.....	41
6.1.1. Scenario 1: Water.....	41

6.1.2.	Scenario 2: Fire.....	43
6.1.3.	Scenario 3: Combination.....	45
6.1.4.	Scenario 4: Extinguishment 16.7kW	46
6.1.5.	Scenario 5: Extinguishment 25kW	47
6.2.	Experiments	48
6.2.1.	Scenario 1: Water.....	49
6.2.2.	Scenario 2: Fire.....	51
6.2.3.	Scenario 3: Combination.....	53
6.2.4.	Scenario 4: Extinguishment 16.7kW	54
6.2.5.	Scenario 5: Extinguishment 25kW	55
6.3.	Result Comparison	56
7.	Discussion.....	57
8.	Conclusion.....	62
9.	Future Work(s)	64
10.	References	65
Annex	I
A.	Porosity Test Procedure.....	I
A.1.	Porosity Test 1	I
A.2.	Porosity Test 2	IV
B.	Danfoss 1910 Hollow Cone Technical Specifications.....	VII
C.	Water Mist Flow Rate Test.....	IX
D.	Sample FDS Script File (Scenario 5).....	X
E.	Experimental (1-5) Procedure.....	XIII
F.	Experimental Risk Assessment.....	XXIII

1. Introduction

Water mist systems share a similarity with conventional sprinklers where water is used as a suppressing/ extinguishing medium against potential fires in various applications. The main difference is that water mist systems utilise higher pressures to atomise the water. This results in much smaller water droplet sizes which increase the ratio of surface area to volume, leading to increased evaporation efficiency. Water mist particles are more susceptible to air flow profiles and turbulences, and therefore in settings of low volume enclosures, it has an enhanced capability to be well distributed within the room; potentially allowing for more efficient suppression of obstructed fires. Other benefits of water mist systems over the conventional sprinklers given a particular scenario include the reduction of water required and mitigated water damage. In comparison to alternative extinguishing agents, the use of water is safe for both the environment and people within the vicinity. These collective benefits make water mist systems specifically preferable for applications in marine, transportation and museum settings. Water mist systems gained more communal exposure due to events such as the Manchester air crash in 1984, phasing out the use of Halons as extinguishing agent and the International Maritime Organisation (IMO) ruling in its support for water mist systems after the MS Scandinavian Star fire in 1990.

Its potential is however not fully tapped upon due to the lack of confidence in its accurate transition to simulations using computational fluid dynamic software such as fire dynamic simulator, FDS (Large Eddy Simulation) where the water is represented by Lagrangian particles. This is reflected in the National Fire Protection Association's, NFPA, widely accepted document NFPA750, "Standard for water mist fire protection systems" which explicitly states the need for full scale fire testing for the scenario of its intended use, making the current procedure for authenticating the performance of specific water mists systems very expensive and therefore less attractive as an alternative. Other disadvantages of water mist systems are the requirement of increased skill competency in installation/maintenance, potential blockage of its smaller orifices and increased costs (including pump system, high pressure resistant piping and possibly for maintenance).

1.1. Objectives & Research Questions

The main objective of this project is to study the effects of water mist on a controlled fire. To make it more manageable, several sub objectives that translate to research questions were created:

- Achieve accurate simulation of water mist spray
 - *Possible to accurately model a water mist spray in FDS?*
- Achieve as uniform of a water vapour distribution within enclosure for experimental setup
 - *Extent of FDS correctly predicting water distribution within an enclosure?*

- Investigate accuracy of FDS's prediction of fire-related outputs
 - *Extent of FDS accuracy on predicting temperatures in the presence of a fire within an enclosure?*
- Investigate effect of (specific) water mist system on fire
 - *Can FDS predict extinguishment?*
- Identify simulation shortcomings (if any)

These objectives are set to be achieved in the order they are presented in. The project is based solely on a specific water mist nozzle (Danfoss 1910 hollow cone) therefore quantitative results attained are specific to it. However, the approaches/ principles used to achieve more accurate simulation and to better understand effects of extinguishing mechanism are transferable as fundamental knowledge.

1.2. Limitations

The main limitation in simulating water mists is that the water particles involved are of much smaller dimensions (commonly assumed to be spherical). As such, fully resolving all turbulence within a water mist simulation would be close to impossible and with reduced water particle dimensions, the effect of turbulence on their movements is also increased. These factors greatly increase the reliance on the software's turbulence sub-grid model (as default FDS 6 uses the Deardorff model) which is still an approximation and not solved by the Navier Stokes equation. The default timestep constraint is used and its capability to adequately resolve the positions of the Lagrangian particles is not known.

Water mist systems can be differentiated by several factors, each likely to result in different output values given the same experimental setup. This limits the relevance of study(s) performed about a specific water mist system when compared to quantitative knowledge of water mists systems in general.

This thesis schedule being only 14 weeks long, introduces a certain time constraint to the depth and spectrum of analysis. The availability of equipment and ideal materials may also contribute to certain errors, although efforts should be made to mitigate them. There is a vast spectrum of factors that require refinement to successfully simulate water mist in a computational fluid dynamics (CFD) software. However, the objectives would be more focused in this project. The fore mentioned time limitation also influences the availability of ideal materials such as the material of the enclosure.

There is also limited knowledge on devices to accurately measure water concentration, which increases the reliance on simulation data.

2. Literature Review

2.1. Suppression Mechanisms

From relevant literature, there is a general consensus on the factors causing suppression/ extinguishment when water mist systems are involved. The factors are gas phase cooling (direct cooling of flame and plume), oxygen depletion, oxygen displacement and wetting/ cooling of fuel surface [5,8,9]. Certain studies have also included the effects of radiation attenuation [1,3,4]. Back et al. [6] expanded on the theory, further characterising factors into primary and secondary mechanisms to suppression where the primary are listed as;

- Gas phase cooling
- Oxygen depletion and flammable vapour dilution
- Wetting / cooling of fuel surface

And the secondary factors are listed as;

- Radiation attenuation
- Kinetic effects

Some factors are interlinked; an example is when more heat is extracted by gas phase cooling, the compartmental temperature would decrease causing a reduction in radiation feedback to the fuel surface. This then indirectly reduces the temperature of the fuel surface which in turn reduces the rate fuel vapours are produced.

Gas Phase Cooling:

This refers to the direct cooling of the flame and plume (hot gases) resulting from the raising of the water particles' temperature to boiling point and eventually their evaporation. This effect is improved when using water mists systems when compared to conventional sprinkler systems due to the reduced water particle sizes which increase the surface area given a certain volume thus maximising the heat transfer and evaporation rate. The faster the water evaporates, the faster the rate of heat extraction from the flame and smoke plume. The threshold for flame extinction is when the flame temperature is cooled below the limiting adiabatic flame temperature (critical flame temperature) and not to ambient temperatures [6]. Research has also been done to identify the critical mist concentration required for extinguishment, and it was found to be within the range of 150-200 g/m^3 when water particle size of $D_{v_{50}} \approx 100\mu m$ was used [10,11]. The challenge for quantifying gas phase cooling is not being able to accurately predict or measure the amount water particles reaching the fire and hot gases. For ease of calculation and predictability, water particles

produced should have a homogeneous concentration in the compartment to be protected. This is difficult to achieve and is supported by studies proving hardware limitations in water particles achieving gas like characteristics [12,13] as particle concentration significantly decreases after travelling for a short span (Concentration more than halved after one and a half meter) [2]. Some have turned to water mists systems that produce higher initial velocities in hopes to encourage a better mix of water particles in the compartment. Efforts also been made to establish terms to quantify gas cooling, the first being Spray Heat Absorption Ratio (SHAR) which connects the fire size to required amount of water for extinguishment [14] and is given as:

$$SHAR = \frac{Q_w}{Q_f} \quad (1)$$

Where $Q_w = \text{Rate of heat absorption by evaporation}$

$Q_f = \text{Heat release rate of fire}$

A SHAR value as low as 0.3 was found under optimal conditions but a more realistic value of 0.6 was found for scenarios such as machinery spaces where fires were potentially shielded by obstructions [14]. Another term developed was the Required Extinguishing Medium Portion (REMP) which is a relation between extinguishing agent (water mist) application rate and pyrolysis rate of the fuel [10]. REMP also measures the critical value to achieve extinguishment and is given as:

$$REMP = \frac{m'_e}{m'_g} \quad (2)$$

Where $m'_e = \text{Mass application of extinguishing agent}$

$m'_g = \text{Mass rate of fuel consumed}$

As a gauge, REMP values for propane flames was found to be a range of 1.2 to 2.2 when using a water mist system, which converts to a water particle concentration of 100 to 200 g/m^3 [10]. Andersson et al. also noted that the Heat Release Rate (HRR) remains unchanged till extinguishment occurred. The experiments conducted to attain both SHAR [14] and REMP [10] values were performed with maximum turbulent mixing where the water mist was positioned directly above the flame and therefore should only be referred to as minimum values due to inefficiencies in reality. These terms are useful as concepts but are not straight forward to calculate as the efficiency of water particles' evaporation is often unpredictable.

Oxygen depletion and flammable vapour dilution:

Upon evaporation, water's volume expands significantly (over three orders of magnitude [2,6]) and can affect flame extinguishment both directly and indirectly. When occurring near/in the flame, the volumetric expansion of water vapours can dilute fuel vapours present and reduce entrainment into the flame which directly affects the presence of combustible mixture forming. On a compartmental scale where oxygen depletion is more effective due to enclosure effects [8,33], a similar phenomenon occurs resulting in rapid volume occupation by water vapours created that reduces the overall oxygen concentration. This was shown in several research papers [16-22] where fires in regions of low water particle concentrations could still be extinguished. The threshold for extinguishment is when the oxygen concentration (in flame region) falls below the fuel's Limiting Oxygen Concentration (LOC). Back et al. [22,23] performed full scale tests for machinery spaces and concluded that with saturated vapour at elevated temperatures, the oxygen concentration was greatly reduced. He further noted that water vapour saturated in air at temperatures above 80°C is enough to reduce oxygen concentration below majority of fuels' LOC. A typical LOC value for hydrocarbon fuels is 13 to 14% [2,24,25]. Oxygen depletion is the dominant extinguishing mechanism in scenarios where water mist spray is not in direct contact with the flame as effects from gas phase cooling is reduced.

Wetting / Cooling of Fuel Surface:

If the momentum of water particles is high enough to penetrate the flame and impinge onto the fuel, it reduces the fuel surface temperature with governs the pyrolysis rate. With conventional sprinklers, the water droplets are much larger and therefore have higher potential to reach the fuel surface. This factor is particularly effective if the fuel does not produce combustible mixtures at ambient conditions [2,6]. The threshold for extinguishment is when the fuel surface temperature is low enough that it cannot maintain production of a combustible mixture above it. Studies have been performed [27-30] to investigate extinguishment by wetting / cooling of fuel surfaces but the data is restricted to only Class A materials.

Radiation Attenuation:

With the lowering of flame temperature, the radiation feedback to fuel surface is reduced. Water mist application effectively introduces water vapour into the air, this mixture if present above the fuel absorbs radiation that is reflected back to the fuel surface at a dampened value [6]. Water

vapour in the air also mitigates radiant energy transfer between the heat source and other combustibles within the region. This reduction is dependent on radiative wavelength size, water particle size and water vapour concentration [31,32].

Kinetic Effect:

This is a secondary factor attributed to gas phase cooling and oxygen depletion [6]. However, it may also increase a fire's HRR by supplying more oxygen upon the mist's first contact with the fire. For this to happen, the fuel evaporation rate has to be intense enough.

2.2. Findings

Within water mist systems, there is a spectrum of variable system factors and scenario specific factors that affects its overall performance. Some of the factors are listed as [1] full/ hollow cone, droplet size, water flow rate, spray angle, properties of fire source and ventilation conditions. A numerical study [34] investigated their effects and concluded that a water mist of solid cone with smaller droplet size has superior extinguishing properties to one of solid cone with larger droplet size. The common gauge of system performances is the respective extinguishment time given a controlled experiment. Arvidsson [7] however, argued that water spray systems should be evaluated on more than just the time to extinguishment. Citing additional performance criteria related to egress and fire spread, he suggested other measurements to validate system performance; they are fire suppression capability, gas temperature reduction and its ability to mix water vapour in compartment space.

Sung et al. [1] performed experiments using pool fire with a water mist nozzle positioned directly above it and also did the parallel scenario simulations. On the contrary, he discovered that the introduction of water mist increased the fire's HRR measurements which he attributed to air entrainment from the mist providing increased turbulence mixing between oxygen and fuel vapours. Expanding on this theory, Sung et al. [1] introduced the concept of increasing the HRR in the simulation after water mist activation which resulted in his simulations closely representing the experimental results. Further tests showed that HRR increased with water flow rate and decreased as fire size increased. The flaw in this concept is that this increase in HRR would vary with different scenarios; therefore experiments have to be done before simulations which defeat the purpose of simulation predictions. Sung et al. [1] found that if the spray momentum was greater than the plume buoyancy, the main extinguishing mechanism was gas phase cooling as water could penetrate into the flame region. Otherwise, oxygen depletion was the main contributing factor for extinguishment.

2.3. Models

Back et al. [2] established a model to estimate time to extinguishment by oxygen depletion and flammable vapour dilution. Obstructed fires were used in his experiments to minimise the effect of gas phase cooling where mist and fire interactions were ultimately neglected. The objective of the model was to predict steady state compartmental temperature, steady state oxygen concentration and the critical fire size given certain compartment dimensions. His results reflected the same conclusion found by previous researches [3,16-23,26] that as the fire's HRR increases, the extinguishment time reduces. With increased HRR, compartment temperature increases which accelerates water evaporation and amplifies the oxygen depletion effect. In addition, a larger flame also consumes more oxygen. The model was used in researches [22,23,26] where the predicted time to extinguishment showed close resemblance to actual experimental values.

A couple of transient zone models for oxygen depletion have also been developed [25,35]. Where conservation of species is solved instead of conservation of mass and evaporation algorithms for water particles were used. The main advantage of the transient models is they allow scenarios that do not reach steady state conditions to be studied as well.

2.4. Simulation

Advances in accurate simulation play an important role in the water mist industry as its potential is being masked by the current wide spread legislation requiring full scale fire testing. In the past decades, significant progress has been made in the simulation of fire suppression and extinguishment though more research is required for sub-grid scale modelling of gas phase suppression / extinguishment.

Previously, suppression by flame cooling was dependant on an empirical coefficient " a " which is a relationship between fuel vapour production rate and water mass on the fuel's surface. This therefore prevented the use of blind simulation for prediction. Jenft et al. [5] introduced a new model originating from the Arrhenius equation to circumvent the need for prior experimental values and has been since implemented in FDS v6.1.2. (Chapter 12.3).

FDS adopts the extinguishment concept of critical flame temperature by Beyler [36], where extinguishment occurs if the flame temperature falls below it. The extinction model has since been further improved where FDS now computes the enthalpies of the fuel and gas mixture in cell with both local temperature and critical flame temperature [5]. If the enthalpy difference is greater than the mixture's heat of combustion, the combustion within the cell ceases.

Jenft et al. [5] also noted that simulating using a pyrolysis model, rather than the commonly used prescribed HRR, yielded a more accurate prediction of time to extinguishment. Extinguishment could however, still be determined when using the prescribed HRR method. It should be noted that pyrolysis models are more sophisticated and are only available for very well defined fuels.

Several research have been done using simulations [1,3-5] each having different set-ups to study the extinguishment mechanisms. With reference to HRR to time curves, Zhu et al. [3] found that a gradual downward gradient upon water mist activation represents the gas phase cooling effect and a sudden HRR drop (extinguishment) represents the oxygen depletion effect. Andersson [10] however, noted that the HRR does not vary due to gas phase cooling unless the water concentration is sufficient to cause extinguishment. Li et al. [4] showed that existing radiation scattering models in FDS is adequate for particle sizes around $100\mu m$.

2.5. Previous Work

This project extends on previous doctorate thesis work and academic article(s) [38,39] performed by the author's supervisor, Associate Professor Bjarne Paulsen Husted. Husted explored several measurement techniques for water particle size, velocity and distribution. Values for the Danfoss 1910 mist nozzle were of particular interest for this project. An attempt was also made to quantify the volumetric distribution of water in areas of interest.

In measurement of water volumetric distribution (density), three methods were used; they were Phase Doppler Anemometry (PDA), laser tomography and water density apparatus. Unfortunately, limited success was achieved where reliability of most results were questionable and only qualitative results from laser tomography were acceptable.

The distribution of particle size and distribution is specified by a cumulative volume fraction of formulae [37] shown below. It was established that values attained from a scan of the entire spray was most representative where it accurately simulated the distribution 30-60mm radially from the spray's axis; the parameter values are $\sigma = 0.43107$, $\gamma = 3.9609$ and $D_{v,0.5} = 46\mu m$.

$$F(D) = \begin{cases} \frac{1}{\sqrt{2\pi}} \int_0^D \frac{1}{\sigma D'} \exp\left(-\frac{[\ln(D'/D_{v,0.5})]^2}{2\sigma^2}\right) dD' & (D \leq D_{v,0.5}) \\ 1 - \exp\left(-0.693 \left(\frac{D}{D_{v,0.5}}\right)^\gamma\right) & (D > D_{v,0.5}) \end{cases} \quad (3)$$

Where $\sigma = \text{width of lognormal distribution}$

$\gamma = \text{Width of Rosin – Rammler distribution}$

$D_{v,0.5} = \text{Median volumetric diameter}$

For particle velocity, three methods were utilised; they were Particle Image Velocimetry (PIV), PDA and high-speed camera. The most reliable velocity data set due to the difference in data acquisition methods was from the PIV and shall be used as baseline for comparison with simulation results; they are shown below (Figure 1). For the graphs on the right in Figure 1, the solid green lines which represent the mean velocity from PIV measurements were referred to.

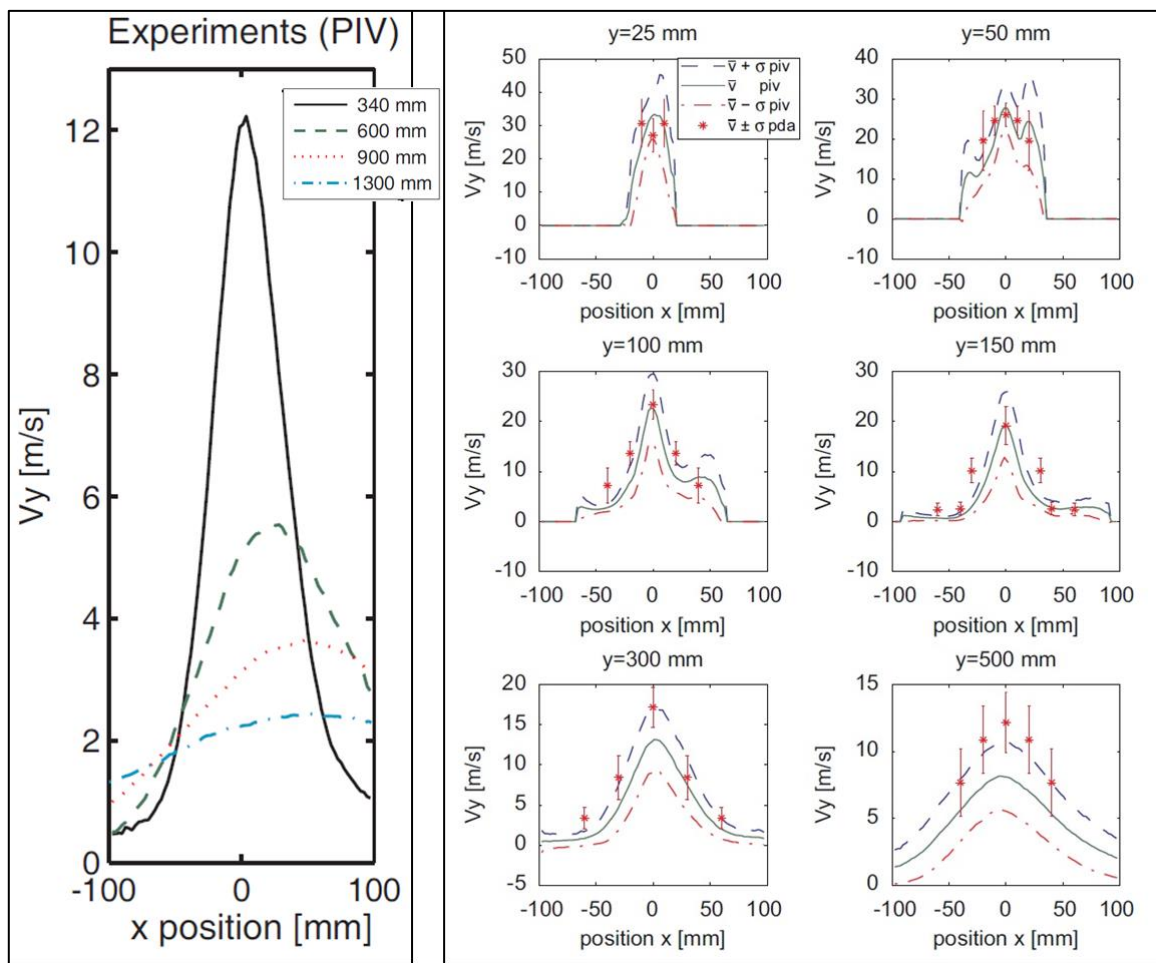


Figure 1. PIV particle velocity measurements [38,39]

Assuming the particles are small enough to share the velocity with the air stream that carries it, their distribution (spray diameter) can be estimated by the x positions from the spray axis in the velocity graphs above.

3. Methodology

The approach taken to answer the research questions raised is to identify appropriate scenarios and examine them by performing simulations and experiments. In the case of studying extinguishment, an extinguishing model was also explored. For all scenarios, the simulations were run prior to performing the experiments to ensure unbiased analysis of simulation data and to avoid unwanted adjustment(s) of input values based on experimental results in retrospect. Results from preliminary simulations influenced the eventual scenarios' setups in hopes to better investigate the particular research question it was designed to answer. These preliminary simulations include the exploration of various concepts to better simulate the water mist system (based on the velocity profiles data from Husted [38,39]) and the study of which configuration would provide the best water distribution within the enclosure; more details can be found in Chapters 4.3, "*Concepts to improve simulation accuracy (Step 3)*" and 4.6, "*Best possible distribution of water particles in enclosure (Step 4)*" respectively.

As extinguishing effects are amplified by enclosure effects, an enclosure shall be used throughout. The scale of the enclosure was determined from the findings in Chapter 4.6, and kept constant throughout the scenarios. A gas burner supplied with propane will be used in scenarios where a fire source is required. Considering the gas burner is supplied with a constant flow rate of gaseous fuel, extinguishing effects from fuel surface wetting/ cooling and radiation attenuation will be ignored. Several scenarios, each built on the previous, were decided upon in reference to the research questions and are elaborated on below.

"Extent of FDS correctly predicting water distribution within an enclosure?"

Scenario 1: (Water)

An enclosure with arbitrary dimensions would suffice to provide the desired enclosure effect. For familiarity sake, the enclosure size will be scaled according to the International Organisation of Standardisation's (ISO) room corner dimensions.

A horizontal water mist nozzle orientation will be adopted to accommodate the orientation of the enclosure's opening along with other factors explained later.

"Extent of FDS accuracy on predicting temperatures in the presence of a fire within an enclosure?"

Scenario 2: (Fire)

In reference to the enclosure used in scenario 1, a fire source of an arbitrary HRR (10kW chosen) is now added and positioned on the middle of the enclosure floor.

“ Can FDS predict extinguishment?”

In majority of researches done on water mist system's effect on fire, the water mist nozzle is positioned directly above the fire. This encompasses the interaction between the water spray's momentum and fire plume's buoyancy causing maximum turbulence mixing at the interface/zone of collision. Though it represents the conventional nozzle orientation, it requires the consideration of the turbulent mixing and identifying the balance between spray momentum and plume buoyancy which affects the efficiency of main extinguishing mechanisms according to Sung et al. [1]. By using a horizontal nozzle orientation in the scenarios, the ambiguity of the respective extinguishing mechanisms' effects can be reduced.

Scenario 3: (Combination)

Here the water mist system and the fire source used in previous scenarios are combined to investigate any possible effects that the water mist might have on the fire.

From past experiments done [38] with the water mist nozzle of interest (Danfoss 1910 hollow cone), the estimated peak water particle velocity interpolated from data measured by PIV at a distance of one meter from the nozzle is 3m/s. In scenario 3, the water mist nozzle is aligned with the gas burner (fire) but with the burner length being 0.17m, the particles would pass it in a fraction of a second. In light of this, it is expected that the effect of direct gas phase cooling of the flame would be minimised. What remains are the suppression effects of indirect gas phase cooling, oxygen depletion, fuel vapour dilution and secondary extinguishing mechanisms.

Scenario 4 & 5: (Extinguishment)

Upon initial simulation results of scenario 3, it was noted that the water mist system entrained a significant amount of ambient air into the enclosure; affecting both the massflow rate into the enclosure and the amount of oxygen available at the flame region. As these scenarios are more tailored to investigating extinguishment, the water mist nozzle was then positioned at the opening rather than a distance away. Apart from that, they share similar set ups to scenario 3 but have different HRR values. The actual values used were determined by using an extinguishing model

developed by Back et.al [2] which will be explained in the next Chapter 3.1, “*Quasi Steady State (Extinguishment) Model [2]*”.

Here, the water mist nozzle and the burner are positioned off-centered. This further reduces the direct effect from gas phase cooling and limits it to mainly particles that rebound off the enclosure’s back wall and into the flames which is negligible. Therefore, the main extinguishing mechanisms to achieve extinguishment (if any) should be indirect gas phase cooling and oxygen depletion.

3.1. Quasi Steady State (Extinguishment) Model [2]

In order to identify HRRs to use for scenarios 4 and 5, the extinguishment model for steady state conditions introduced by Back et al. [2] was used. It predicts the steady state gas temperatures in the enclosure and time to extinguishment (if any) given certain enclosure dimension and heat release rate inputs. Theoretical calculations using the approach of this extinguishment model were performed for the scenarios at hand. The inputs required include details on the enclosure, vent and fuel used. Upon analysis of preliminary simulation results discussed in Chapter 4.6, “*Best possible distribution of water particles in enclosure (Step 4)*”, the quarter scale ISO room corner scale was chosen therefore its dimensions shall be used here. Several assumptions were made while developing this model and they are listed as:

- Complete combustion within enclosure boundaries
- Uniform HRR
- Uniform temperature in enclosure
- Exhaust gases through vent are at temperature in enclosure
- Gases in compartment and exhaust are saturated with water vapour
- An overall heat transfer coefficient can be used for entire enclosure
- Uni-dimensional heat transfer at enclosure boundaries (edges and corners ignored)
- Boundaries assumed to be thermally thick
- Mist particles are heated to temperatures in enclosure
- Mass flow rates of fuel and water negligible

The model is based the energy balance within a fire cell (enclosure) which is expressed by the equation:

$$\dot{Q}_{Fire} = \dot{Q}_{Boundary} + \dot{Q}_{Vent} + \dot{Q}_{Water} + \dot{Q}_{H_2O\ vapour} \quad (4)$$

Where \dot{Q}_{Fire} = Fire's heat release rate (HRR)

\dot{Q}_{Vent} = Energy lost due to exhaust gas

$\dot{Q}_{Water} = \text{Energy absorbed by water particles}$

$\dot{Q}_{H_2O \text{ vapour}} = \text{Energy required to vaporise water particles}$

The calculation of HRR is particular to the equipment used in the actual experiment where an unknown correction factor needs to be applied. The HRR can be adjusted to a desired value during experiments and calculated based on oxygen depletion shown in Equations (20,21) of Chapter 6.2, "Experiments".

$$\dot{Q}_{Fire} = CF_{Burner} * \chi * \dot{V}_f * \rho_f * \Delta H_c \quad (5)$$

Where $CF_{Burner} = \text{Correction factor for burner used}$

$\chi, \text{Combustion efficiency} \approx 0.7$

$$\dot{V}_f, \text{Fuel volumetric flow rate} = \frac{\text{Fuel flow rate } [\frac{l}{min}]}{60*1000}$$

$$\rho_f, \text{Fuel density (Propane)} = 1.882 [\frac{kg}{m^3}]$$

$$\Delta H_c, \text{Heat of combustion (Propane)} = 46450 [\frac{kJ}{kg}]$$

The energy lost to the enclosure boundaries:

$$\dot{Q}_{Boundary} = h_T * A * \Delta T \quad (6)$$

Where $h_T, \text{Overall heat transfer coefficient} \approx 30 [\frac{W}{m^2K}]$

$A = \text{Internal surface area of enclosure } [m^2]$

$\Delta T, \text{Temperature difference between steady state and ambient} = T_g - T_\infty$

$T_g = \text{Steady state gas temperature } [K]$

$T_\infty, \text{Ambient temperature} \approx 293 [K]$

Assuming $\dot{m}_{gas} \approx \dot{m}_{air}$, energy lost through hot exhaust gases is estimated:

$$\dot{Q}_{vent} = \dot{m}_{air} * C_{p_g} * \Delta T \quad (7)$$

Where $\dot{m}_{gas} = \text{Mass flow rate of exhaust gases } [\frac{kg}{s}]$

$$\dot{m}_{air} = \text{Mass flow rate of ambient air into enclosure} \left[\frac{kg}{s} \right]$$

$$C_{pg}, \text{ Specific heat of hot gas} \approx 1 \left[\frac{kJ}{kgK} \right]$$

The mass flow rate of incoming ambient air, \dot{m}_{air} , is calculated below assuming the gases within the enclosure are homogeneously distributed:

$$\dot{m}_{air} = \frac{2}{3} * A_v * C_d * \rho_o \sqrt{\frac{2g * H_v * \left(\frac{\rho_{\infty} - \rho_g}{\rho_{\infty}} \right)}{\left[1 + \left(\frac{\rho_{\infty}}{\rho_g} \right)^{\frac{1}{3}} \right]^3}} \quad (8)$$

Where $A_v = \text{Vent opening area} [m^2]$

C_d , Discharge coefficient ≈ 0.7

ρ_{∞} , Density of ambient air $\approx 1.2 \left[\frac{kg}{m^3} \right]$

g , Gravity $\approx 9.81 \left[\frac{m}{s^2} \right]$

ρ_g , Density of hot gas $= \frac{353}{T_g [K]}$

$H_v = \text{Height of vent opening} [m]$

The energy absorbed by water particles:

$$\dot{Q}_{water} = \dot{m}_{water} * C_{pw} * \Delta T \quad (9)$$

Where \dot{m}_{water} , Mass flow rate of water injection from nozzle $= \frac{0.42 \left[\frac{l}{min} \right]}{60}$

C_{pw} , Specific heat of water $\approx 4.181 \left[\frac{kJ}{kgK} \right]$

Assuming dry air enters the enclosure and exhaust gases are saturated with water vapours, the energy lost due to vaporisation :

$$\dot{Q}_{H_2O \text{ vapour}} = \dot{m}_{air} * \gamma_{H_2O \text{ vapour}} * L_v \quad (10)$$

Where $\gamma_{H_2O \text{ vapour}} = \text{Mass fraction of water vapour in exhaust gas}$

$$L_v, \text{ Latent heat of vaporisation for water} = 2260 \left[\frac{\text{kJ}}{\text{kgK}} \right]$$

The water vapour mass fraction can be estimated using Dalton's law that requires the partial pressure of water vapour [2]. Assuming the water vapour acts as an ideal gas, the partial pressure of water vapour, P_v [mm Hg] :

$$P_v = e^{\left\{18.3 - \left[\frac{3816.44}{T_g - 46.13} \right] \right\}} \quad (11)$$

Where P_v , Partial pressure of water vapour [mm Hg]

From Equation (11), Dalton's law can be solved to attain the mass fraction of water vapour:

$$\gamma_{H_2O \text{ vapour}} = \frac{\left(\frac{P_v}{P_\infty} \right) M_{W_{H_2O}}}{\left(\frac{P_v}{P_\infty} \right) M_{W_{H_2O}} + \left(1 - \frac{P_v}{P_\infty} \right) M_{W_{air}}} \quad (12)$$

Where P_∞ , Atmospheric pressure = 760 [mm Hg]

$M_{W_{H_2O}}$, Molecular mass of water = 18 $\left[\frac{\text{kg}}{\text{mol}} \right]$

$M_{W_{air}}$, Molecular mass of air $\approx 28.97 \left[\frac{\text{kg}}{\text{mol}} \right]$

The mass fraction of water vapour, $\gamma_{H_2O \text{ vapour}}$, from Equation (12) is then subbed back to Equation (10). Next by putting Equations (4-7,9,10) together, the elevated steady state enclosure temperature, T_g , can be found which also allows the mass flow rate of ambient air into the enclosure, \dot{m}_{air} , to be calculated.

The following steps quantify the steady state oxygen concentration which first requires the calculation of the amount of oxygen consumed by the fire in the next equation; which momentarily assumes the absence of water particles:

$$\dot{Q}_{Fire} = \dot{m}_{air} * \Delta H_{R,O_2} (\gamma_{O_2 \infty} - \gamma_{O_2 \text{ dry}}) \quad (13)$$

Where $\Delta H_{R,O_2}$, Heat of reaction of oxygen $\approx 13,100 \left[\frac{\text{kJ}}{\text{kg}} \right]$

$\gamma_{O_2 \infty}$, Mass fraction of oxygen in **inflow** air ≈ 0.21

$$\gamma_{O_2 \text{ dry}} = \text{Mass fraction of oxygen in } \mathbf{outflow} \text{ air}$$

Assuming the exhaust gases are saturated with water vapour, the steady state oxygen concentration can be found by:

$$\gamma_{O_2 \text{ ss}} = \gamma_{O_2 \text{ dry}}(1 - \gamma_{H_2O \text{ vapour}}) \quad (14)$$

Where $\gamma_{O_2 \text{ ss}} = \text{Steady state oxygen concentration}$

By tweaking the HRR input, solving for T_g and substituting it into equation (14) to match a $\gamma_{O_2 \text{ ss}}$ value equal to the LOC of fuel used, the critical fire size can be estimated. The critical fire size for the quarter scale ISO room corner is 18.5kW, where its steady state oxygen concentration barely falls below the LOC of propane of 11.5% illustrated by the horizontal black dashed line shown in Figure 2. Next, the oxygen concentration at a given time can be calculated from:

$$\Delta C_{O_2}(t) = \Delta C_{O_2}(ss)(1 - e^{-\frac{\dot{v}t}{v}}) \quad (15)$$

Where $C_{O_2}(t)$, Oxygen concentration in enclosure at 't' secs [%]

$C_{O_2}(ss)$, Steady state oxygen concentration [%]

$\dot{v} = \text{Volumetric flow rate of air/gas through the enclosure opening } [\frac{m^3}{s}]$

$t = \text{time of interest [sec]}$

$v = \text{Volume of enclosure } [m^3]$

From Equation (15), the time to extinguishment can be predicted by substituting the value $C_{O_2}(t)$ in reference to the fuel's LOC.

Considering the degree of calculations required for this quasi steady state extinguishment model, the equations were formatted into an excel file that required minimal user intervention. With this excel file, the oxygen concentration behaviour can be estimated by solving Equations (14,15) by solving it multiple times with a varying time step (1 second used) of user's choice. Although the model was meant for steady state values, this oxygen concentration behaviour can be used as a gauge.

The results when using the quarter scale ISO room corner are displayed in Table 1 and shown graphically in Figure 2. The flame extinguishment characteristics for HRRs values shown below can now be predicted by analysing the oxygen concentration behaviour graph. With reference to Figure 2, it should be noted that the curves which eventually fall below the LOC threshold do not represent the actual oxygen concentration behaviour; as upon flame extinguishment, the steady state concentration would be expected to level out at the fuel's LOC.

Table 1. Time to extinguishment for various heat release rates

HRR [kW]	Predicted steady state oxygen concentration [%]	Time to extinguishment [sec]
10	15.2	N/a
16.7	12.2	N/a
18.5	11.4	70
21.7	10.1	29
25	8.9	21

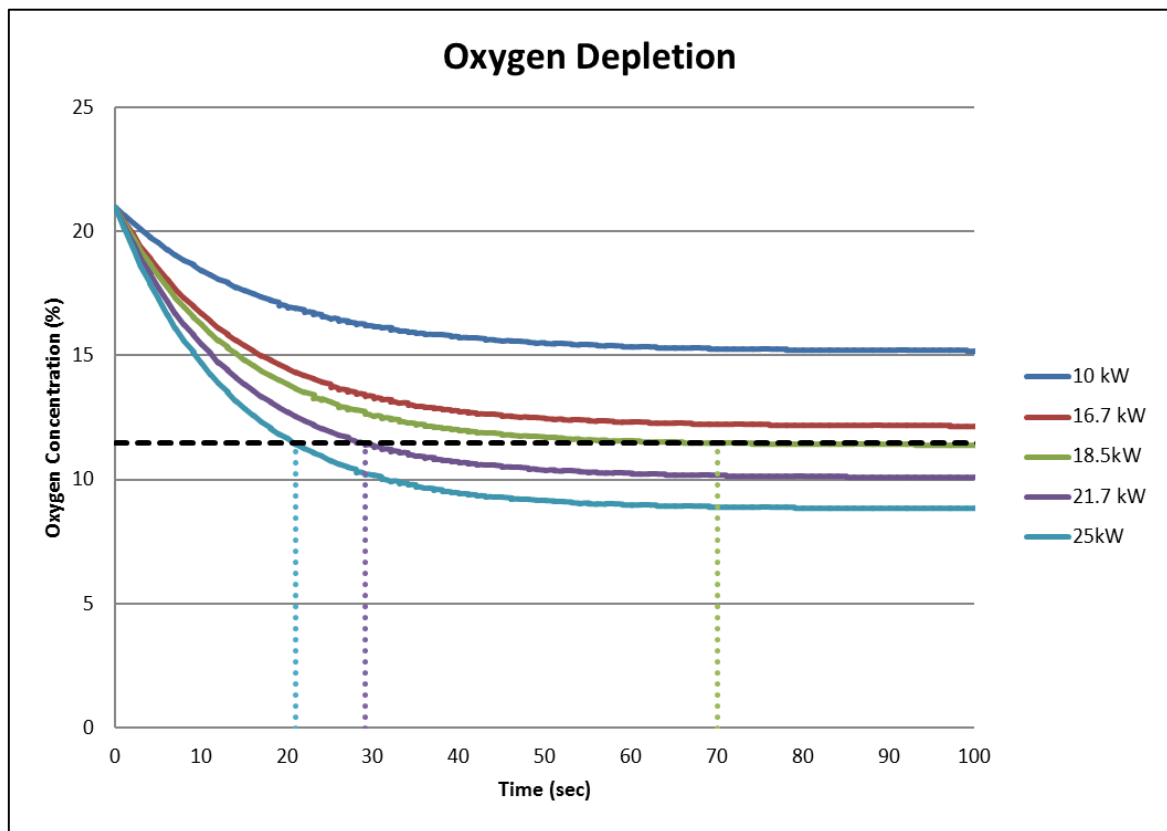


Figure 2. Oxygen concentration behaviour

Referring to Figure 2 above, HRRs with steady state oxygen concentration lower than the LOC for propane (11.5% as indicated by black horizontal dashed line) are expected to be extinguished and vice versa. For scenario 4, the HRR of 16.7kW was chosen as it was close to the critical fire size of 18.5kW; where the flame should theoretically not be extinguished. In view of the laboratory's limitations and safety, a maximum HRR of 25kW was chosen for scenario 5 where the flame is expected to be extinguished in 21 seconds upon activating the water mist system.

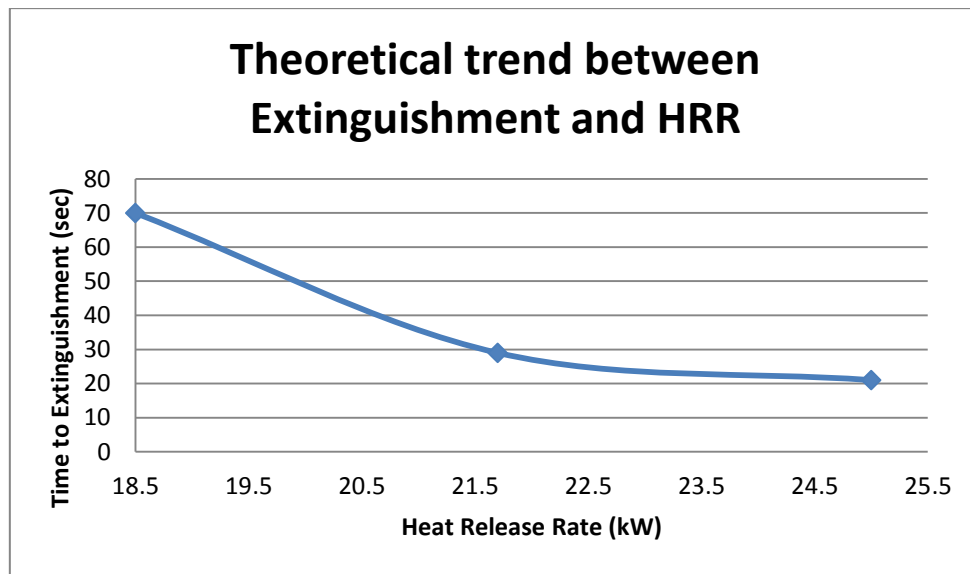


Figure 3. Theoretical trend between Extinguishment and HRR

A trend indicating that the likelihood and rate of extinguishment is increased as the fire's HRR gets larger can be observed (refer to Figure 3). This aligns with theory that given the same mean water particle surface area, a larger fire is capable of evaporating the water particles quicker and also consumes more oxygen; resulting in a lower oxygen concentration levels which causes extinguishment once it falls below the fuel's LOC value.

3.2. Overview of Steps

Several steps were identified and sequenced appropriately for the build-up of confidence in equipment performance and certain input values involved thus far. An overview of the Steps is as follow:

1. Material (PROMATECT-H) porosity test
2. Replication and comparison of previous study's water mist system data *
3. Concepts to improve simulation accuracy *
4. Decide on method to quantify water distribution in enclosure

5. Best possible distribution of water particles in enclosure *
6. **Scenario 1:** Water
 - Evaluate simulation accuracy of water distribution
7. **Scenario 2:** Fire (10 kW)
 - Evaluate HRR accuracy
8. **Scenario 3:** Combination (10 kW)
 - Analyse effect of water mist on flame
9. Evaluate quasi steady state model prediction
 - **Scenario 4:** Extinguishment Test A (16.7 kW)
 - **Scenario 5:** Extinguishment Test B (25 kW)

(*) Indicates solely simulation work

3.3. Material (PROMATECT H) Porosity Test (Step 1)

PROMATECT-H was used to construct the existing enclosure due to its resilience for high temperatures. The material was tested for its performance with relation to water mist interaction. Details on the setup and procedure for an initial test, before attaining the water mist equipment, can be found in **Annex A.1**. It involved several assumptions such as representation of water mist with a film of water and the ideal adhesion between scotch tape and specimens. However from observations and the results, it was deemed as a misrepresentation of the scenarios being considered.

Once in possession of the water mist system, an alternative test was performed to investigate on the porosity behaviour of the enclosure's material. The experiment procedure document can be found in **Annex A.2**. The specimen size of 12.5cmx12.5cm was meant to be large enough to represent the area exposed to majority of the water mist's spray cone. This porosity test was performed at two "nozzle to specimen" distances of 0.9m and 1.5m representing distances from nozzle to the internal back wall of enclosure in scenarios.

The known inaccuracies are that the sides (thickness) of the specimens were not waterproofed due to complications arising from using them in the initial porosity test. By test observations, the bottom faces of the specimens were also exposed to water due to turbulence and reflection off the ground.

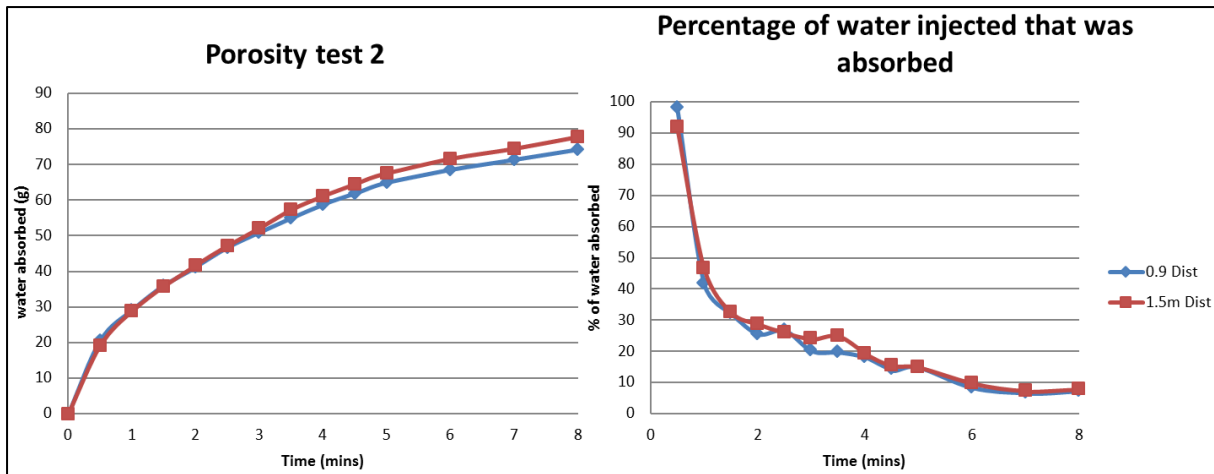


Figure 4. Porosity test 2 results

From the Figure 4 above, both cases exhibited very similar trends. A rapid absorption of water can be seen initially, this rate of water absorption evens out after eventually where the material absorbs approximately 7 to 8% of water injected from the water mist system. These results show that PROMATECT is not the ideal material for water mist interaction. However, the actual physical enclosure had been used for fire experiments previously and thus has accumulated a relatively thick internal coating of soot. This soot coating, enclosure induced turbulence, along with the decision to precondition the enclosure by exposing it to the water mist ten minutes before conducting any experiment, the water absorbed by the enclosure during actual experimental runs would be significantly mitigated.

4. Simulation Setup

4.1. Grid Size Resolution

As grid size increases, the error due to averaging increases, the resolution of data available given a certain volume in space reduces and the reliance on turbulence sub grid scale models increases. However, the user would enjoy a shorter computational time with a larger grid size. A method to quantify the suitability of a certain grid size [37] when buoyant plumes are involved exists. Although not all the simulations done for this project involve fire or plume, this method shall be used as a gauge.

$$D^* = \left(\frac{\dot{Q}_{Fire}}{\rho_{\infty} * C_{p_{\infty}} * T_{\infty} \sqrt{g}} \right)^{\frac{2}{5}} \quad (16)$$

Where $D^* = \text{Characteristic fire diameter}$

Equation (17) then links the characteristic fire diameter to the grid size used in a simulation.

$$\frac{D^*}{dx} \quad (17)$$

Where $dx = \text{Grid size [m]}$

The U.S. Nuclear Regulatory Commission used a range of $4 \leq \frac{D^*}{dx} \leq 16$ for their validation studies [37] and for Danish best practice, $10 \leq \frac{D^*}{dx}$ is used. In the initial simulations to study the water mist system, a grid size of 1cm was used. For the simulations of scenarios 1 to 5, two meshes were used with grid sizes of 1 and 2cm. Table 2 below provides an overview of the suitability of grid sizes used. The minimum $\frac{D^*}{dx}$ value of 4 is met for all HRRs of interest, though the Danish best practice recommendation is not met throughout.

Table 2. Grid size resolution study

\dot{Q}_{Fire} [kW]	D^*	dx [m] when $D^*/dx = 4$	dx [m] when $D^*/dx = 10$	dx [m] when $D^*/dx = 16$	D^*/dx when dx=0.02m	D^*/dx when dx=0.01m
10	0.152	0.038	0.015	0.010	7.6	15.2
16.7	0.187	0.047	0.019	0.012	9.4	18.7
25	0.220	0.055	0.022	0.014	11.0	22.0

4.2. Replication of Previous Study's Water Mist System Data (Step 2)

In reference with Chapter 2.5, "Previous Work", where a vertical water mist nozzle orientation was used, initial open vented simulations as such were conducted. This allowed an equal comparison to results attained in the past. The vertical velocities were measured at respective vertical distances from the nozzle head (25, 50, 100, 150, 300, 340, 500, 600, 900 and 1300mm) to match Husted's [38,39] work shown in Figure 1. The simulation inputs for the water mist nozzle used, Danfoss 1910 hollow cone, are as follow:

- Median volumetric diameter, $D_{v,0.5} = 46 \mu m$
- Rosin-Rammler distribution, $\gamma = 3.96$
- K-Factor= $0.0418 \frac{l}{min\sqrt{bar}}$
- Operating pressure= $100 bar$
- Initial particle velocity = $60 \frac{m}{s}$
- Offset = $0.1 m$
- Spray angle = 24°

According to Danfoss product specifications (**Annex B**), the water flow rate of the water mist nozzle at an operating pressure of 100 bar should be $0.42 \frac{l}{min}$. A simple bucket test was performed (details in **Annex C**) and the actual water flow rate was calculated to be $0.418 \frac{l}{min}$ which closely replicates the expected value. The bucket test value was used as input for the simulations which can be calculated from the K-factor and operating pressure shown above.

Using FDS 4.07, Husted [38] previously found that the spray of water particles lost their momentum too drastically to the surrounding air. He introduced the concept of adding an air inlet behind the water mist nozzle to supplement this lost momentum. This approach was adopted and worked upon in Step 3. Due to the water mist system's ability to achieve steady state quickly in 180ms [38], the initial simulations were of only five seconds. The different concepts were then simulated with very fine grids of 1cm and the velocity profiles at the respective distance from the nozzles were compared to experimental values shown in Figure 1 and used as a gauge of simulation accuracy.

Firstly, the water mist nozzle was simulated as is to serve as a baseline of simulation data for the current version of FDS 6.1.2. The result is displayed alongside past simulation result using FDS 4.07 [38] and the same grid size (1cm) in Figure 5 below. From this figure, it is clear that significant improvements have been achieved where the lost in momentum is now, to a large extent, captured in the latest version of FDS. In comparison with Figure 1, the simulation results at 300mm and onward are slightly higher than but within the same magnitude of the experimental values.

However, the velocity profiles at distances of 25, 50 and 100mm poorly represent the expected values where the initial particle velocity measured by Husted [38] and inputted in the simulation was 60m/s. Also, the velocity profile at 150mm indicates a lower velocity than that at 300mm, which in theory should not be the case. The inaccuracy of velocity readings at 25, 50, 100 and 150mm can be explained by the insertion of particles only at a distance from the nozzle as shown in Figure 6. Ideally, the particles should be inserted as near to the nozzle as possible, on the other hand, a distance is also required to avoid complex calculations of particles near the nozzle due to phenomenon such as collision and coalescence [38]. FDS uses a distance of approximately 150mm.

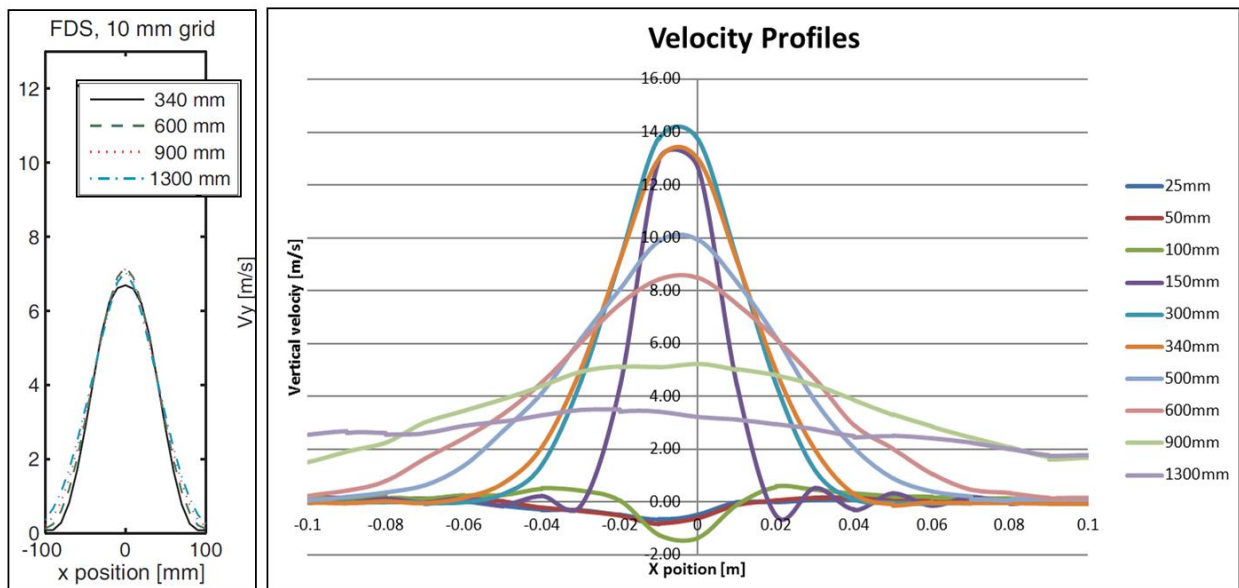


Figure 5. Velocity profile comparison between FDS 4.07 performed by Husted [38] (left) and FDS 6.1.2 (right)

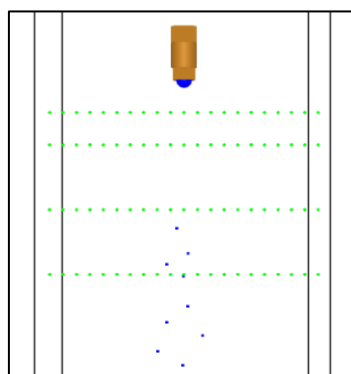


Figure 6. Particle insertion distance

The number of particles used to simulate the water mist spray was 15000, which showed to be adequate in reference to Kolstad [40], rather than the default of 5000 set in FDS.

4.3. Concepts to Improve Simulation Accuracy (Step 3)

“Possible to accurately model a water mist spray in FDS?”

Setup with air inlet:

Next, the concept of introducing an air inlet behind the water mist nozzle was explored. Although the velocity profiles from the original simulation setup already show higher velocities at 300mm and beyond, the concept was carried out as previously done to understand its effect on the results. The conditions of the air inlet used in Husted’s study [38] of $0.054 \frac{kg}{s}$ from a 80x80mm obstruction and positioned 100mm behind the nozzle were used as a guide. The same obstruction dimension and position were used and the flow rate of inlet air was represented by a volume fraction of $0.045 \frac{m^3}{s}$ which was calculated using an ambient air density of $1.2 \frac{kg}{m^3}$. The initial velocity of the air from the air inlet can be calculated, by dividing the volume fraction with the surface area, as $7 \frac{m}{s}$.

Referencing Figure 7 below, velocities at every distance were increased due to the added momentum from the air inlet. The effect of the air inlet’s dimension can also be seen where nearing and beyond X positions of 0.08m magnitude, the added velocity quickly dissipates. When comparing to Figure 1 (experimental results), the velocity profiles’ distribution at distances 500mm to 900mm of the current simulation can be improved, especially at the further X positions.

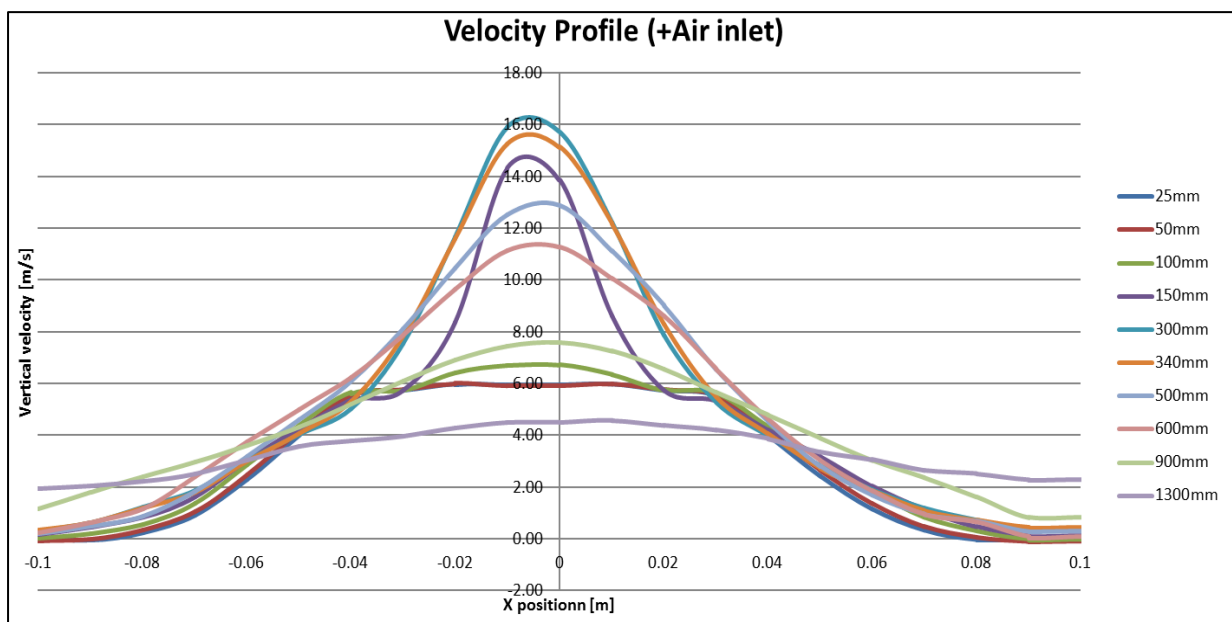


Figure 7. Velocity Profile (with air inlet)

Setup with air inlet and turbulence obstruction meshes:

Two additional obstruction meshes constructed with 1cm cubes were introduced in between the air inlet and water mist nozzle to encourage turbulence that would in turn improve the velocity distribution along the x axis.

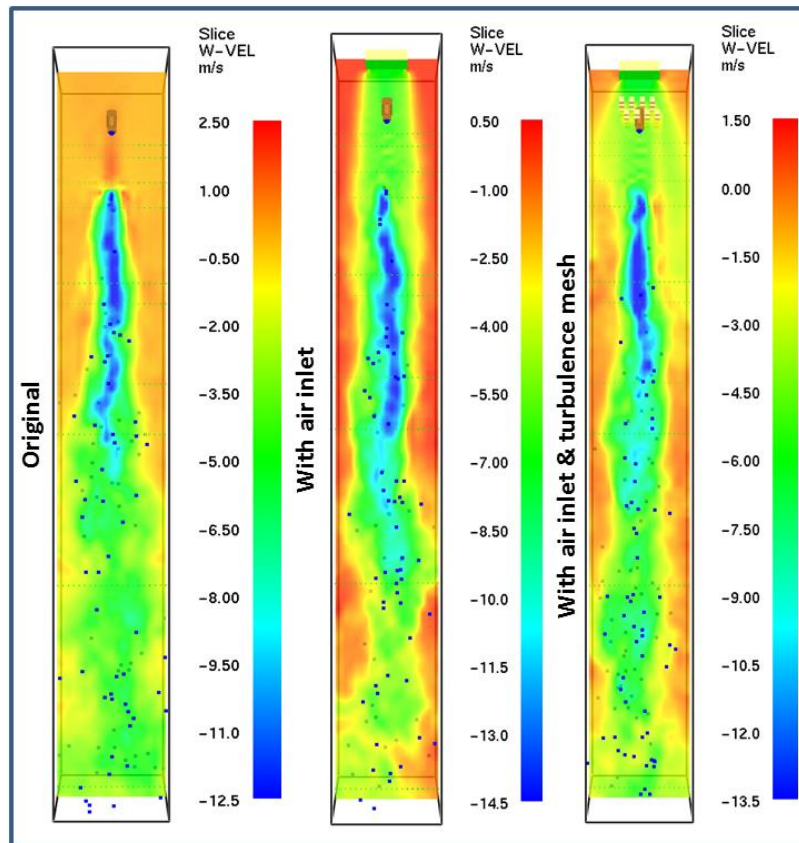


Figure 8. Vertical velocity slices of concepts

Figure 8 show Smokeview screenshots of the vertical velocity slices for the three concepts. In the 2nd case, the air from the air inlet is seen to engulf the water mist spray which would result in a narrower water particle velocity profile. In the 3rd case, turbulence indeed is generated in between the air inlet and the nozzle for the case with the addition of the obstruction meshes.

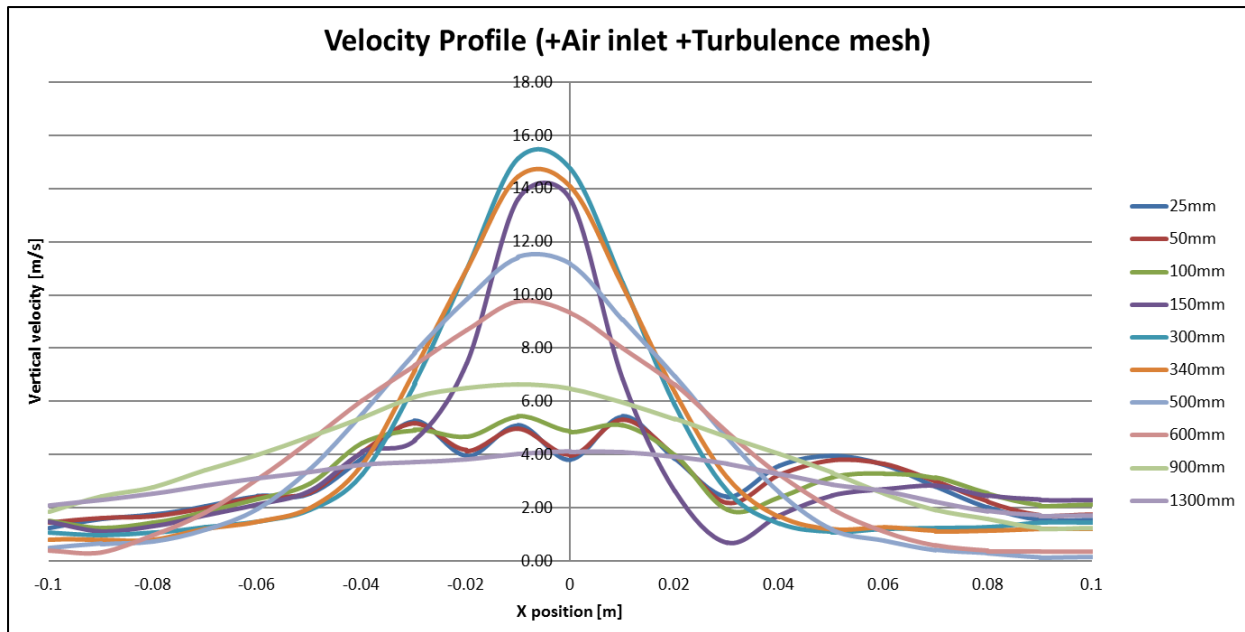


Figure 9. Velocity profile (with air inlet and turbulence mesh)

Comparing the velocity profiles of the 3rd case (Figure 9) and the 2nd case (Figure 7), the peak velocities were reduced indicating the momentum added by the air inlet to the water mist spray is now better distributed along the X axis.

Setup with air inlet, turbulence obstruction meshes and reduced initial particle velocity:

Simulation results from the original concept already showed that velocities were too high at distances of 300mm and beyond. This discrepancy was only made worse with the introduction of the air inlet. Although it was improved by adding the obstruction meshes, the velocity magnitudes were still too large. There were two options to reduce the velocity magnitudes, namely reduce either the air inlet's mass flow rate or the particle's initial velocity. For the former, the combined effect of the air inlet and obstruction meshes would be reduced as the contribution of the obstruction meshes is reliant on the air inlet's mass flow rate. Therefore, the particle's initial velocity was chosen to be reduced instead. Varying this factor does not affect the water's mass flow rate or the mean volumetric diameter, preserving the remaining aspects of the water mist system. Several fraction variations of the initial particle velocity were investigated, and where the peak velocities at the distances from the nozzle were used to analyse them (refer to Table 3 below). The values for distances of 100mm and below are neglected due to the particle insertion distance in simulation. The mid-range distances, 300-500mm, were of priority weightage when comparing to the values from the experiment.

Table 3. Initial particle velocity investigation

Distance from nozzle (mm)	Exp V_{peak}	Simulation							
		100%		70%		65%		60%	
		V_{peak}	Diff	V_{peak}	Diff	V_{peak}	Diff	V_{peak}	Diff
25	32.00	5.44	-26.56	5.56	-26.44	5.48	-26.52	5.53	-26.47
50	26.00	5.34	-20.66	5.49	-20.51	5.38	-20.62	5.44	-20.56
100	21.00	5.45	-15.55	6.11	-14.89	6.07	-14.93	6.09	-14.91
150	18.00	13.63	-4.37	12.57	-5.43	11.48	-6.52	11.17	-6.83
300	12.50	15.13	2.63	13.01	0.51	12.32	-0.18	11.78	-0.72
340	12.00	14.45	2.45	12.55	0.55	11.74	-0.26	11.23	-0.77
500	8.00	11.42	3.42	9.90	1.90	9.56	1.56	9.11	1.11
600	5.40	9.76	4.36	8.38	2.98	8.31	2.91	8.00	2.60
900	3.60	6.65	3.05	5.52	1.92	5.78	2.18	5.36	1.76
1300	2.20	4.14	1.94	3.59	1.39	3.58	1.38	3.39	1.19

The best suited concept to represent the Danfoss 1910 hollow cone in a simulation is therefore with an air inlet ($0.045 \frac{m^3}{s}$, area of $80 \times 80 \text{ mm}^2$, 100mm behind water mist nozzle), turbulence obstruction meshes and 65% ($39 \frac{m}{s}$) of the original initial particle velocity.

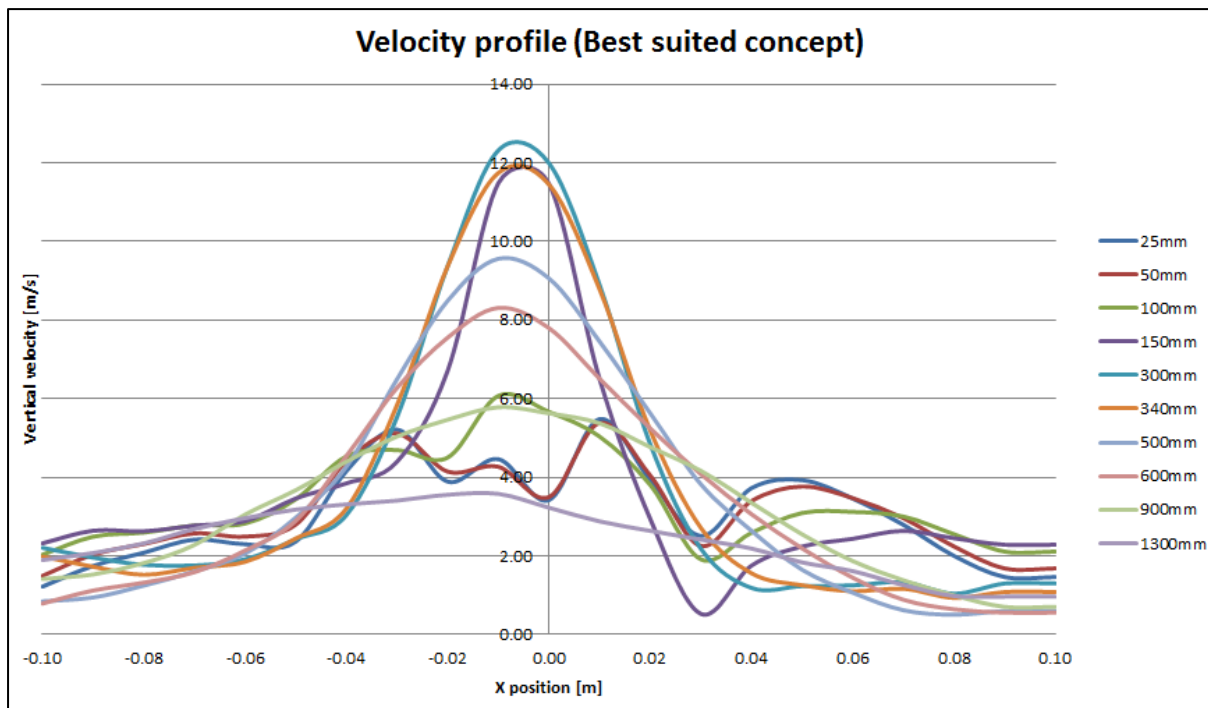


Figure 10. Velocity profile (with best suited concept)

From the resultant velocity profiles achieved, the characteristic of the water mist system remains unchanged. The velocity profile using the chosen concept closely represents the experimental values in Figure 1, especially in the mid distance range. It should be noted that the far field velocity profiles

are of slightly higher magnitudes. This chosen concept shall be utilised for the simulation of the scenarios.

4.4. Turbulence Intensity

Turbulence intensity can also be referred to as the turbulence level, where a higher value indicates more turbulence in that region. The turbulence intensity can be attained from Equation (18) shown below, they were calculated for simulations using the original and respective concepts.

$$I = \frac{\sqrt{\frac{1}{3} * [Var(u) + Var(v) + Var(w)]}}{\sqrt{\bar{u}^2 + \bar{v}^2 + \bar{w}^2}} \quad (18)$$

Where $I =$ Turbulence intensity

$Var(u) =$ Variance of velocity along x axis

$Var(v) =$ Variance of velocity along y axis

$Var(w) =$ Variance of velocity along z axis

$\bar{u} =$ Mean velocity along x axis

$\bar{v} =$ Mean velocity along y axis

$\bar{w} =$ Mean velocity along z axis

The variance and mean velocities were taken from a one second sample size (last second, between the 4th and 5th second). Turbulence intensity is calculated with velocity values from a single point, and therefore velocity measurements were made along the water mist's axis at the respective distances. Figure 11 below displays the results for the different concepts at respective distances from the water mist nozzle.

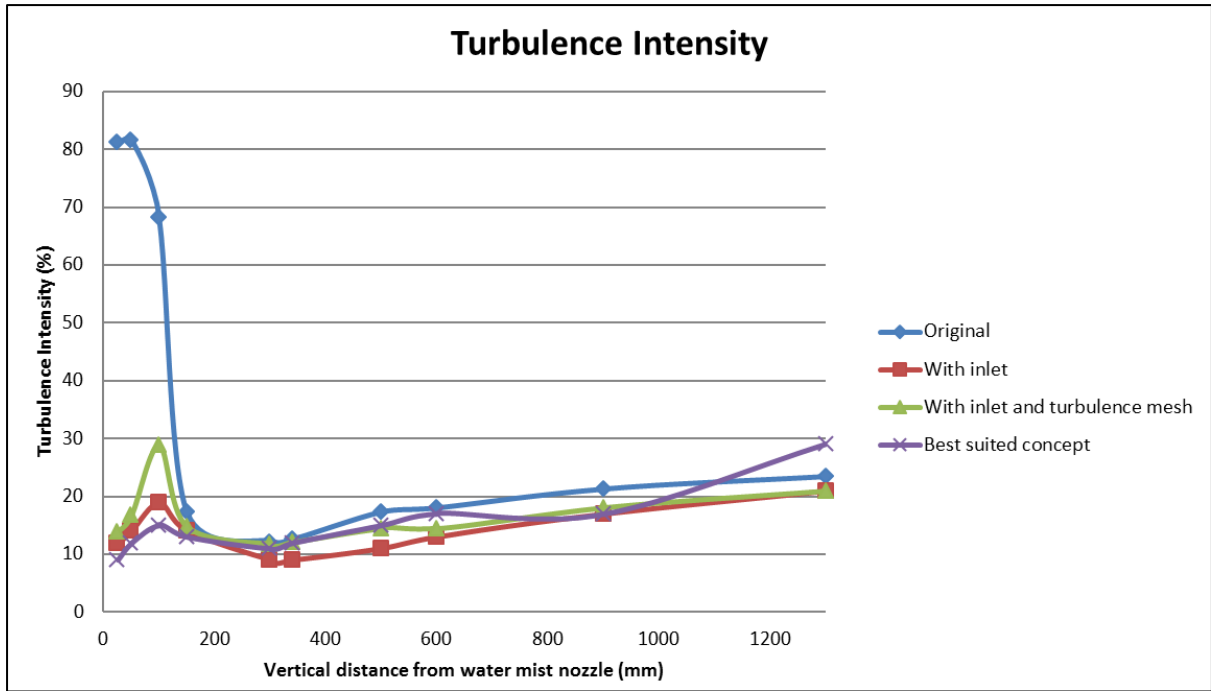


Figure 11. Turbulence intensity

The high turbulence intensity for the original simulation near the nozzle is due to the particle insertion distance, and does not affect the distribution of the water mist spray. A trend of increasing turbulence intensity from 300mm onwards is observed, aligning with theory of water particles and airflow losing their momentum with distance travelled resulting in more chaotic down-stream behaviour. Previously mentioned, the introduction of turbulence meshes between the air inlet and the water mist nozzle was meant to encourage turbulence down-stream the spray. This however, is not reflected in the results above. A likely explanation could be the formation of structured air flows created by the air inlet and turbulence mesh which improves the dispersion of the water particles but is not registered as actual turbulence. The wavy averaged velocity profiles in the middle for distances 25, 50 and 100mm in Figure 10 attest to the presence of such structured air flows.

A qualitative measure of turbulence can be made from the turbulence intensity values [46] where:

- High-turbulence case ($5\% \leq I \leq 20\%$)
- Medium-turbulence case ($1\% \leq I < 5\%$)
- Low-turbulence case ($I < 1\%$)

A gauge for a typical high turbulence case is for flows inside complex geometries (heat exchangers) or in rotating machinery. Referring to Figure 11, all points studied are within the high turbulence range (several points even exceeding 20%).

4.5. Turbulence Resolution

Ideally, all turbulence should be captured in any simulation to fully incorporate the flows' behaviour and their effects on the specific scenario of interest. Doing so however, requires the grid size used to be as small as the smallest turbulence swirl, also known as the Kolmogorov scale, which vastly increases the computational time required and for most cases is not even possible given current computational limitations. For a CFD software to be truly considered a LES, it should be capable of resolving 80% of the turbulence involved. Turbulence resolution measures the amount of turbulent energy that is unresolved in a simulation (should be below 20%) and can be calculated by:

$$mtr = \frac{k_{subgrid}}{k_{LES} + k_{subgrid}} \quad (19)$$

Where $mtr = \text{Measure of turbulence resolution}$

$k_{subgrid} = \text{Kinetic energy within sub grid scales}$

$k_{LES} = \text{Kinetic energy resolved by "LES" software}$

The calculations are in-built in FDS and can be displayed as slices, the results for slices in the X plane along the axis of the water mist system for each of the concepts are shown below in Figure 12. The bounds were set to match among the scenarios and a range of 1% - 20% is displayed, where regions in red indicate area of turbulence resolution exceeds 20% which is undesirable. Noting that a fine grid size of 1cm is already being used, it is clear that the capability of FDS to capture turbulence fully when simulating water mists can be improved. Fortunately, majority of the region within the mist's spray have acceptable turbulence resolution values.

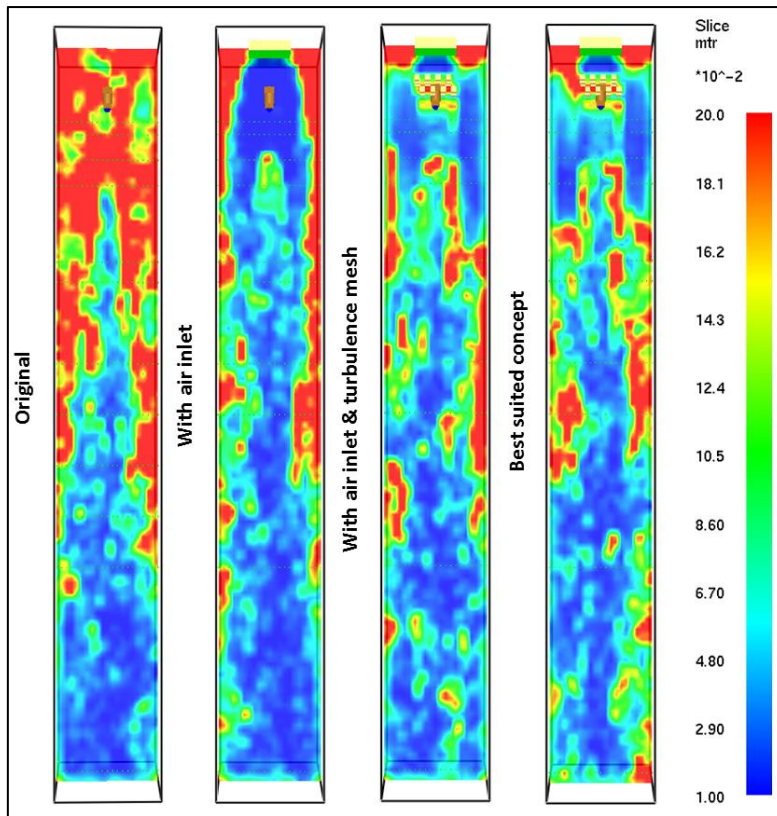


Figure 12. Turbulence resolution slices

4.6. Best Possible Distribution of Water Particles in Enclosure (Step 4 & 5)

To evaluate Step 5, a method to measure the water distribution within the enclosure that could be translated physically to incorporate in experiment 1 was required. A simple method of using cups positioned in a grid format (Figure 13) was decided upon. Although this method may seem crude, it enables an effective comparison between simulation and experiment. In the simulation, these cups were represented by multiple devices measuring the Accumulated Mass Per Unit Area (AMPUA). This measurement characteristic closely mimics the physical one as water particles would only be accounted for once when they reach the device. A limitation of AMPUA measurement devices are they must be placed on an obstruction's surface, in this case, the enclosure's ground. Whereas in the experiment, collection of water would be at the cups' height. Other inconsistencies are the area of water collection and the inability of the simulation to accurately demarcate areas with dimensions consisting of odd numbers (as grid size used is 2cm and cup diameter is 7cm).

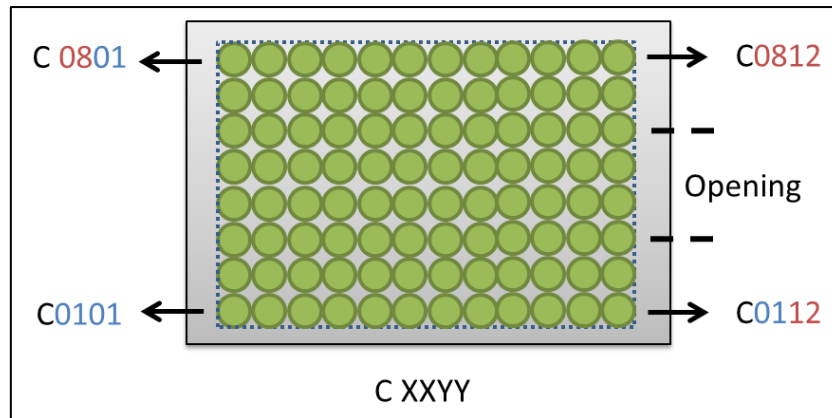


Figure 13. Cups' grid format

As previously mentioned, a horizontal water mist nozzle orientation shall be adopted to improve the water mist distribution in the enclosure. Apart from that, two other factors affecting the water mist distribution were investigated; ISO room corner (enclosure) scale and the nozzle distance from enclosure opening (shown in Figure 14 below). Note that the original concept to simulate the water mist (refer to Figure 8) was used due to the tediousness of shifting the obstruction mesh and to avoid multiple meshes domains from being used.

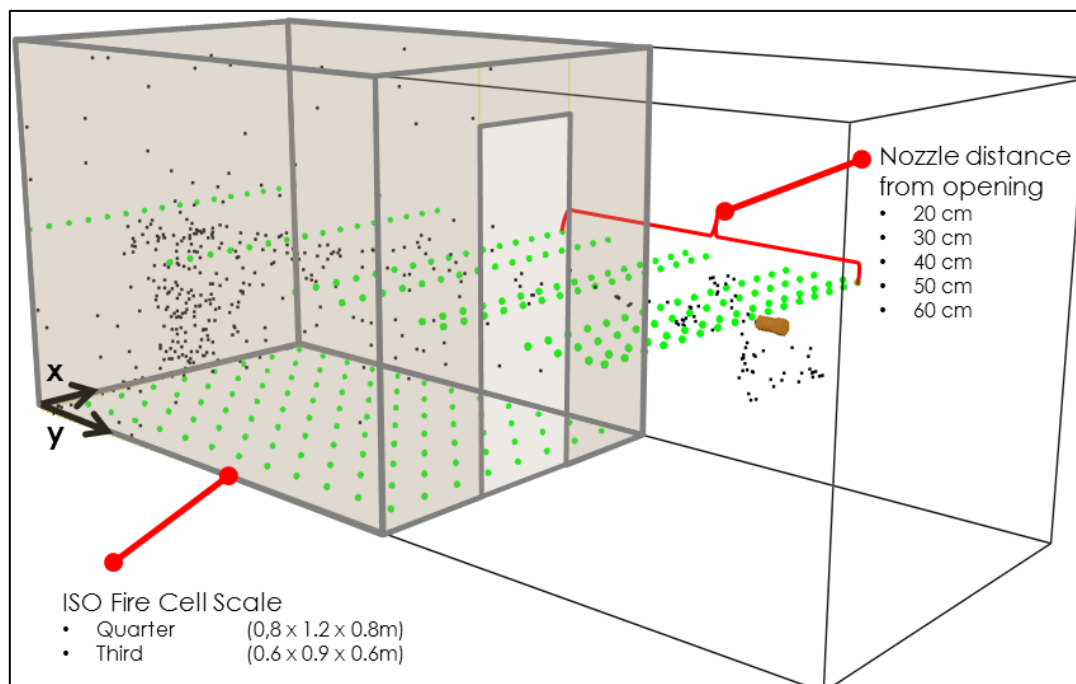


Figure 14. Factors affecting water distribution

Considering the time for the water mist to achieve steady state, all permutations of nozzle distance and ISO room corner scale were simulated for five seconds and AMPUA devices used were of 6x6cm to avoid possible area overlap. The AMPUA measurements were then analysed to identify the case

with the best water distribution. The case of “third scale ISO cell and 20mm nozzle distance” shall be used as an example to illustrate the analysis method where the AMPUA results are shown below in Figure 15 where the enclosure opening is along the right edge. To attain a quantifiable comparison, an appropriate threshold value of 5×10^{-5} kg was decided upon visually by analysing the AMPUA results of all ten cases. Next, the ratio of number of measurements exceeding the threshold value to total number of measurements is calculated. In the example below, this ratio was $\frac{21}{187}$, giving an overall percentage of 11%. The same was done for the other permutations and the results are compiled in Table 4 below.

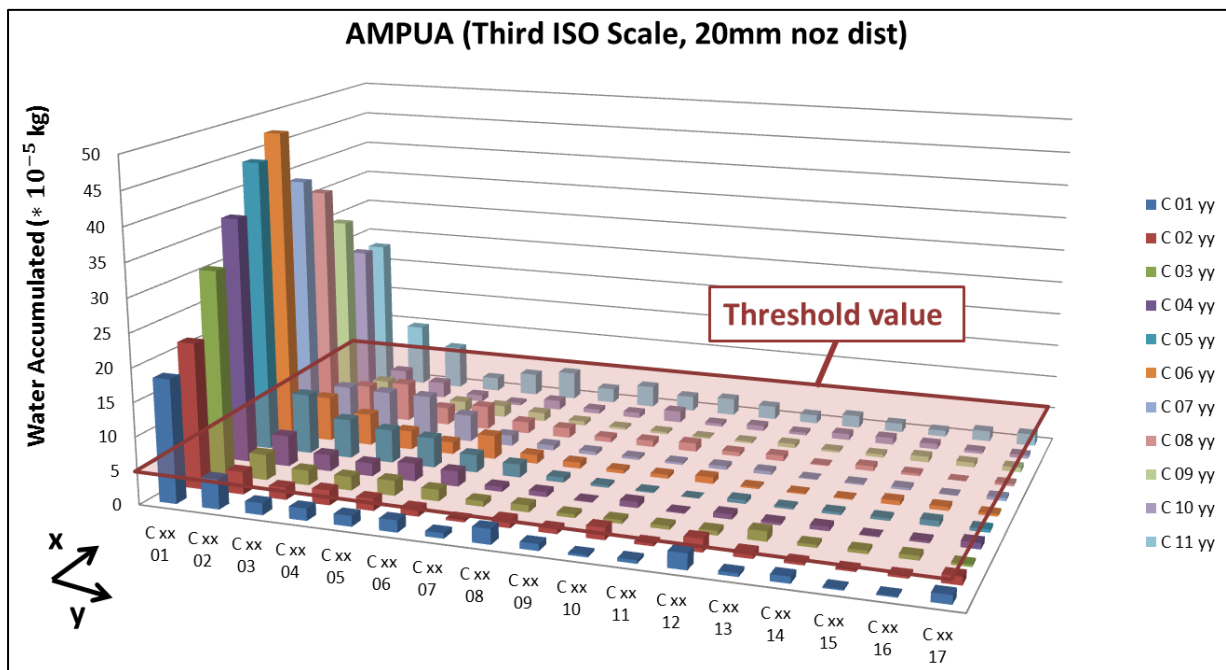


Figure 15. Water distribution analysis (example showing 11% of device measurements exceeding threshold value)

Table 4. Water distribution analysis (Higher percentage indicates better distribution)

Nozzle distance from opening (cm)	ISO room corner scale	
	Quarter	Third
20	8%	11%
30	14%	16%
40	24%	18%
50	31%	24%
60	38%	28%

The use of a bigger enclosure seems to be beneficial only when low distance between the nozzle and open is used. A common trend of improved water distribution as the nozzle distance from opening

increases can be observed. There are however, limitations on how far the nozzle can be positioned from the opening which includes the laboratory's layout (position of the hood calorimeter and structure to position the water mist nozzle) and the distance where water particles would start impinging on the edges of the enclosure opening. To determine the latter limitation, velocity profiles at additional distances from the nozzle were investigated (shown in Figure 16 below). The maximum distance was found to be 600mm as with a distance of 100mm increment, velocity profiles at the extreme X positions (coincides with enclosure opening's width of 0.2m) have a non-zero magnitude.

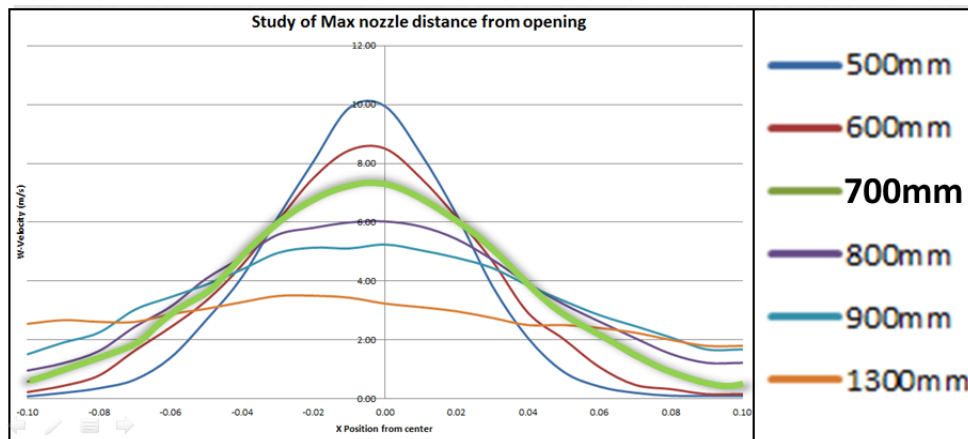


Figure 16. Study of maximum nozzle distance from opening

The distance limitation from the laboratory setup is of roughly 1m; therefore the limiting maximum nozzle distance from the opening is 600mm, governed by the water mist spray width. Finally, the combination for best water distribution can be said to be the use of a quarter scale ISO room corner with a 600mm distance between the water mist nozzle and enclosure opening.

4.7. Scenarios' Simulation (Steps 6-9)

In step 6, the result attained from simulating the combination for best water distribution (quarter scale ISO room corner and 600mm nozzle distance) using the best suited concept was compared to those of the different permutations. The main intention now is to show that when using the best suited concept, the water distribution is at least as good when compared to using the original concept. By using the same technique to analyse the AMPUA data, the result comparison was not as clear and thus the mean and standard deviation values were used instead (Figure 17). The distribution among the AMPUA measurements seen for the best suited concept (indicated as purple diamond in figure) is better than that of similar simulation when using the original water mist concept (indicated as green dash in figure). This was deduced by comparing the two error bars which indicate the extent of the measurement range from the respective mean values.

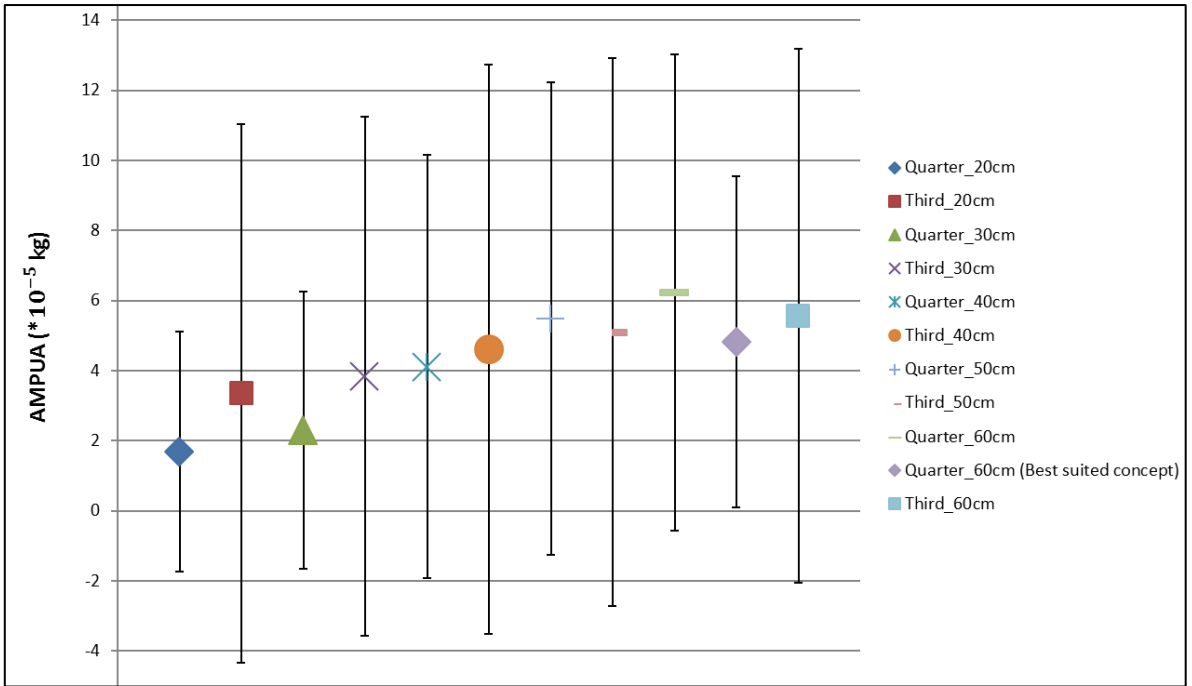


Figure 17. Mean and standard deviation analysis of water distribution (All simulations performed with original water mist concept except for 2nd last where best suited concept was used)

For all scenarios (Steps 6-9), the simulations were constructed to mimic the respective experiments. The best suited concept to simulate the water mist was adopted which requires a grid size of 1cm in the region of the turbulence meshes. Two meshes were used where the first mesh was of 1cm grids and encompassed the air inlet and the turbulence meshes. In view of computational costs, the enclosure was mostly within the second mesh of 2cm grid size. For simulations involving water mist (scenarios 1,3-5), the effect of the water preconditioning of the enclosures on the enclosure material's properties were not taken into account. Two types of output data, temperatures from thermocouples (refer to Figure 20 for positions) and HRR, were collected. A sample of a FDS script written (Scenario 5) is provided in **Annex D**.

5. Experimental Setup / Details

The experimental setups are influenced by simulation limitations, preliminary simulation setup results and theoretical findings (Extinguishment model). The detailed experimental procedure for experiments 1-5 and the physical layout of the laboratory can be found in **Annex E**. The risk assessment performed for the experiments can be found in **Annex F**.

Experiment 1: Water

The smallest cups available (7cm diameter) were used and were formed in a grid (8 by 12) that fit the maximum number of cups in the enclosure. The cups' positions in grid and labels as well as the buffer dimensions are shown in Figure 18 below (Note: enclosure opening on the right). The water mist nozzle is centered with reference to the enclosure's opening. Each cup was weighed before and after the experiment and the weight difference was recorded as the amount of water accumulated. Experiment 1 had a five minute duration.

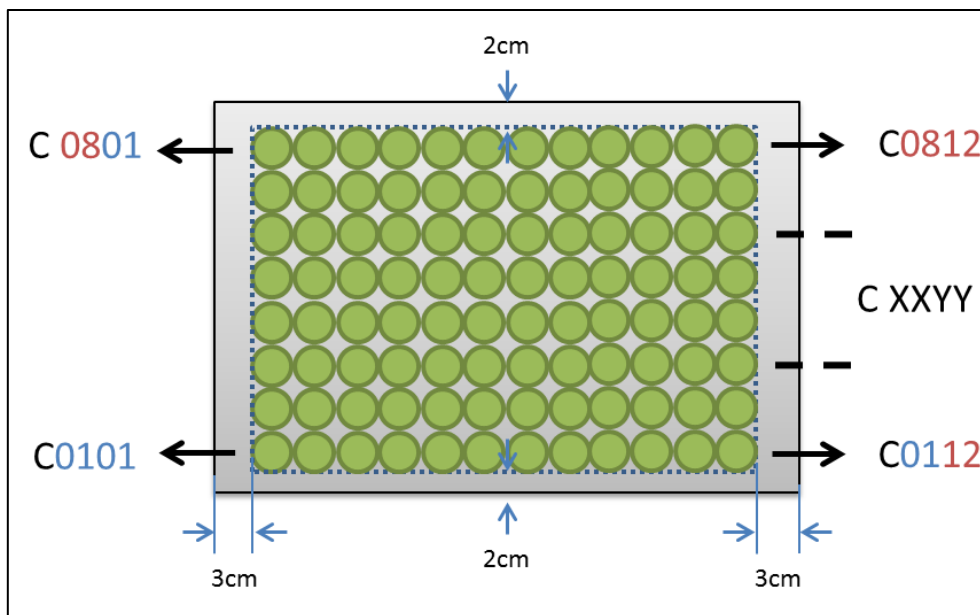


Figure 18. Cups' Position and Label

Experiment 2: Fire

A prior test is performed where the burner was ignited and placed below the hood calorimeter and the fuel flow rate toggled to achieve the desired HRR of 10kW. The experiment was then done with the experimental setup shown in Figure 20 using the same fuel flow rate setting. The output data consist of temperatures varying in height and HRR. The HRR will be calculated based on oxygen depletion by analysing the difference of current to ambient oxygen concentration levels. The thermocouple tree was positioned at the corner, which consists of ten thermocouples at heights of 56, 52, 47.5, 42, 36, 30.5, 25, 19, 13.5 and 8mm off the enclosure floor. Experiment 2 had an eight minute duration.

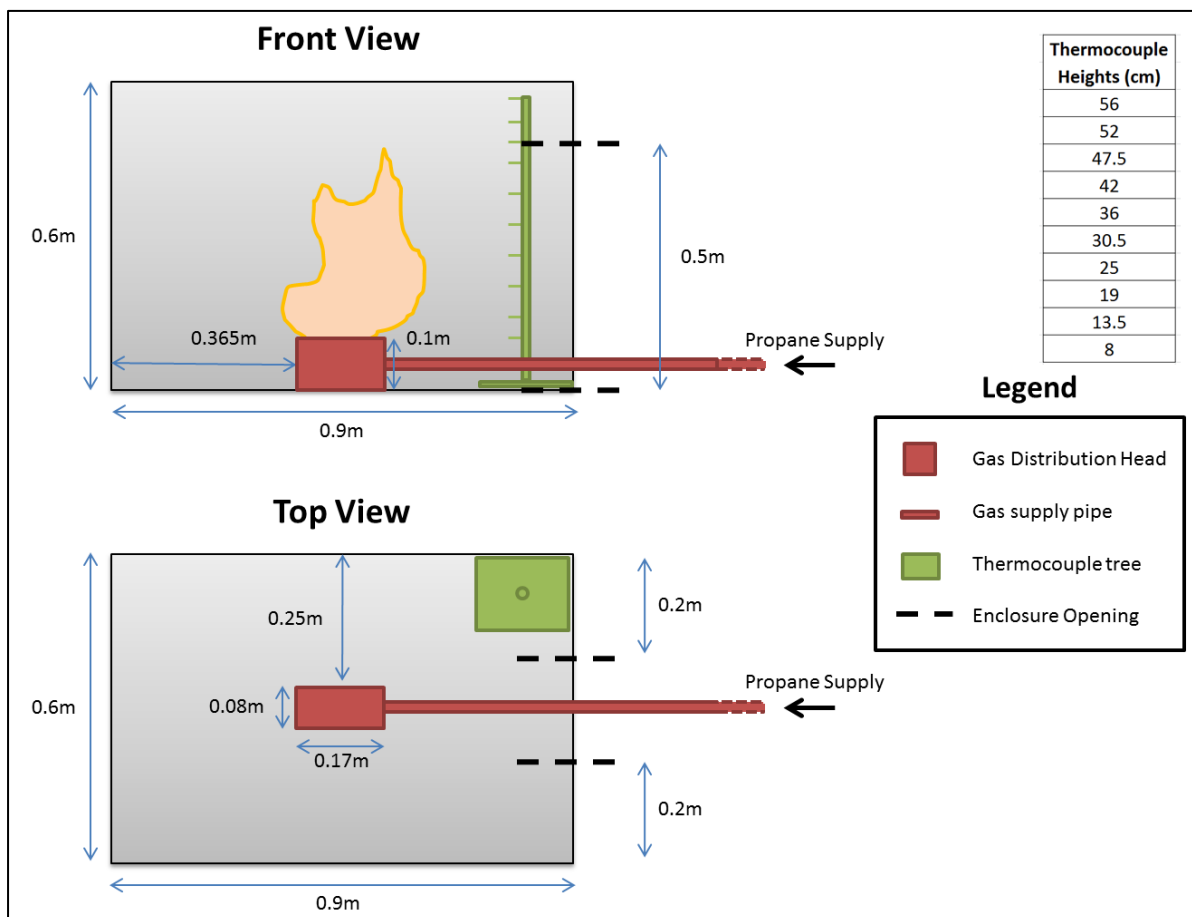


Figure 20. Experiment 2 setup

Experiment 3: Combination

Experiment 3 is a combination of experiments 1 and 2, where the effects of water mist on the flame can be observed and analysed. The temperature readings off the thermocouples and the HRR readings from the hood calorimeter can be used to affirm observations and possible theories. The same outputs, temperatures varying with respective heights and HRR, were measured for comparison against experiment 2's result. Experiment 3 had an eight minute duration, which consisted of three initial minutes of free burn before activation of the water mist system. The experimental setup is as shown below (Figure 21).

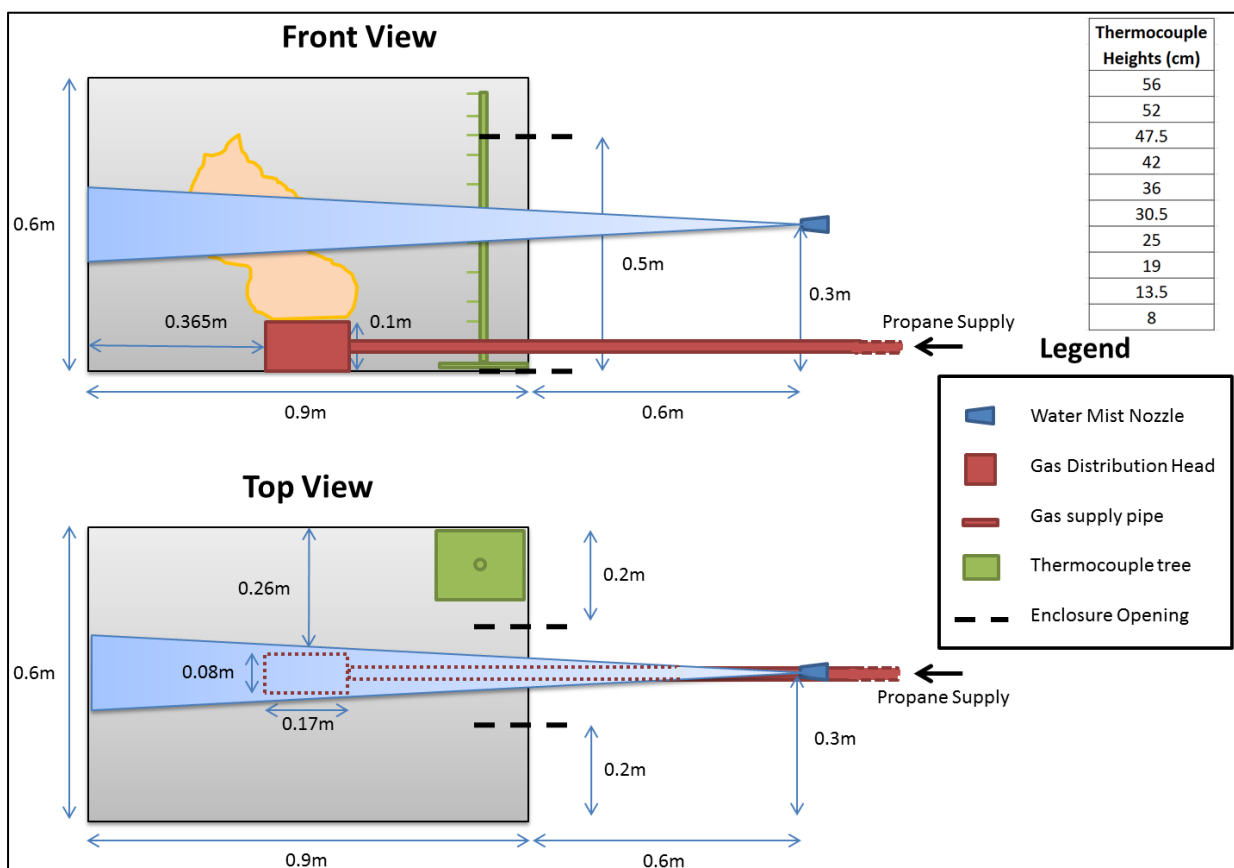


Figure 21. Experiment 3 setup

Experiments 4 & 5: Extinguishment

The motivation for these scenarios is to study how reliable the quasi steady state extinguishment model [2] is. This said model was developed using obstructed fires, which therefore focuses on extinguishment by oxygen dilution. From preliminary simulation results of scenario 3, a large amount of oxygen was being introduced into the enclosure due to entrainment, therefore the water mist nozzle would now be placed right at the opening instead. To reduce the effect of direct gas phase cooling, the water mist and burner axes were deliberately misaligned. By using the best suited concept in simulations, the nozzle cannot be placed at the edge of the opening. HRRs of 16.7 and 25kW were used for scenarios 4 and 5 respectively. Output data of temperature and HRR were measured for analysis. Due to the higher HRRs used, there is a concern for the enclosure's integrity therefore a shorter free burning time is used. Experiments 4 and 5 each had a six minute duration, which consisted of an initial minute of free burn before activation of the water mist system. The experimental setup is as shown below (Figure 22).

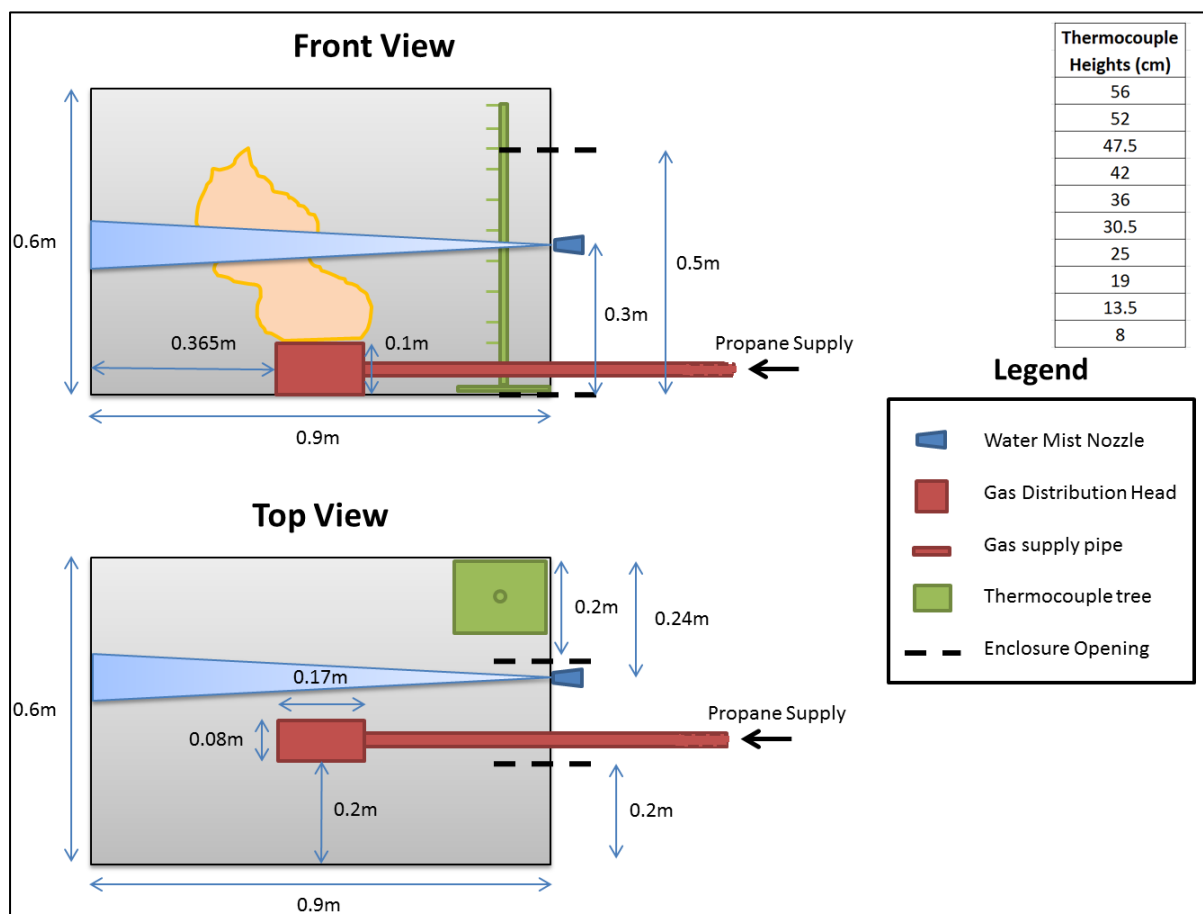


Figure 22. Experiment 4 and 5 setup

6. Results

6.1. Simulations

The simulations' timestep were automatically generated based on the choice of grid size where a smaller timestep is used for a smaller grid size. The timesteps of the simulations were less than one second and due to the degree of measurement fluctuations, a large amount of fluctuation in the data was created. HRR data averaging over one second intervals (to correspond to time interval used in experiments) were performed to reduce this "noise". The thermocouple devices used to measure temperature in the simulations have a slight resistance to measurement change and thus have lesser fluctuations and do not require averaging.

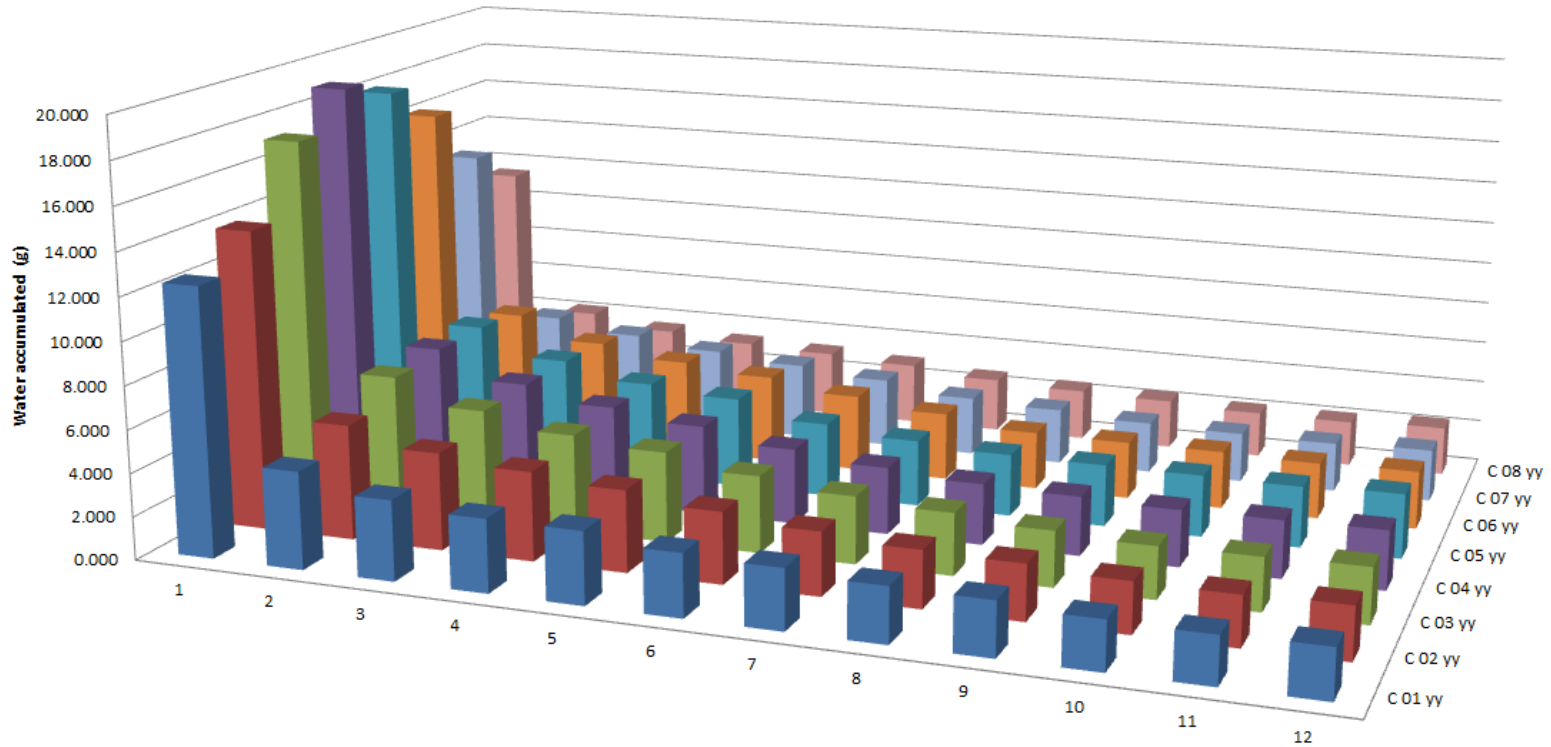
The thermocouple labelling sequence starts from the highest thermocouple downwards (ie. TEMP1= temperature measurement of highest thermocouple). In cases where steady state temperatures are of interest, the final temperature values of the respective height were used.

In scenarios where the water mist system was used, the time of activation is indicated as a light blue dashed vertical line in the results. The best suited concept was used in simulations of all scenarios involving the water mist system.

6.1.1. Scenario 1: Water

Results from the full length simulation of 5 minutes (Figure 23, Note that opening is along the right edge) show similar trends as the preliminary 5 second simulations; where the devices nearest to the back wall collected the most amount of water. Apart from that row of devices, the distribution of water collected by the rest of the devices seem relatively even in magnitude thus indicating an improvement in overall water distribution with time.

(Simulation) Scenario 1, Water Accumulated



	1	2	3	4	5	6	7	8	9	10	11	12
C 01 yy	12.450	4.516	3.712	3.377	3.350	2.904	2.785	2.549	2.498	2.256	2.188	2.269
C 02 yy	13.951	5.362	4.536	4.147	3.796	3.320	2.940	2.648	2.572	2.355	2.317	2.419
C 03 yy	17.222	6.440	5.274	4.566	4.226	3.589	3.154	2.893	2.595	2.418	2.467	2.556
C 04 yy	18.945	6.674	5.360	4.668	4.189	3.549	3.148	2.862	2.764	2.645	2.683	2.737
C 05 yy	18.034	6.676	5.376	4.627	4.311	3.519	3.151	2.943	2.917	2.902	2.862	3.005
C 06 yy	16.160	6.226	5.147	4.582	4.232	3.688	3.235	2.753	2.723	2.735	2.644	2.724
C 07 yy	13.225	5.022	4.476	4.026	3.696	3.347	2.833	2.671	2.446	2.369	2.330	2.454
C 08 yy	11.445	4.208	3.615	3.338	3.190	2.975	2.621	2.458	2.364	2.189	2.165	2.312

Figure 23. (Simulation) Scenario 1, Water Accumulated

6.1.2. Scenario 2: Fire

The mean HRR after achieving steady state was 10.01kW. This low margin of error is expected as the simple prescribed HRR approach was used in FDS which tailors the fire's HRR according to the inputs of Heat Release Rate per Unit Area (HRRPUA) and the burner's surface area.

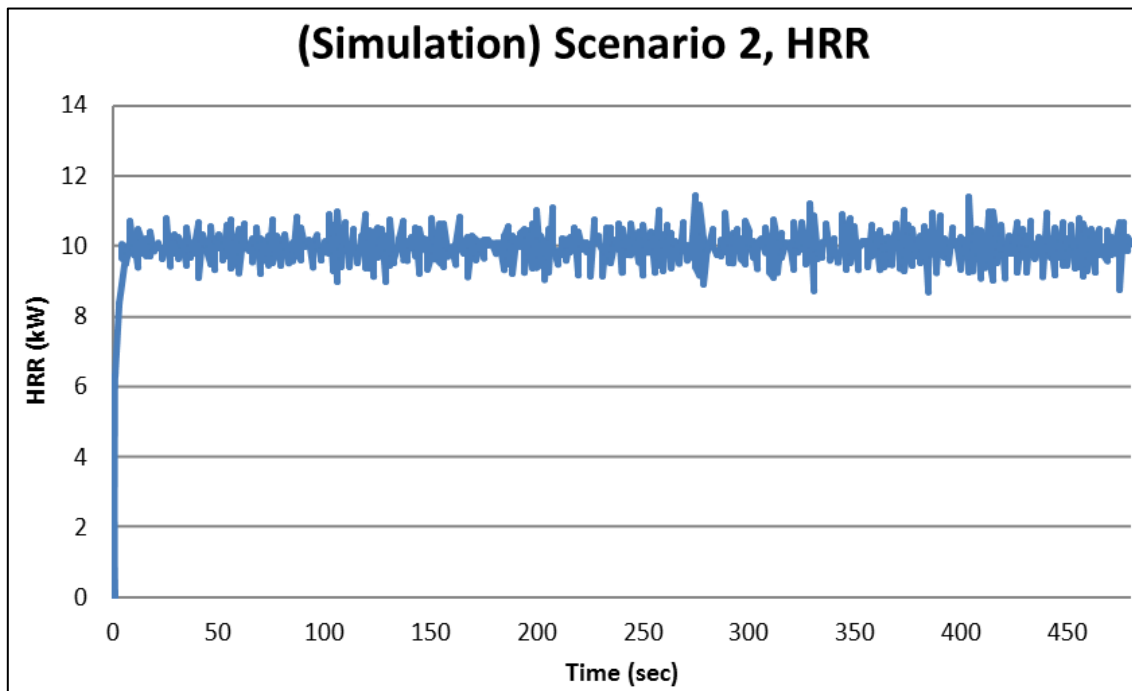


Figure 24. (Simulation) Scenario 2, HRR

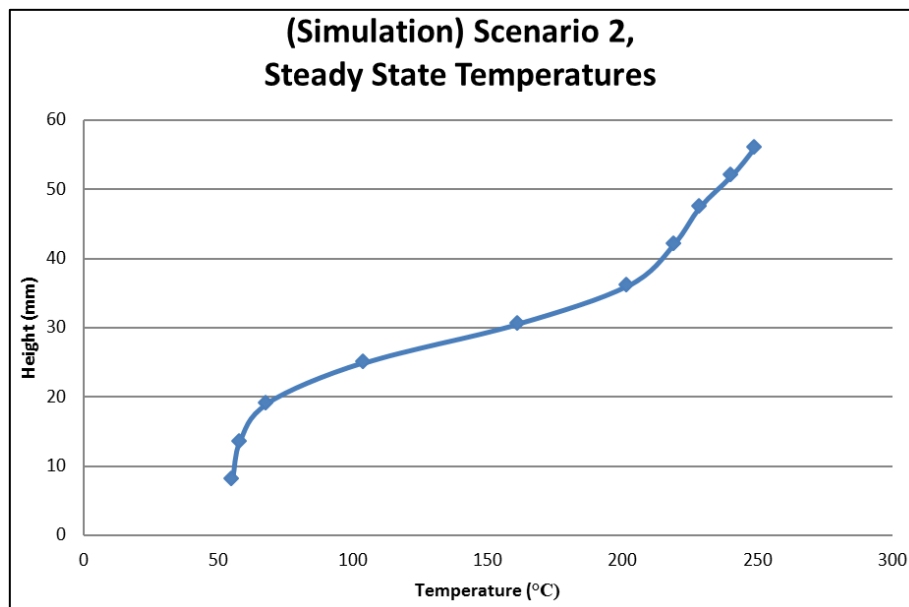


Figure 25. (Simulation) Scenario 2, Steady State Temperatures

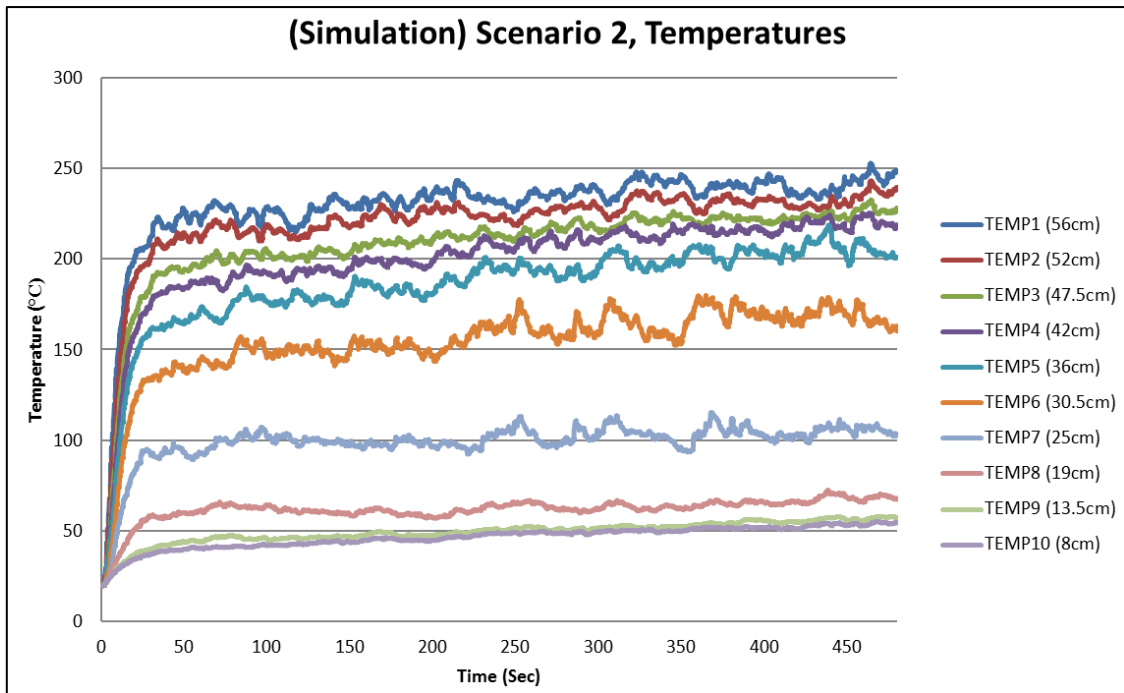


Figure 26. (Simulation) Scenario 2, Temperatures

Both the steady state temperature and rate of temperature change increases with the height of thermocouple, especially with heights beyond the smoke layer which is estimated from Figure 25 to be at 30mm. A gradual temperature increment after relative steady state has been reached is seen in all the thermocouple measurements. This is likely due to re-radiation from the enclosure boundaries where their temperatures change according to their interaction with heat and the specific heat of the material, PROMATECT-H, used.

6.1.3. Scenario 3: Combination

The average steady state HRR achieved was 9.97kW which did not waver much upon activation of the water mist, resulting in the fire not being extinguished.

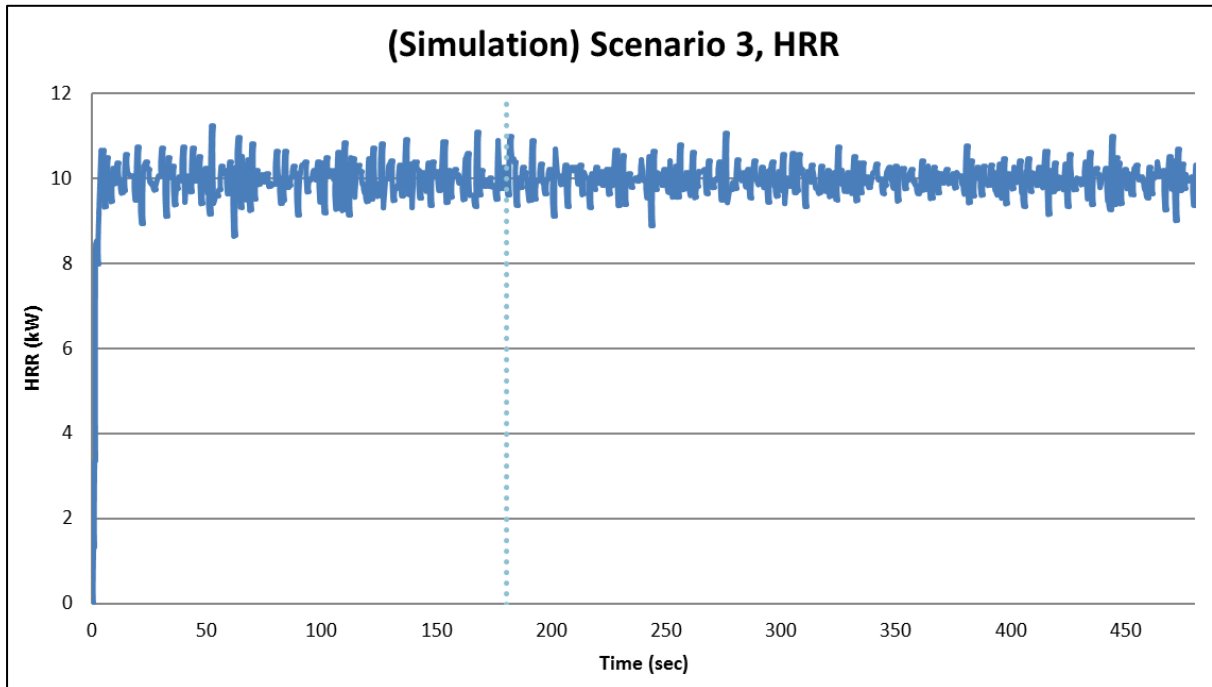


Figure 27. (Simulation) Scenario 3, HRR

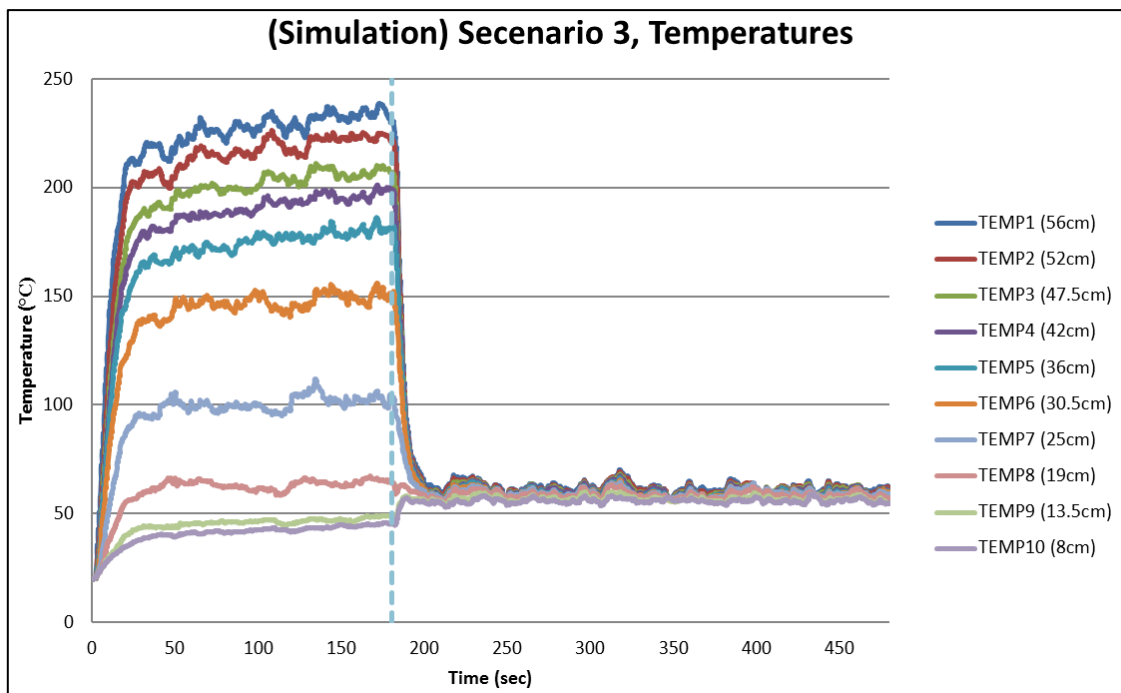


Figure 28. (Simulation) Scenario 3, Temperatures

6.1.4. Scenario 4: Extinguishment 16.7kW

The average steady state HRR achieved was 16.71kW which did not waver much upon activation of the water mist, resulting in the fire not being extinguished.

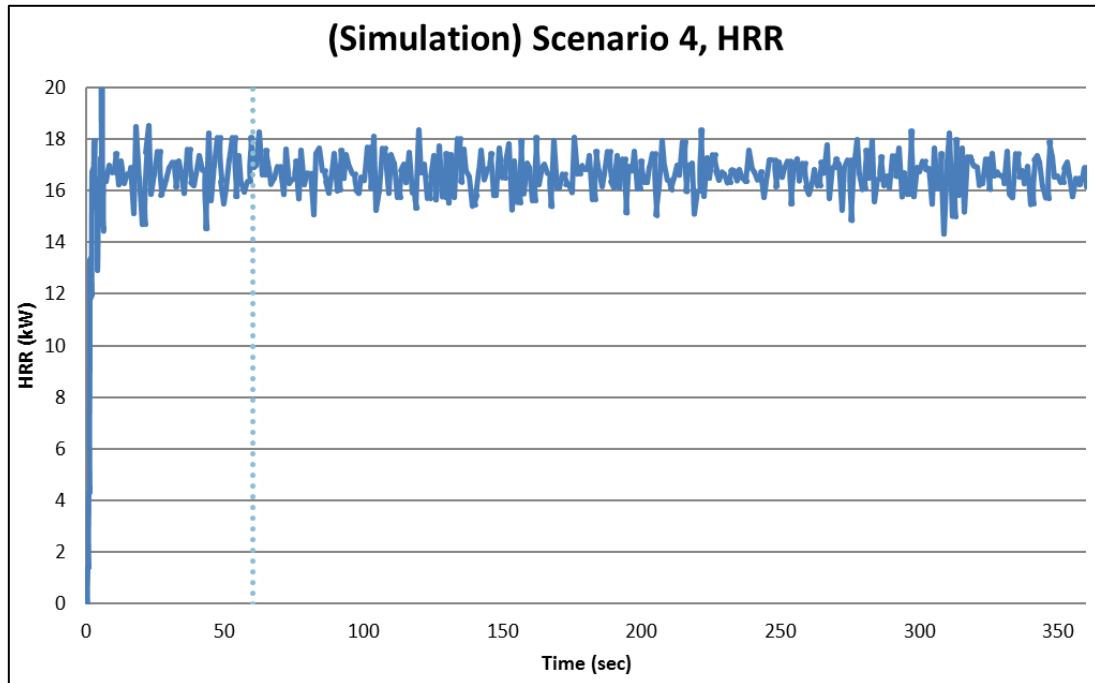


Figure 29. (Simulation) Scenario 4, HRR

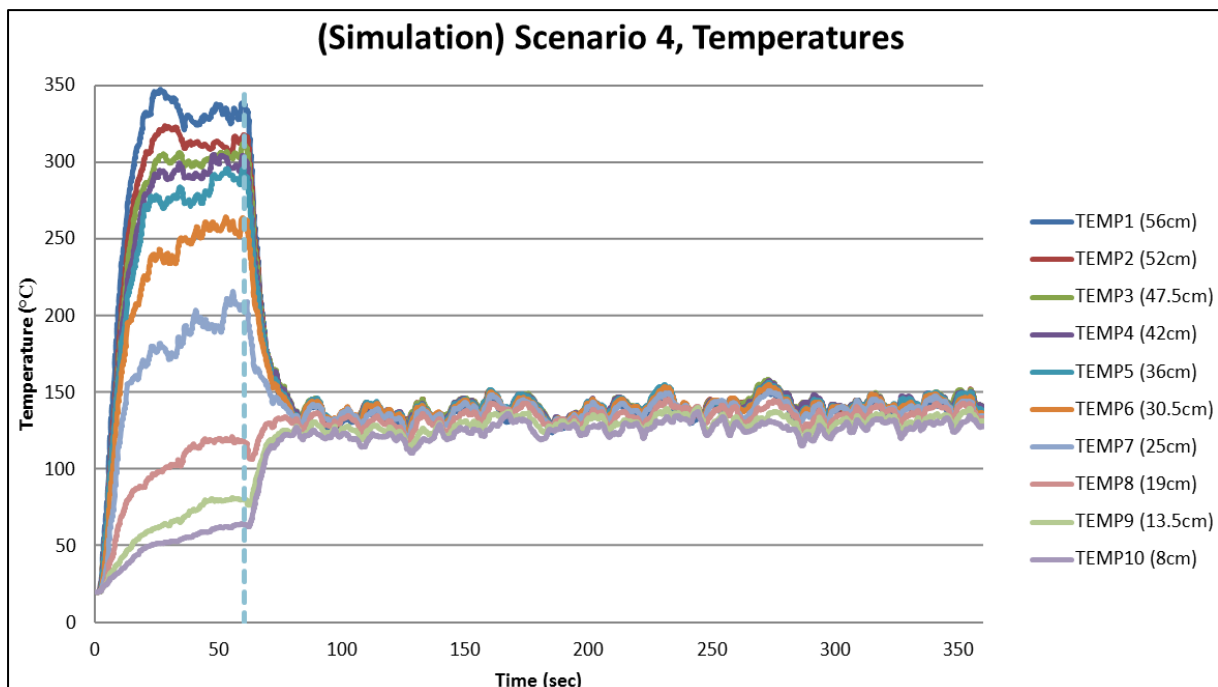


Figure 30. (Simulation) Scenario 4, Temperatures

6.1.5. Scenario 5: Extinguishment 25kW

The average steady state HRR achieved was 25.01kW which did not waver much upon activation of the water mist, resulting in the fire not being extinguished.

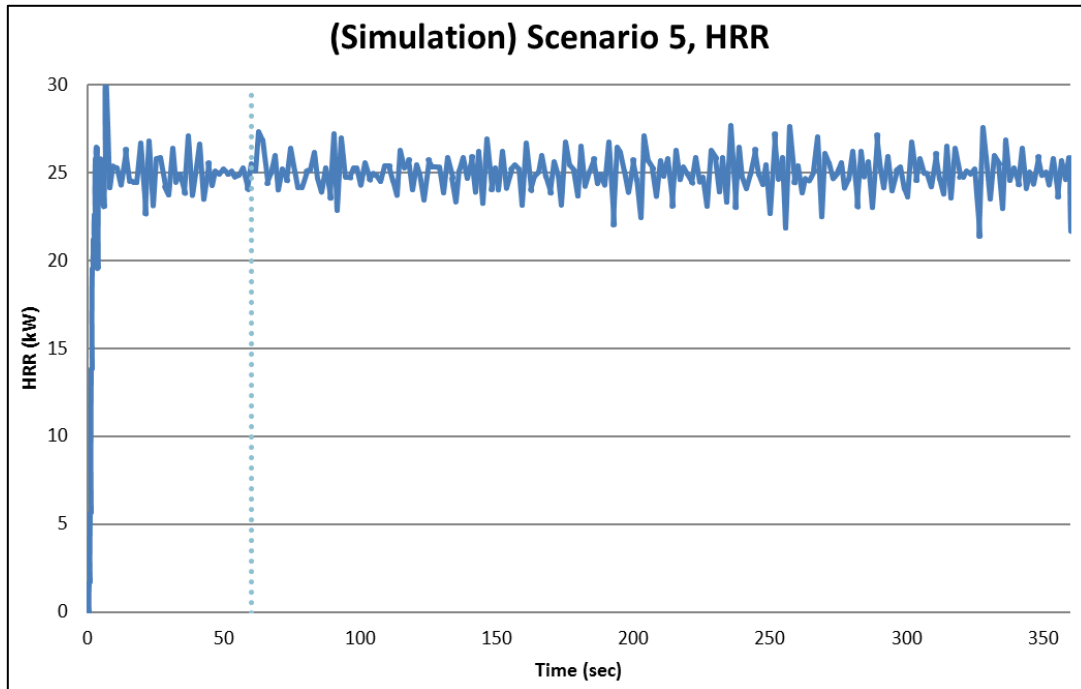


Figure 31. (Simulation) Scenario 5, HRR

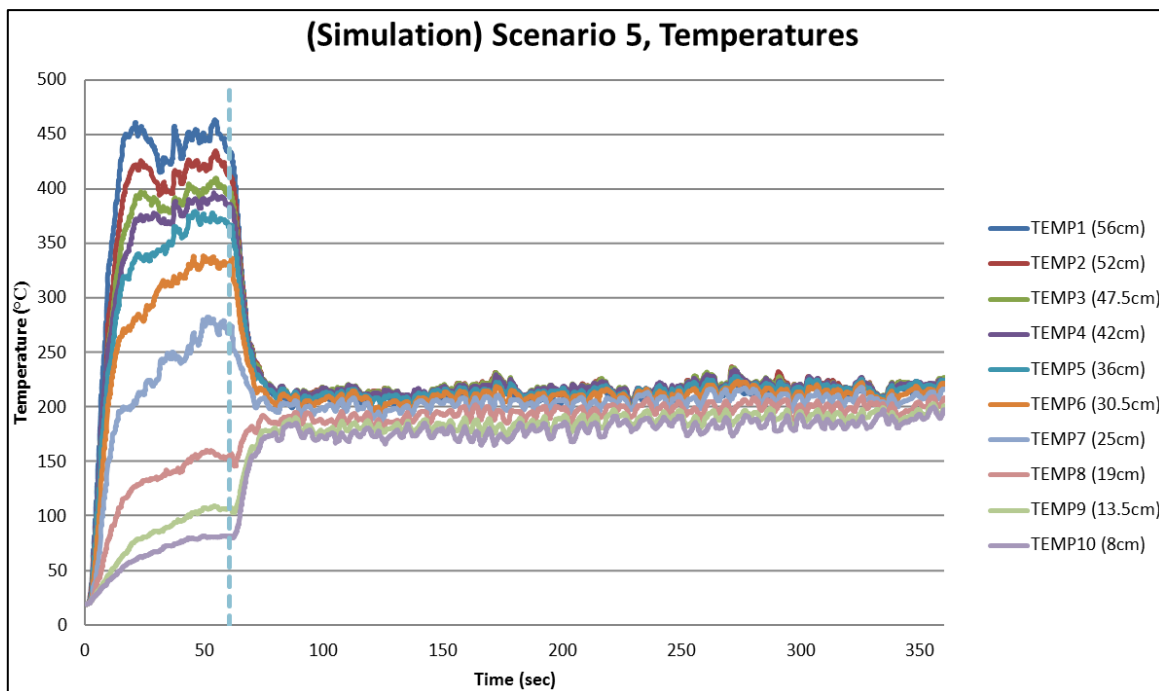


Figure 32. (Simulation) Scenario 5, Temperatures

6.2. Experiments

Each experiment was run twice and relative repeatability was confirmed unless mentioned otherwise.

HRR calculation

While there was a live display of the HRR readings in the software “LSHR Calc”, the data exported do not include the HRR specifically and must be calculated from the oxygen concentration level and the duct pressure. First, the duct velocity had to be determined using the formula of kinetic energy:

$$\text{Kinetic Energy, } KE = \frac{1}{2}MV^2$$

Where $M = \text{Mass [kg]}$

$$V = \text{Velocity } \left[\frac{m}{s}\right]$$

Making velocity the subject:

$$V = \sqrt{\frac{2 * KE}{M}}$$

Next by comparing the units for appropriate substitutions to be made:

$$\frac{KE}{M} \left[\frac{J}{kg}\right] = \frac{P_d}{\rho_g} \left[\frac{Nm}{kg}\right]$$

Where $P_d = \text{Pressure in duct [Pa]}$

$$\rho_d, \text{Density of gas in duct} = \frac{353}{T_d [K]}$$

$$T_d = \text{Temperature in duct [K]}$$

The velocity in the duct can then be found by:

$$V_d = CF_d \sqrt{\frac{2 * P_d}{\rho_d}} \quad (20)$$

Where $V_d = \text{Velocity in duct } \left[\frac{m}{s}\right]$

$$CF_d, \text{Correction factor for duct} = \frac{0.9}{1.08}$$

With the velocity in the duct known, the HRR can be calculated using the oxygen depletion method using Equation (13) as reference:

$$\dot{Q}_{Fire} = V_d * A_d * \rho_d * \Delta H_{R,O_2} * \left(\frac{C_{O_2}(t) - C_{O_2\infty}}{100} \right) \quad (21)$$

Where $A_d = \text{Area of duct [m}^2\text{]}$

$C_{O_2}(t) = \text{Oxygen concentration at 't' seconds [\%]}$

$C_{O_2\infty} = \text{Ambient oxygen concentration [\%]}$

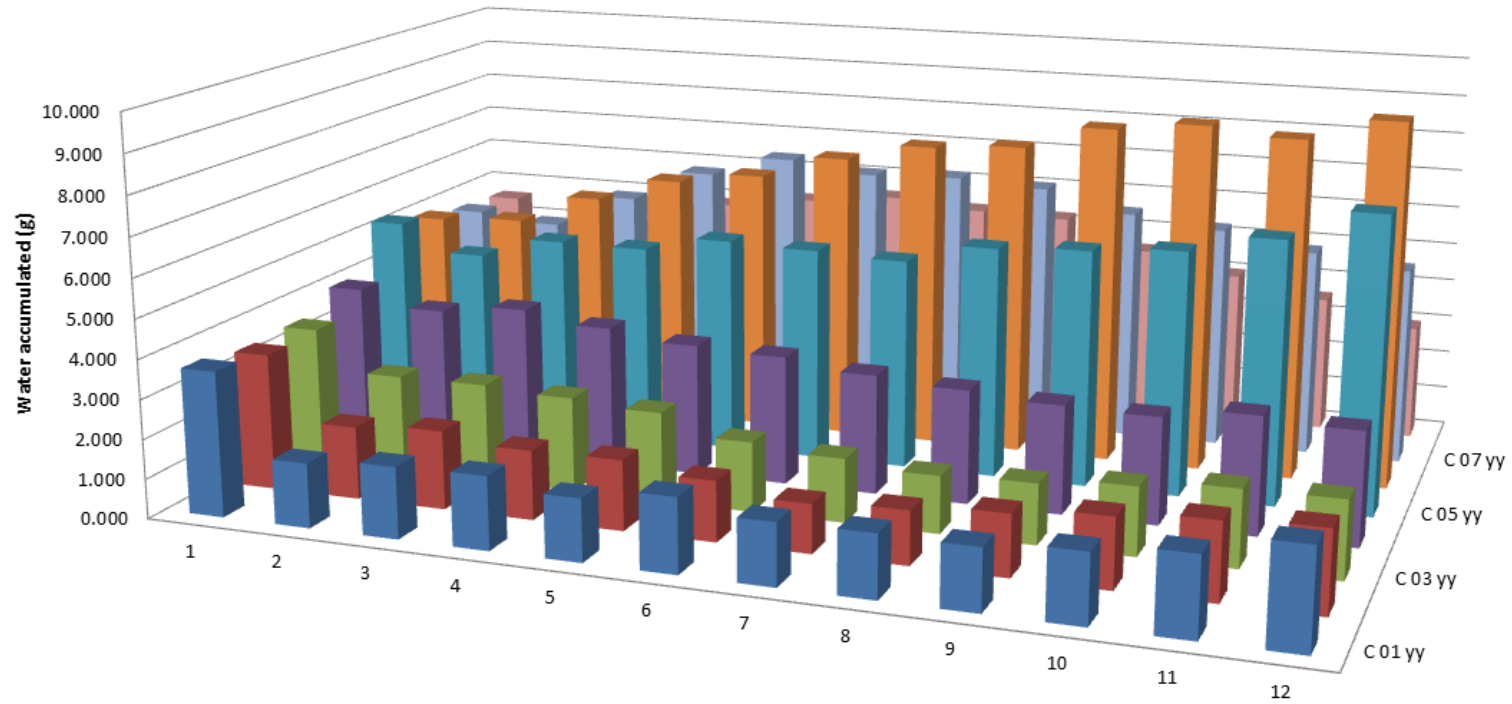
Extinguishment

There can be a large subjectivity to the exact time to extinguishment when determined visually; therefore a more quantitative method is required for repeatability. In this project, extinguishment will be assumed when the HRR drops to half of the average steady state HRR value.

6.2.1. Scenario 1: Water

From observations during the experiment, the water mist spray seemed to have a slight torsion causing a tendency for the water particles to veer to the right of the water mist nozzle's axis. This is reflected in the averaged experimental result shown in Figure 33 (Note that opening is along the right edge). Physically, there are gaps in between the cups which are not present in the simulation of this scenario; thus for a fair comparison to be made, the water collection rate about the cup's opening is assumed to be constant throughout the square area which encompasses the circle. The values shown in the result below have already been subjected to the appropriate area ratio correction factor.

(Experiment) Scenario 1, Water Accumulated



	1	2	3	4	5	6	7	8	9	10	11	12
C 01 yy	3.673	1.628	1.801	1.842	1.571	1.877	1.560	1.580	1.548	1.734	1.975	2.469
C 02 yy	3.468	1.844	1.994	1.758	1.776	1.528	1.235	1.353	1.551	1.762	1.953	2.055
C 03 yy	3.522	2.502	2.520	2.415	2.281	1.777	1.620	1.455	1.531	1.727	1.942	1.959
C 04 yy	4.030	3.658	3.889	3.615	3.377	3.300	3.060	2.914	2.772	2.724	3.002	2.882
C 05 yy	5.317	4.628	5.183	5.169	5.571	5.510	5.420	5.936	6.065	6.244	6.726	7.531
C 06 yy	4.961	5.097	5.876	6.522	6.830	7.454	7.920	8.073	8.696	8.940	8.739	9.328
C 07 yy	4.684	4.494	5.414	6.280	6.843	6.583	6.663	6.531	6.018	5.765	5.355	5.074
C 08 yy	4.607	3.923	4.523	4.903	5.218	5.477	5.279	5.221	4.498	3.998	3.549	2.965

Figure 33. (Experiment) Scenario 1, Water accumulation

6.2.2. Scenario 2: Fire

The HRRs values calculated with Equations (20,21) were slightly less than those shown on the software's display. Figure 34 below shows the average HRR values between both runs where the mean HRR after achieving steady state is approximately 9.3kW. The motivation for scenarios 2 and 3 however, is to study generic interaction effects between the flame and the water mist and therefore this lowered HRR is accepted so long it was kept constant in experiment 3's free burning period.

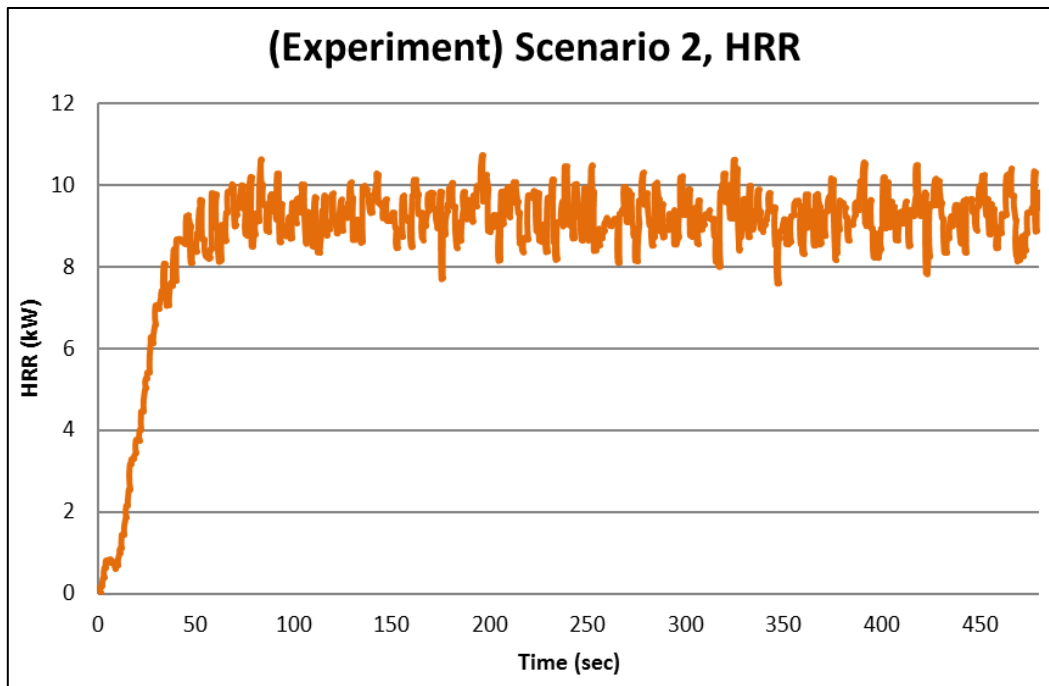


Figure 34. (Experiment) Scenario 2, HRR

There were questionable temperature measurements for the second run where temperatures from thermocouple 3 were higher than thermocouple 2. By using an air flow to cool the enclosure between the runs, the positions of the thermocouples may have been shifted. Therefore for temperature, results from the first run are more representative and are used in Figure 35 and Figure 36.

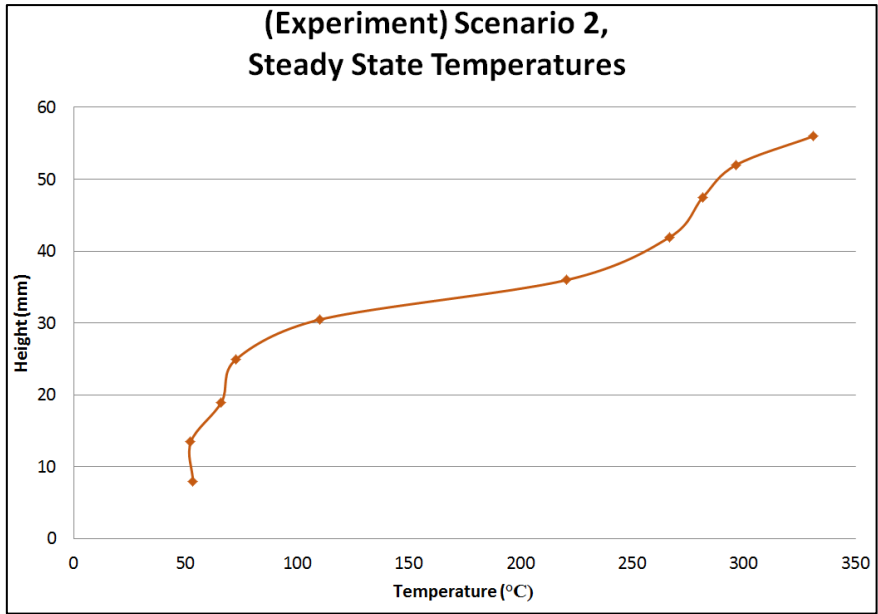


Figure 35. (Experiment) Scenario 2, Steady State Temperatures

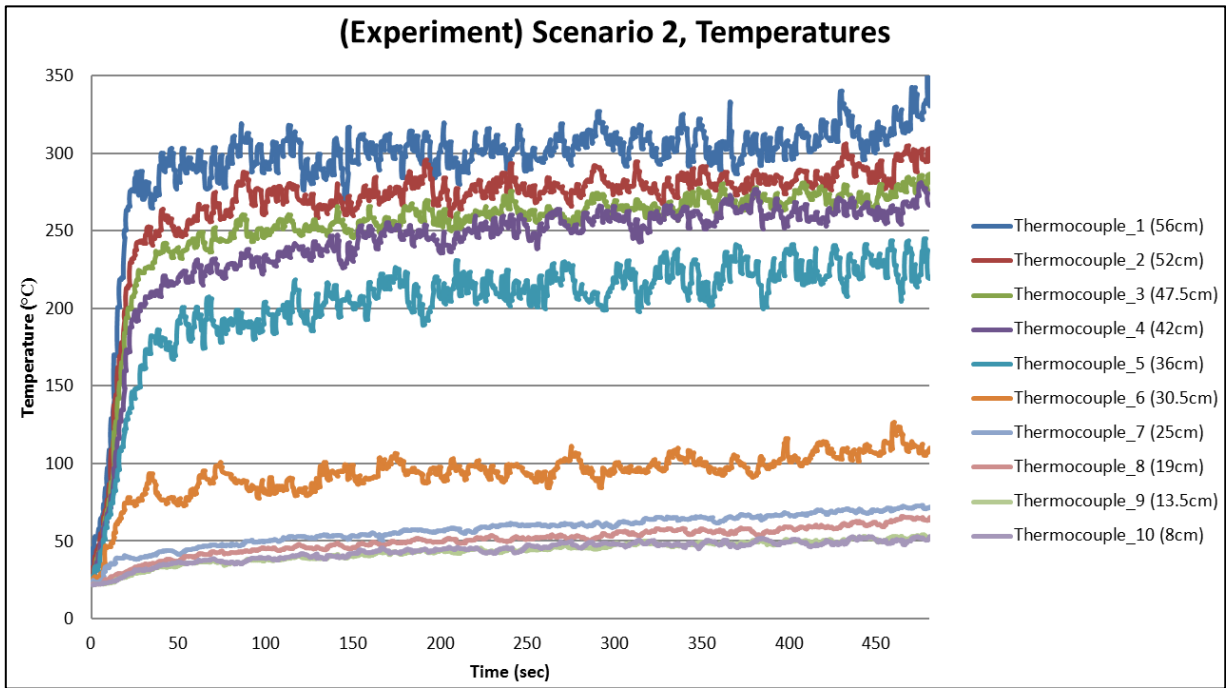


Figure 36. (Experiment) Scenario 2, Temperatures

Similar trend observations from the simulation result can be made here, though the smoke layer height estimation from Figure 35 seems higher at 33mm for the experiment.

6.2.3. Scenario 3: Combination

The result trends were repeatable but due to human errors were of recording the exact ignition time and activation of the water mist, results from a single run would be more representative and thus are used for Figure 37 and Figure 38. The average steady state HRR achieved was 9.4kW and the time to extinguishment was 13 seconds.

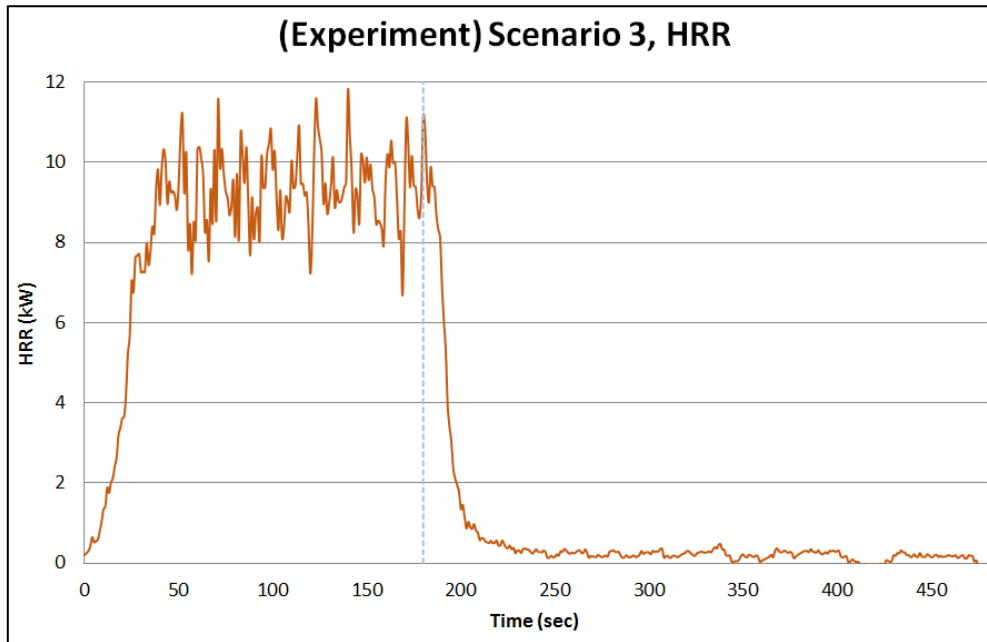


Figure 37. (Experiment) Scenario 3, HRR

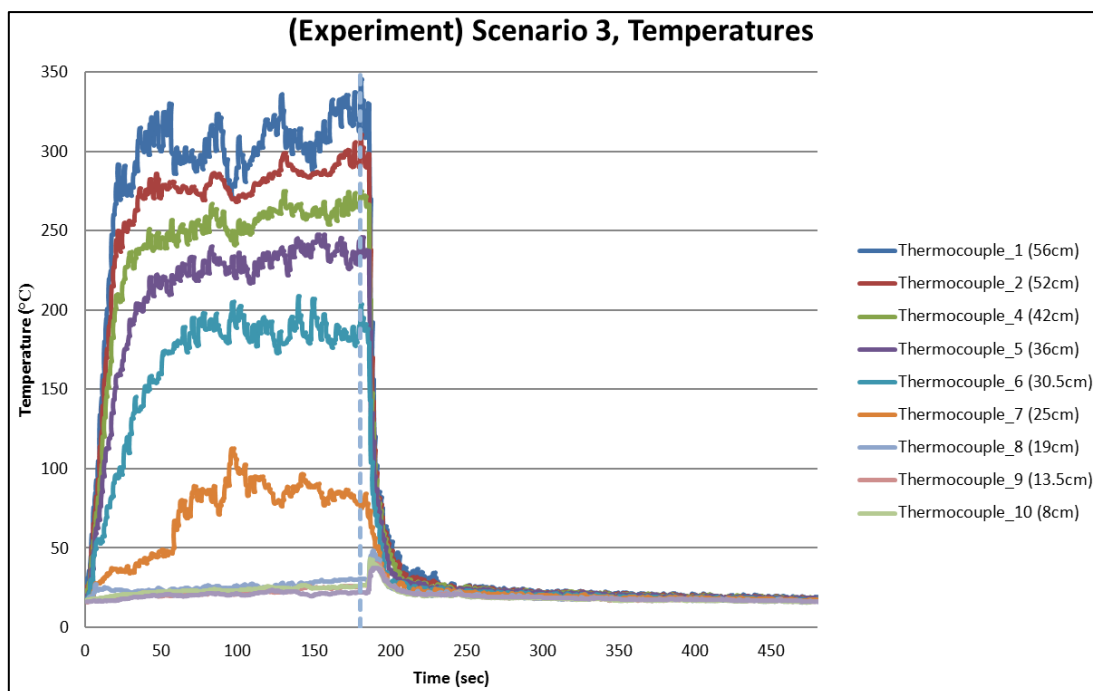


Figure 38. (Experiment) Scenario 3, Temperatures

6.2.4. Scenario 4: Extinguishment 16.7kW

By consulting the live HRR values shown in the software “LSHR Calc” during experiments of scenario 4, the HRR at the predetermined free burning time of one minute did not seem to be at steady state; the water mist activation was therefore delayed to two minutes instead. The average HRR achieved in the last free burning minute was 16.8kW and the time to extinguishment was 12 seconds.

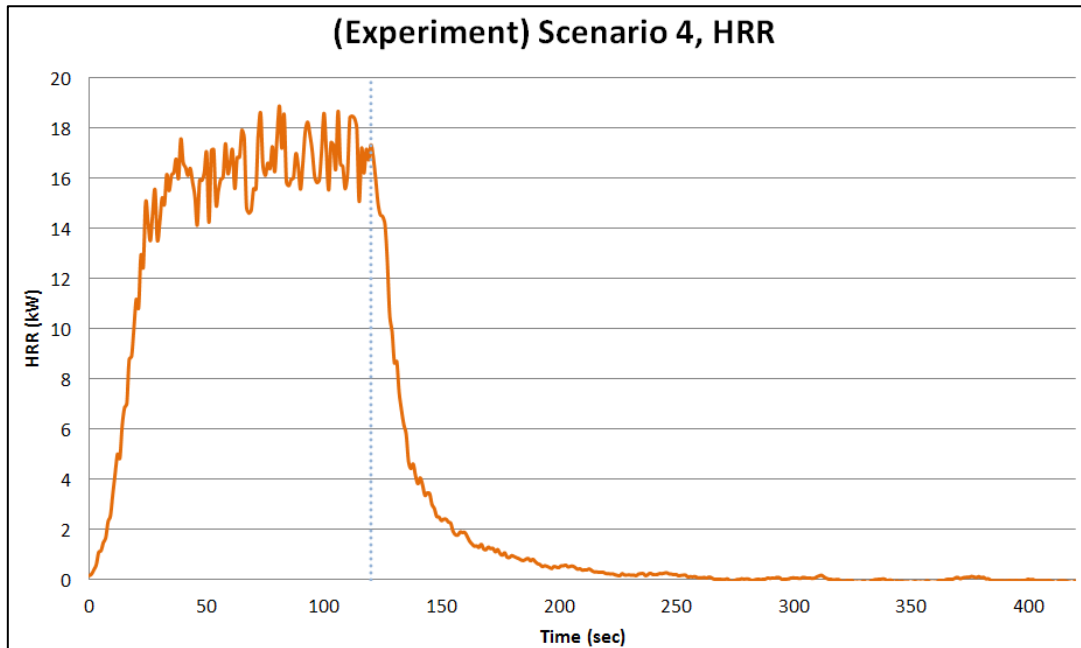


Figure 39. (Experiment) Scenario 4, HRR

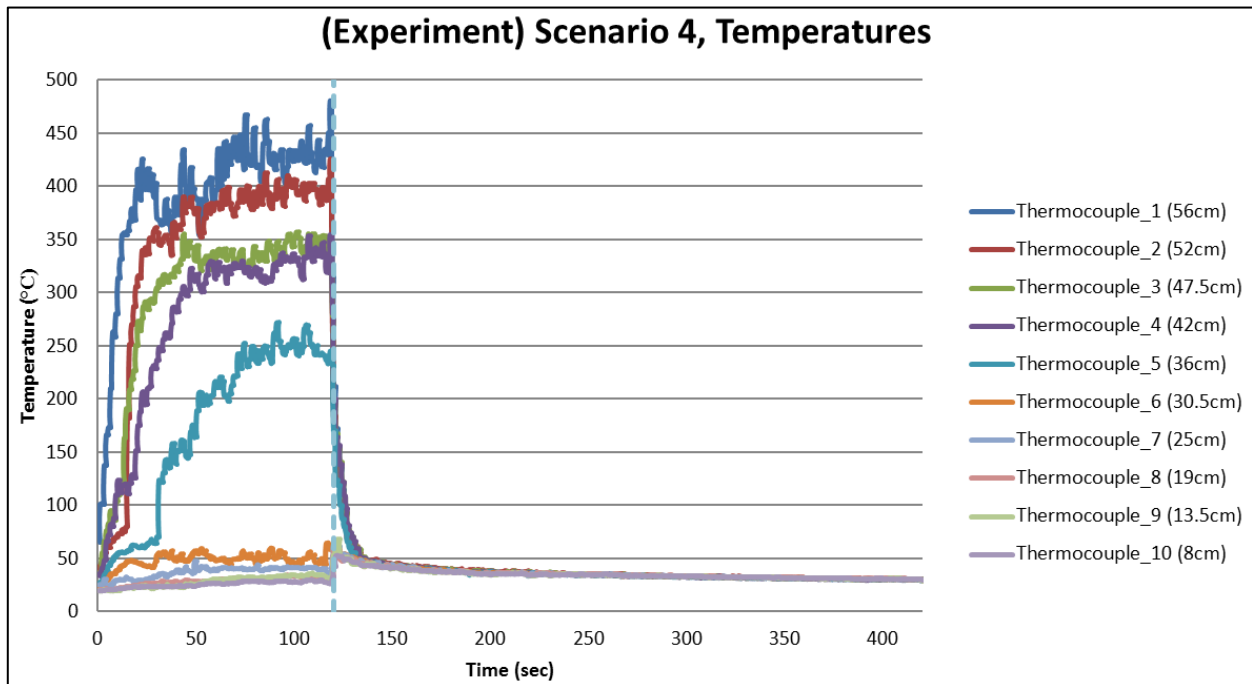


Figure 40. (Experiment) Scenario 4, Temperatures

6.2.5. Scenario 5: Extinguishment 25kW

As per explanation of the previous experiment, a two minute free burning was carried out before activation of the water mist. The average steady state HRR achieved was 25.5kW and the time to extinguishment was 24 seconds.

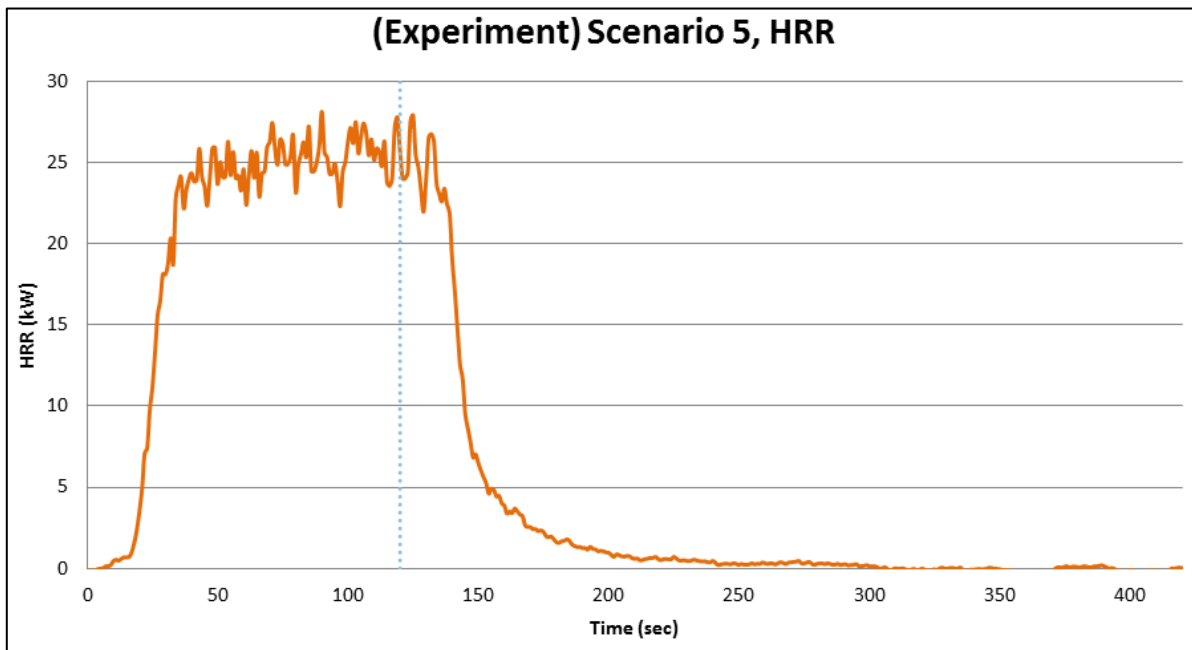


Figure 41. (Experiment) Scenario, HRR

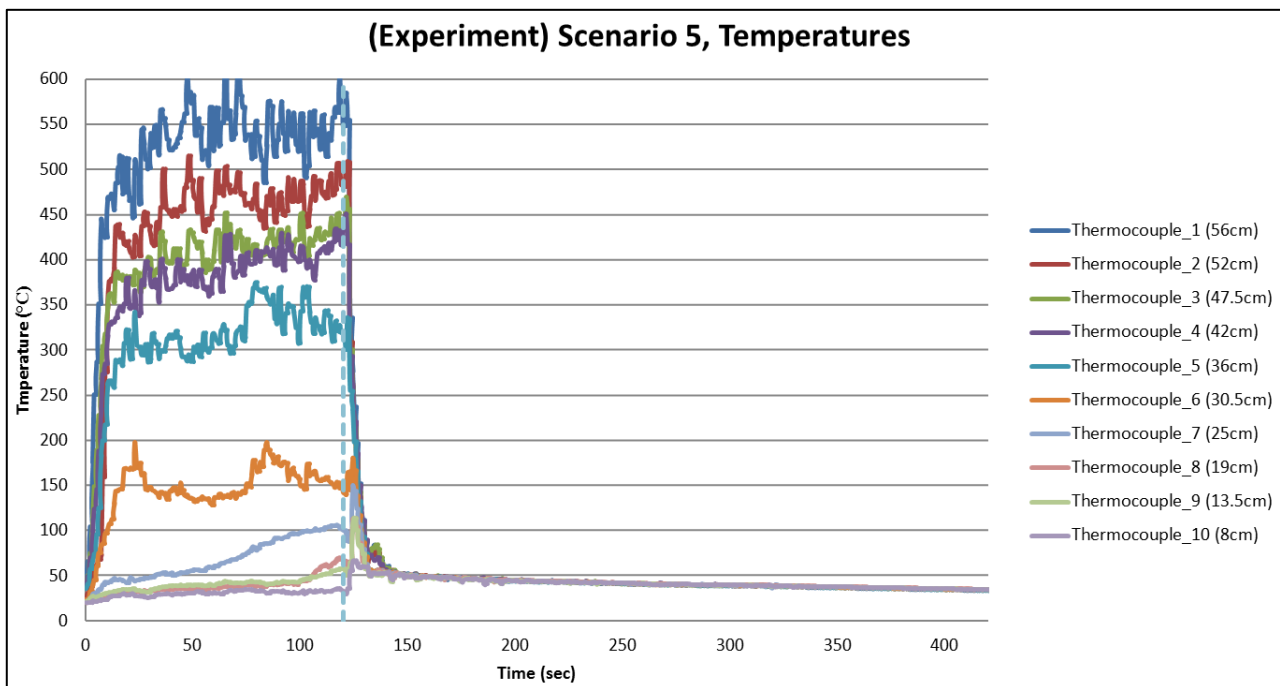


Figure 42. (Experiment) Scenario 5, Temperatures

6.3. Result Comparison

Result overviews between simulation and experimental results for each scenario will be displayed below for comparison. Error percentage values displayed in columns after the factors of interest are in reference to the experimental values.

Table 5. Scenario 1 comparison

	Total Water Collected (g)	Error	Standard Deviation (g)	Error
Simulation	421	7 %	3.52	65 %
Experiment	392		2.13	

Table 6. Scenario 2 comparison

	Ave. Steady State HRR (kW)	Error	Ave. Steady State of Temperature 1 (°C)	Error	Approx. Smoke Layer Height (mm)	Error
Simulation	10.01	8 %	237	-23 %	30	-9 %
Experiment	9.3		306		33	

Table 7. Scenarios 3-5 comparison

		Flame Extinguished	Time to Extinguishment (s)	Error
Scenario 3	Extinguishing Model	No		
	Simulation	No		
	Experiment	Yes	13	n/a
Scenario 4	Extinguishing Model	No		
	Simulation	No		
	Experiment	Yes	12	n/a
Scenario 5	Extinguishing Model	Yes	21	-13 %
	Simulation	No		
	Experiment	Yes	24	n/a

7. Discussion

General discussion

Apart from distances smaller than or close to the particle insertion distance of 150mm (Figure 6), relatively accurate velocity profiles were achieved when the best suited concept was used to simulate the water mist system. It is important to note that the best suited concept revealed here is specific to the water mist used in this project (Danfoss 1910). The practice of introducing such concepts to improve simulation accuracy of a water mist system is therefore warranted. It is however, a tedious process which requires output data as a baseline prior to performing the simulations to study the performance of concepts. Still, the possibility to do so uplifts the potential of accurately simulating water mist systems especially in open environments or large scale enclosures.

Scenario 1:

The simulation result (Figure 23) shows greater water accumulation near the back wall where the water mist spray collides with. Whereas the experimental results (Figure 33) show more water is accumulated in the middle of the room and near the enclosure opening. Liable explanations are FDS's lack of ability to simulate either the turbulence accurately or the effect of turbulence on the small water particles. From Figure 43, the former seems unlikely as majority of the turbulence within the enclosure in the slice (at mid enclosure height of 0.3m) conform to the 20% threshold.

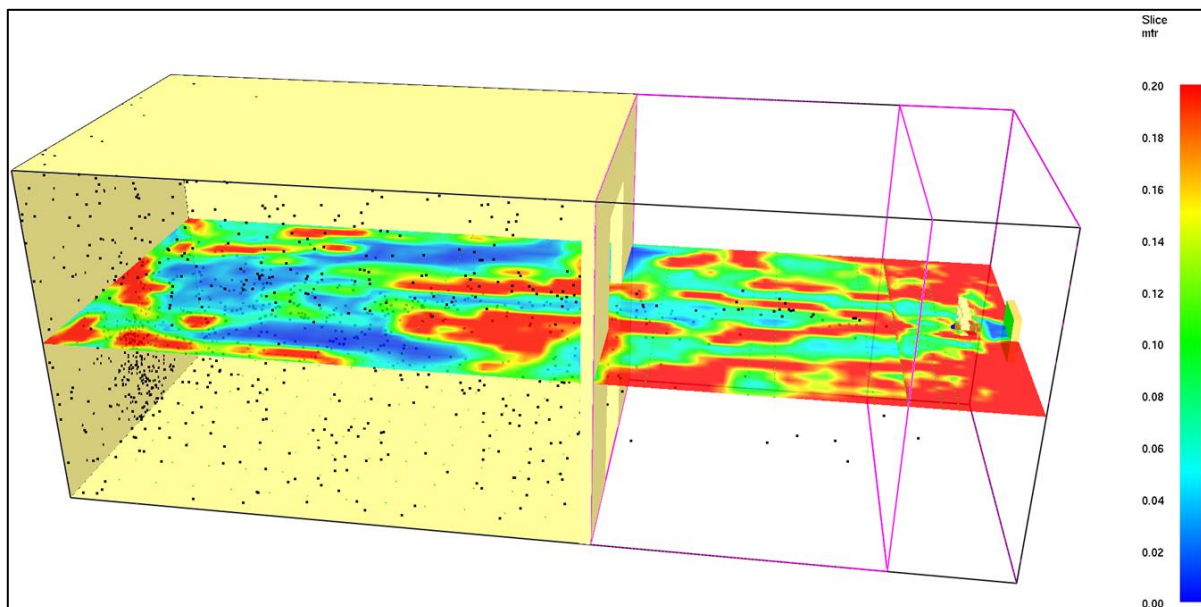


Figure 43. (Simulation) Scenario 1, Measure of turbulence resolution slice at z=0.3m

Although the 7% error for total water collected may seem acceptable, most of the water particles in the simulation are within the buffer zone by the back wall due to the tendency for FDS to reassign a downwards velocity upon particles' collision against a vertical obstruction [37]. This contributes to the discrepancy in standard deviation shown in Chapter 6.3, "Comparison" which suggests that the experiment achieved a better overall water distribution compared to the simulation. On the other hand, from observations during the experiment, some of the water particles had lost their momentum before reaching the enclosure's opening, resulting in them not entering the enclosure and being collected by the cups. Having the spray cone's radius cover the majority of the enclosure opening's area, the outward mass flow of air and water vapours could have counteracted some of the particles' momentum created from the water mist system. Lastly, even with the pre-conditioning step taken, some of the water would be absorbed by the material (PROMATECT-H) the enclosure is constructed with.

Scenario 2:

Temperature measurements from the experiment are considerably higher than the simulation's. This may be due to several potential factors such as the use of a simple pyrolysis model of specific heat release rate and the use of an insufficiently small grid size. It should be noted that after further consultation, the HRR by calculation using the hood calorimeter data likely underestimated the actual HRR. The simulation's prediction of a lower smoke layer may also cause lower predicted temperatures due to the suggested increase of entrainment.

Scenario 3-5:

In simulations, the steady state HRRs before potential extinguishment were not affected by the water mist. Using smokeview screenshots of scenario 5 to illustrate, this could be caused by additional introduction of oxygen from the air inlet into the enclosure (Figure 44) which crippled the extinguishment effect by oxygen dilution. This additional entrainment of air would have likely reduced the average water vapour concentration which was roughly $50 \frac{g}{m^3}$ (Figure 45). This was insufficient to reduce the temperature of the cells within the flame below the critical flame temperature of propane set at $1267^{\circ}C$ (value according to Beyler [36]) indicating a lack of extinguishment effect by gas phase cooling.

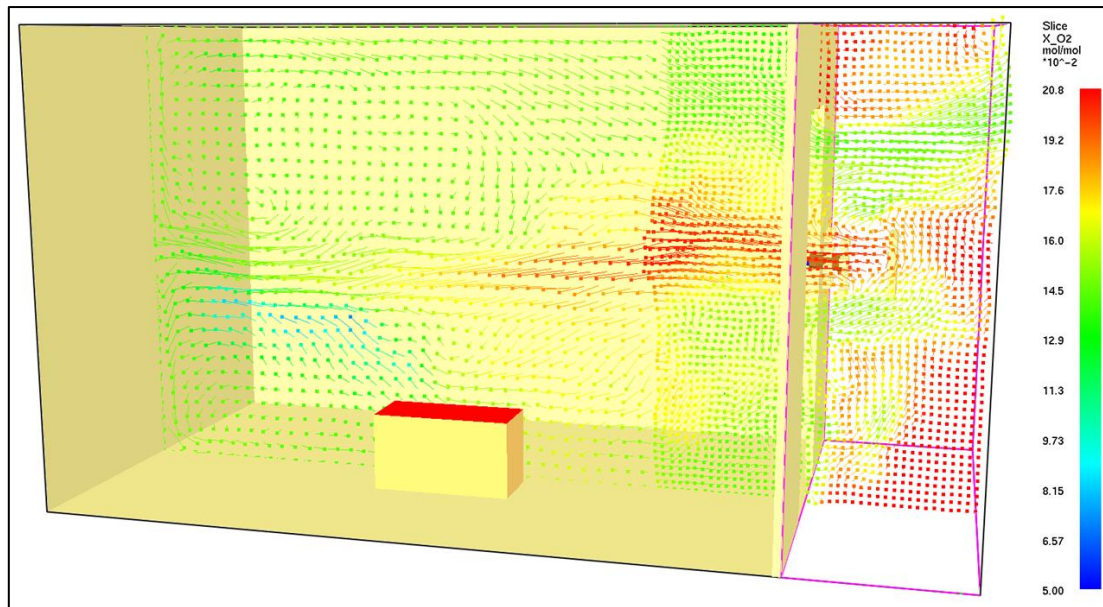


Figure 44. (Simulation) Scenario 5, Oxygen volumetric concentration slice at $x=0.3\text{m}$

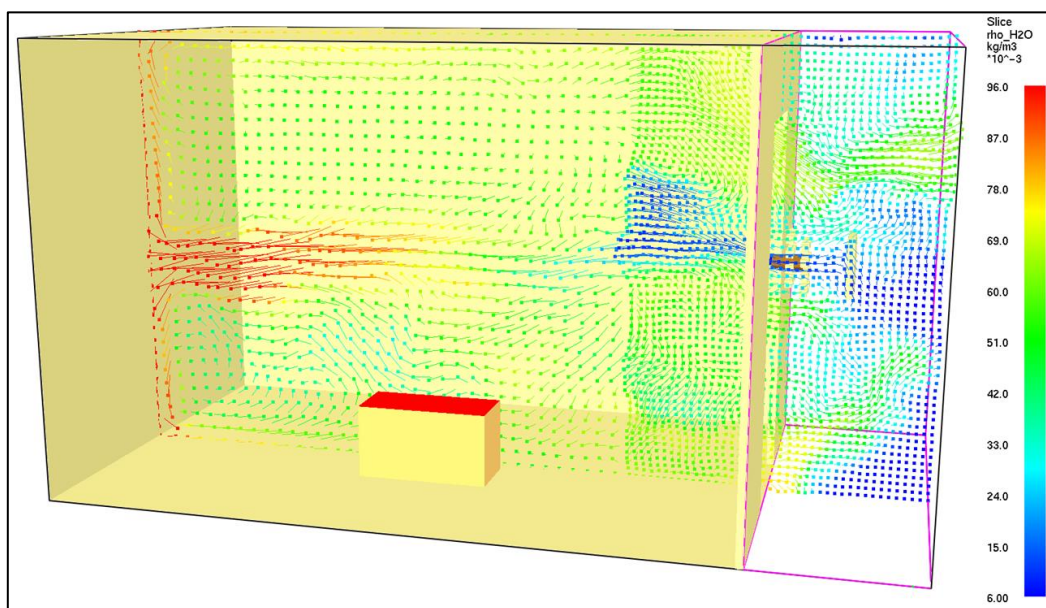


Figure 45. (Simulation) Scenario 5, Water density vector slice at $x=0.3\text{m}$

In theory, the time to extinguishment should decrease as the HRR increases. However in experiments 4 and 5, the opposite trend was observed. The position of the water mist nozzle right at the opening likely produced a significant amount of circulation (velocity) within the enclosure resulting in extinguishment by kinetic effects (flame “blown” out).

For the extinguishing model, the water mist nozzle is assumed to be within the enclosure where any additional entrainment of air outside the enclosure due to the spray is neglected. In scenarios 1 and 3, the water mist nozzle was positioned a distance away from the opening and thus do not conform to the

mentioned assumption. In scenarios 4 and 5, even though the nozzle was positioned at the opening, the additional entrainment caused by the water mist spray cannot be neglected due to the combination of the high pressure water mist system and the relatively small enclosure.

Another assumptions made in the extinguishing model include that exhaust gases are saturated with water vapour, which would not be the case with the circulation created. From visual observations of experiments 4 and 5, the flames were extinguished very quickly (3 and 7-8secs respectively) which are consistent with the theory of kinetic effect being responsible. The close-to immediate temperature drops in experiments 4 and 5 (Figure 40 and Figure 42) also suggest a high turbulence mixing. This phenomenon is also seen for experiment 3, although it took longer upon activation of the water mist. The initial temperature increase of thermocouples 7-10 upon the water mist activation also indicates this. In the simulations however, such strong circulation is not reflected. Figure 46 shows the slices for velocity along the Y axis during steady state where the black portions indicate the separation between positive (inward) and negative (outward) velocity values.

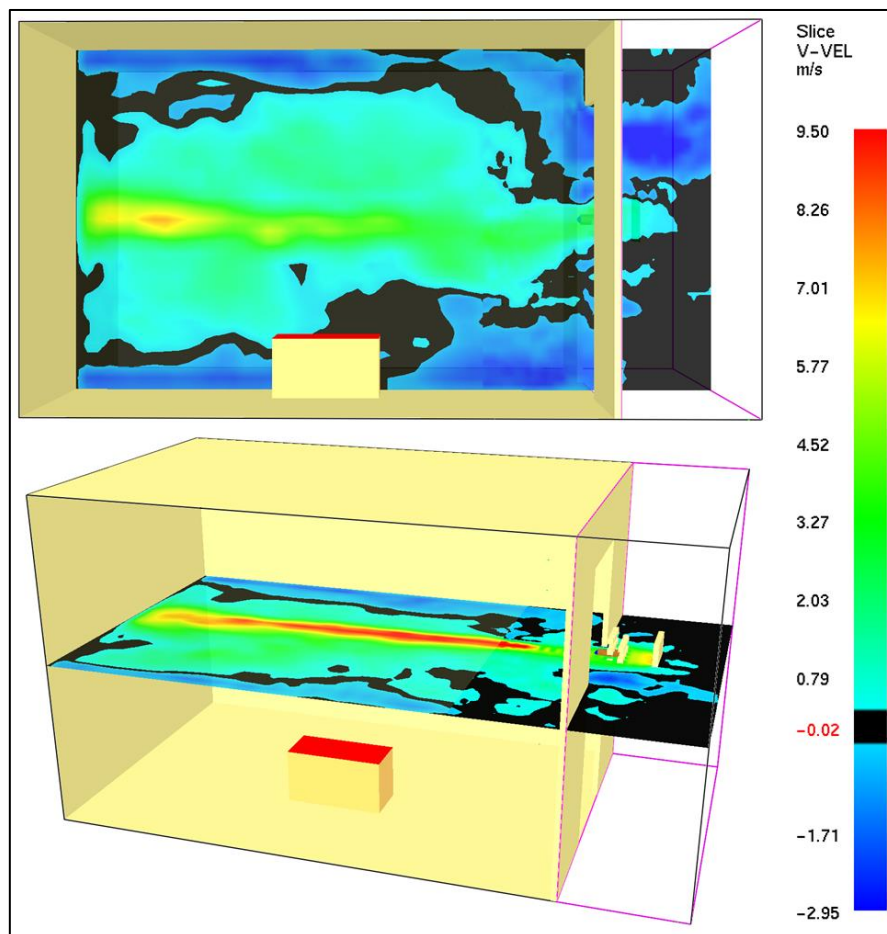


Figure 46. (Simulation) Scenario 5, V-Velocity slices at $x=0.3\text{m}$ (top) and $z=0.3\text{m}$ (bottom)

Evaporation of water particles in FDS are modelled by using predetermined thermal properties of water vapour, number of particles per second to represent water mist spray (15000 used instead of the default 5000) and temperatures the water particles are exposed to. In the simulation of scenarios 4 and 5, the steady state temperatures seem fairly high at 130°C (Figure 30) and 200°C (Figure 32) respectively. Such high temperatures would encourage evaporation of the water particles introduced by the water mist system. By observing the lack of evaporation in the simulations, it indicates that sufficient circulation was created within the enclosure to prevent a high water vapour density.

In the case of temperatures, the results of the simulations and experiments will be considered separately due to the difference in extinguishment status. Firstly in the simulations, the temperatures converged to a relative steady state temperature quickly, where the overall average temperature decreases. This steady state temperature is dependent on the fire size as it controls the rate of hot gases produced which are eventually mixed throughout the enclosure due to the turbulence present. For the experimental temperatures, they are cooled rapidly and converge at a low temperature which cools further gradually over time till it reaches ambient temperature. The likely cause for the delay in achieving steady state HRRs in experiments 4 and 5, where two minutes of free burning time was observed instead of the simulations' one minute, was the presence of water vapour suspended in the enclosure due to the preconditioning procedure done prior to commencing the experiments (refer to Chapter 3.3, "*Material (PROMATECH H) Porosity Test (Step 1)*").

8. Conclusion

General conclusion

The introduction of supply air from the air inlet provides additional oxygen replenishment to the flame which is not present in reality and should be taken into consideration unless water mist nozzle concept is entirely placed within an enclosure.

Due to the assumptions made, application of the extinguishing model developed by Back et al. [2] is limited to larger scale enclosures. An example being the assumption that mass flow rate from the plume and water mist can be neglected, should be made with caution. In scenarios of a small enclosure with large fire and water mist emissions, this assumption becomes highly inaccurate.

The use of a high pressure water mist system with a relatively small enclosure maximised the circulation created, which limited the contribution of extinguishing mechanisms such as gas phase cooling and oxygen dilution. To mitigate this, either scaled down water mist nozzles can be made or larger scale tests that are more representative of its intended uses can be performed for validation. The production of accurate scaled down representations would be very difficult to achieve which questions the liability of the former approach. Standardisation organisations should consider categorising the settings of water mists' intended uses, and conduct representative experiments for each; to eventually compile data for a base line reference. Then by consulting the differences of water mist systems' traits, a more accurate estimation can be made.

“Possible to accurately model a water mist spray in FDS?”

By successfully replicating the water mist spray's velocity profiles in an open simulation (no obstruction interaction other than at the obstruction meshes), the possibility for accurate FDS simulation of water mist systems in open environments or large scale enclosures can be confirmed. The best suited concept identified in this project however, is specifically tailored to the Danfoss 1910 water mist nozzle but the approach used to achieve this can be reused for other water mist nozzles of interest. When relatively small enclosures are involved where a large portion of the water particles collide with an obstruction(s), the accuracy of the simulation suffers due to the method FDS uses where the water particles stick to the obstruction and are reallocated a velocity vector along the obstruction plane.

“Extent of FDS correctly predicting water distribution within an enclosure?”

FDS has the potential to predict water distribution fairly well as it is able to model the spray's momentum loss. However when an enclosure is involved, its accuracy is reduced due to the spray's collision with a

vertical obstruction and its lack of ability to realistically account for effect of turbulence (circulation) on the small water particles. FDS also lacks a model to resolve the varying effects of turbulence which depends on the water particle's size as studied by Andersson [13].

“Extent of FDS accuracy on predicting temperatures in the presence of a fire within an enclosure?”

From results, the simulations tend to underestimate temperatures measured by thermocouples. A grid dependence study could have been done to investigate if a fine enough grid was being used. However, referring to chapter 4.1, *“Grid size resolution”*, the minimum of 2cm grid size used is well within the recommendation range which already required substantial computational time. However, it is important to note that the actual HRRs used in the experiments may have been higher than those calculated and displayed in Chapter 6.2, *“Experiments”* due to errors of the hood calorimeter used.

“Can FDS predict extinguishment?”

The extinguishments seen in the experiments were not replicated in the simulations which may have been caused by several factors. Firstly being the unrealistic distribution of water particles in FDS (most of them are directed to the floor upon collision with back wall) resulting in reduced enclosure water vapour densities of approximately 47 and 52 $\frac{g}{m^3}$ for scenarios 4 and 5 respectively. These values align the theory that as the HRR increases, the overall water vapour density increases which results in more effective extinguishment. They are however, far from the estimated water density required for extinguishment at 160 $\frac{g}{m^3}$ [13,41]. Secondly, when using the simple prescribed HRR simulation approach, the extinguishing kinetic effects are not sufficiently recognised.

9. Future Work(s)

There are several future works that can be considered:

- Exploration of extinguishment using complex pyrolysis model
- Validate with transient extinguishment models available [25,35]
- Use non-gaseous fuel so the effects of surface cooling / wetting can be accounted for
- Scenarios with bigger enclosure
 - reduces particles' velocities and circulation
 - improves ability to better position the fire source to mitigate the effect of additional oxygen from entrainment into the enclosure
 - further reduces enclosure's overall oxygen concentration
- Compilation of validation data for representative range of
 - enclosure dimensions
 - water mist set groups
- Study effects of turbulence depending on particle size and water concentration
- Work on new concepts for water mist simulation without introducing additional air (oxygen) into compartment
- Validate entrainment effects of water mist systems

10. References

1. Sung C.K., Hong S.R., (2003). *The Effect of Water Mist on Burning Rates of Pool Fire*, **Journal of Fire Sciences**
2. Back G.G., Beyler C.L., Hansen R., (2000). *A Quasi-Steady State Model for Predicting fire Suppression in Spaces Protected by Water Mist Systems*, **Fire Safety Journal**
3. De-Ming Zhu, Dong Liang, Jian-Yong Liu, (2014). *Numerical Simulation of Ultra-Fine Water Mist Extinguishing Mechanism*, **Procedia Engineering**
4. Songyang Li, Ragini Achayra, Meredith Colket, Vaidya Sankaran, Poncia Guido, Leena Torpo, (2013). *Modelling Water-Mist Based Suppression of 34GJ Car-Deck Fires using FDS*, **Suppression, Detection and Signaling Research and Applications Symposium (SUPDET 2013)**
5. A. Jenft, P.Boulet, A.Collin, G.Pianet, A.Breton, A.Muller, (2013). *Can We Predict Fire Extinction by Water Mist with FDS?*, **21^{ème} Congrès Français de Mécanique**
6. Jack R. Mawhinney, Gerard G. Back, (2002). *Water Mist Fire Suppression Systems*, **SFPE Handbook of Fire Protection Engineering, 4:311-337**
7. Magnus Arvidsson, (2013). *A Novel Method to Evaluate Fire Test Performance of Water Mist Spray Total Compartment Protection*, **Journal of Fire Protection Engineering**
8. Mawhinney J.R., Dlugogorski B.Z., Kim A.K., (1994). *A Closer Look at the Fire Extinguishing Properties of Water Mist*, **Fire Safety Science – Fourth International Symposium**
9. Holmstedt G., (1993), *Extinction Mechanisms of Water Mist*, **International Conference on Water Mist Fire Suppression Systems, Sweden.**
10. Andersson P., Arvidson M., Holmstedt G., (1996). *Small Scale Experiments and Theoretical Aspects of Flame Extinguishments with Water Mist*, **Department of Fire Safety Engineering, Lund University**
11. Leonard J.T., Back G.G., Di Nenno P.J., (1994). *Small/ Intermediate Scale Studies of Water Mist Fire Suppression Systems*, **Naval Research Laboratory, Washington DC**
12. Back G.G., (1994). *Water Mist: Limits of the Current Technology for use in Total Flooding Applications*, **Society of Fire Protection Engineers, NFPA annual meeting 1994**
13. Andersson P., Holmstedt G., (1999). *Limitations of Water Mists as a Total Flooding Agent*, **J Fire Protection Engineering**
14. Wighus R., (1995). *Engineering relations for Water Mist Fire Suppression System*, **Halon Alternatives Technical Working Conference, Albuquerque**
15. Prasad K., Li C., Kailasanath K., Ndubizu C., Ananth R., Tatem P., (1998). *Numerical Modeling of Fire Suppression using Water Mist*, **Naval Research Laboratory, Washington DC**
16. Back G.G., Di Nenno P.J., Hill S.A., Leonard J.T., (1996). *Full-Scale Testing of Water Mist Fire Extinguishing Systems for Machinery Spaces on US army Warcraft*, **US Coast Guard**
17. Back G.G., Di Nenno P.J., Leonard J.T., Darwin R.L., (1996). *Full-Scale Tests of Water Mist Fire Suppression Systems for Navy Shipboard Machinery Spaces: Phase 1 – Unobstructed Spaces*, **Naval Research Laboratory**
18. Back G.G., Di Nenno P.J., Leonard J.T., Darwin R.L., (1996). *Full-Scale Tests of Water Mist Fire Suppression Systems for Navy Shipboard Machinery Spaces: Phase 2 – Obstructed Spaces*, **Naval Research Laboratory**
19. Bill Jr R.G., Hansen R.L., Richards K., (1997). *Fine Spray (Water Mist) Protection of Shipboard Engine Rooms*. **Fire Safety J**
20. Bill Jr R.G., Ural E.A., (1999). *Water Mist Protection of Combustion Turbine Enclosures*, **Fire Safety Science**

21. Wighus R., (1995). *Engineering Relations of Water Mist Fire Suppression System*, **Halon Alternatives Technical Working Conference**
22. Back G.G., Beyler C.L., De Nanno P.J., Hansen R., Zalosh R., (1998). *Full-Scale Testing of Water Mist Fire Suppression Systems in Machinery Spaces*, **US Coast Guard**
23. Back G.G., Lattimer B.Y., Beyler C.L., Di Nanno P.J., Hansen R., (1999). *Full-Scale Testing of Water Mist Fire Suppression Systems for Small Machinery Spaces and Spaces with Combustible Boundaries*, **US Coast Guard**
24. Zegers E.J.P., Williams B.A., Sheinson R.S., Fleming J.W., (2000). *Water Mist Suppression of Methane / Air and Propane / Air Counterflow Flames*, **Halon Options Technical Working Conference, Albuquerque**
25. Forssell E.W., Back G.G., Beyler C.L., (1999). *A Transient Model for Predicting Fire Suppression in Spaces Protected by Water Mist Systems*, **Hughes Associates**
26. Back G.G., Beyler C.L., Di Nanno P.J., Hansen R., (1999). *Full-Scale Water Mist Design Parameters Testing*, **US Coast Guard**
27. Kung H.C., Hill J.P., (1975). *Extinction of Wood Crib and Pallet Fires*, **Combust Flame**
28. Tamanini F., (1976). *Application of Water Sprays to the Extinguishment of Crib Fires*, **Combust Sci Technol**
29. Magee R.S., Reitz R.D., (1974). *Extinguishment of Radiation Augmented Plastic Fires by Water Spray*, **15th International Symposium on Combustion**
30. Kim M.B., Jang Y.J., Yoon M.O., (1997). *Extinction Limit of a Pool Fire with a Water Mist*, **Fire Safety J**
31. Nedelka D., Bauer B., (1991). *Fire Protection: Water Curtains*, **Fire Safety Journal**
32. Dembele S., Wen J.X., Sacadura J.F., (2001). *Experimental Study of Water Sprays for the Attenuation of Fire Thermal Radiation*, **Journal of Heat Transfer**
33. Liu Z., Kim A., Su J.Z., (1997). *Improvement of Efficiency of Water Mist in Fire Suppression by Cycling Discharges*, **National Institute of Standards and Technology (NIST)**
34. Hua J., Kumar K., Khoo B.C., Xue H., (2002). *A Numerical Study of the Interaction of Water Spray with a Fire Plume*, **Fire Safety Journal**
35. Vaari J., (2000). *A Transient One-Zone Computer Model for Total Flooding Water Mist Fire Suppression in Ventilated Enclosures*, **VTT**
36. Beyler C.L., (2002). *Flammability Limits of Premixed and Diffusion Flames*, **SFPE Handbook of Fire Protection Engineering, 2:172-187**
37. McGrattan K., Hostikka S., McDermott R., Floyd J., Weinschenk C., Overholt K., (2014). *Fire Dynamics Simulator User's Guide (Sixth Edition)*, **National Institute of Standards and Technology (NIST)**
38. Husted B.P., (2007). *Experimental Measurements of Water Mist Systems and Implications for Modelling in CFD*, **Department of Fire Safety Engineering, Lund University**
39. Husted B.P., Petersson P., Lund I., Holmstedt G., (2009). *Comparison of PIV and PDA droplet Velocity Measurement Techniques on Two High Pressure Water Mist Nozzles*, **Fire Safety Journal**
40. Kolstad E.A., (2014). *Effect of Water Mist Suppression System in Engine Room: Case Study of Fire in the Cruise Liner MS Nordlys*, **Department of Physics and Technology, University of Bergen**
41. Dlugogorski B.Z., et al., (1997). *Water Vapour as an Inerting Agent*, **Halon Options Technical Working Conference, Albuquerque**
42. http://www.branz.co.nz/cms_show_download.php?id=6502dc9e0bcd36a863218fc6039fef7e1a2b13f8
43. <http://www.nu-techresources.com/datasheet/PROMATECTH-eng.pdf>
44. http://www.engineeringtoolbox.com/propane-d_1423.html

45. http://www.engineeringtoolbox.com/gas-density-d_158.html
46. http://www.cfd-online.com/Wiki/Turbulence_intensity

ANNEX

A. Porosity Test Procedure

A.1. Porosity Test 1

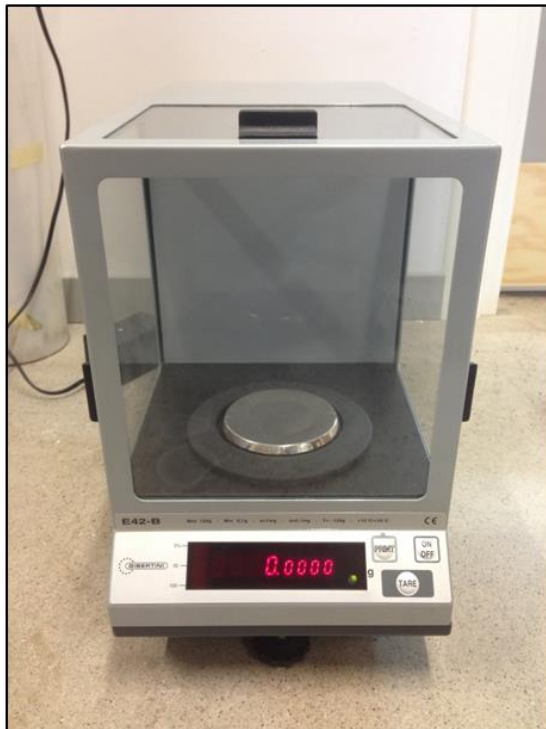
Introduction

This serves as an explicit guide for the experiment to be carried out prior to the main experiments described in “Experiment Procedure II”. This experiment investigates the porosity of the material, PROMATECT-H (used to construct the enclosure used in experiments described in “Experiment Procedure II”) and evaluates the suitability of its use in conjunction with a water mist system.

Equipment

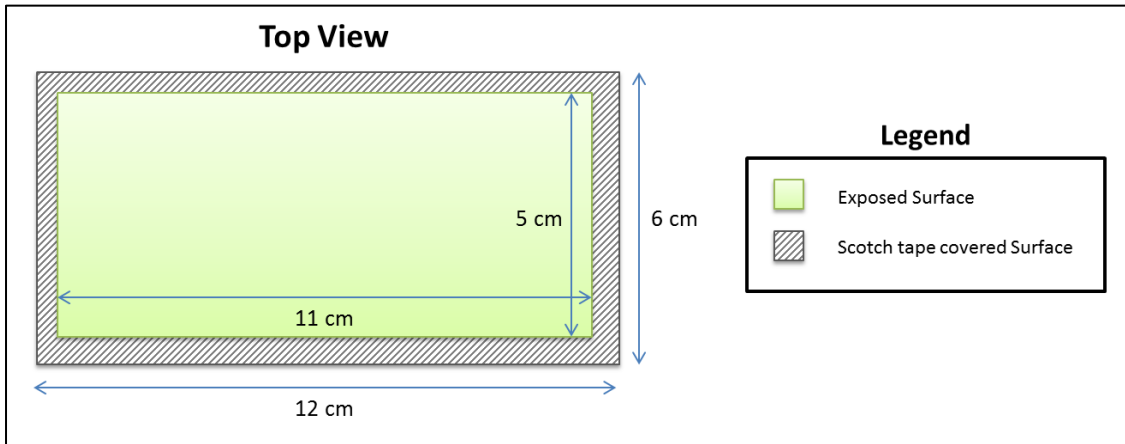
A list of equipment required for the experiments is given below.

- Tray (Container with flat interior base)
- Weight measuring equipment (GIBERTINI – Analytical balances)
- Stopwatch



Experiment

Specimen preparation:

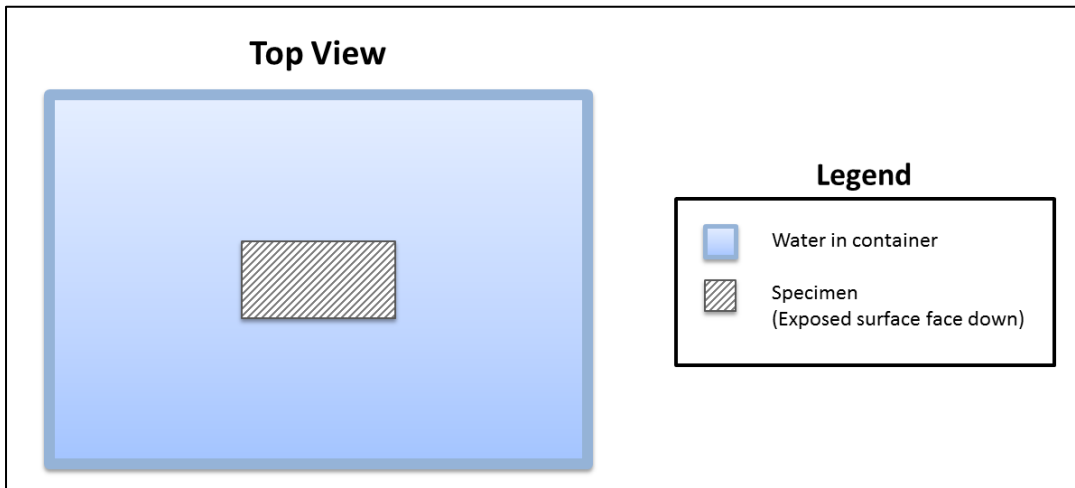


Ten specimens are cut from a sample of PROMATECT-H material, each with the (larger) dimensions shown in the figure above. From the sample material, each side has a different texture. On the side of the smooth surface, apply scotch tape around the edges of the specimens creating the borders also shown in the same figure above. The scotch tape was wrapped about the specimen(s), covering the entire thickness of the specimen(s) on all sides.

Assumptions:

Some assumptions were made to defend the integrity of data acquired from this experiment, and they are as follow:

- Scotch Tape is fully waterproof
- Perfect adhesion between scotch tape and material surface (No seepage of water onto areas covered by scotch tape)
- Human error in producing specimens are negligible
- Horizontal specimen orientation representative wall/floor/ceiling orientation in experiment.

Experiment Set-up:

Water is added into the container (tray) to produce a thin film of water not exceeding the thickness of the specimen (1.1cm). The specimen(s) is placed in the water with the exposed surface facing downwards for the pre-determined time(s).

Specimen Test Duration(s):

Specimen	A	B	C	D	E	F	G	H	I	J
Exposure Time (min)	0.5	1	1.5	2	2.5	3	3.5	4	4.5	5

Procedure Sequence:

1. Prepare experiment setup
2. Ensure weighing equipment is on a stable and flat surface
3. Place specimen (dry) on weighing equipment and 'zero' measurement once reading stabilises
4. Place specimen (exposed surface downwards) onto water in container, Start timing
5. Once respective time elapsed (According to "Specimen Test Duration(s)"), remove specimen and remove excess water
6. Place specimen (wet) with exposed surface facing upwards on weighing equipment
7. Wait one minute before recording difference in weight (water absorbed in time exposed)
8. Repeat steps (a – e) for next specimen

A.2. Porosity Test 2

Introduction

This document serves as an explicit guide for the experiment to be carried out prior to the main experiments described in “Experiment Procedure II”. This experiment investigates the porosity of the material, PROMATECT-H (used to construct the enclosure used in experiments described in “Experiment Procedure II”) and evaluates the suitability of its use in conjunction with a water mist system.

Equipment

A list of equipment required for the experiments is given below.

- Danfoss 1910 hollow cone water mist system
- ‘L’ bracket
- Weight measuring equipment (Mettler PE 6000)
- Stopwatch



Experiment

Specimen preparation:

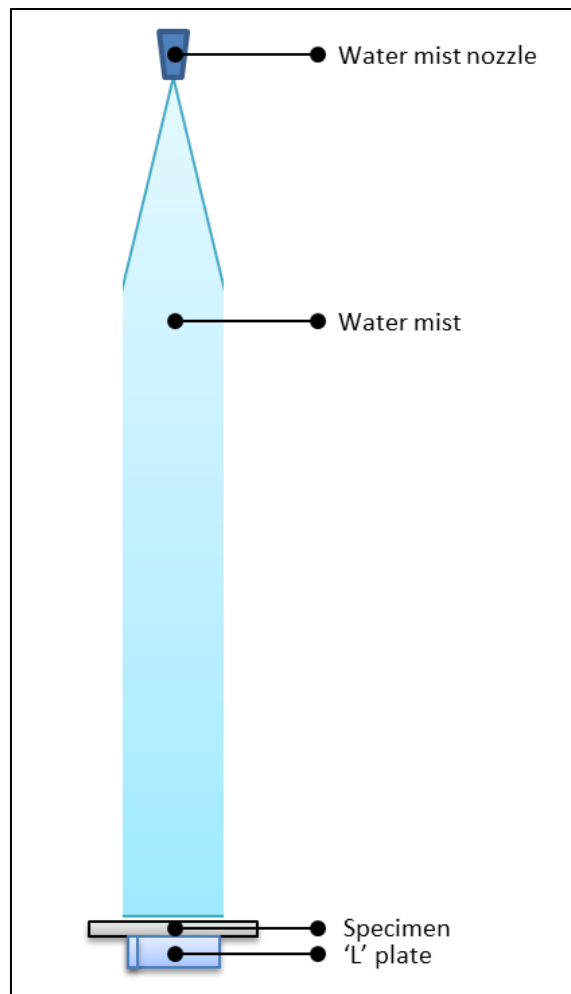
Two specimens are cut from a sample of PROMATECT-H material, each with dimensions of 12.5 x 12.5cm.

Assumptions:

Some assumptions were made to defend the integrity of data acquired from this experiment, and they are as follow:

- The specimen area represents area on experiment enclosure's back wall where majority of water would come into contact with
- Specimens' exposed sides (thickness) only absorbs amount of water
- Human error in producing specimens and experiment alignment are negligible
- Horizontal specimen orientation representative wall/floor/ceiling orientation in experiment.

Experiment Set-up:



Specimen is positioned on top of 'L' plate and aligned to the water mist's center axis.

Test Variations:

Exposure Time (min)	0.5	1	1.5	2	2.5	3	3.5	4	4.5	5	6	7	8
----------------------------	-----	---	-----	---	-----	---	-----	---	-----	---	---	---	---

The test is to be performed twice at distances **1.5m** (to represent Experiments 1 and 3) and **0.9m** (to represent Experiments 4 and 5).

Procedure Sequence:

1. Prepare experiment setup
2. Ensure weighing equipment is on a stable and flat surface
3. Place specimen (dry) on weighing equipment and record initial weight
4. Adjust water mist height off the ground to distance of interest (account for thickness of 'L' plate and specimen)
5. Start water mist system
6. Place 'L' plate on ground and align to water mist's axis
7. Place specimen smooth side up on 'L' plate and align to water mist's axis, Start timing
8. Once respective time elapsed (According to "Specimen Test Duration(s)"), remove specimen and remove excess water
9. Place specimen (wet) on weighing equipment and record weight
10. Place specimen back on 'L' plate and align to water mist's axis, Continue timing
11. Repeat steps (h – j) till all exposure time of interest is completed
12. Repeat steps (c-k) for second specimen

B. Danfoss 1910 Hollow Cone Technical Specifications

Extracted from "Danfoss technical data sheet, Water Mist Nozzles"

http://www.danfoss.com/NR/rdonlyres/CB7DD9DF-9AD2-476F-A2C3-5E5B6ABECA96/0/521B0563_DKCFNPD091A702_WaterMistNozzles_GB.pdf

Generic data on water mist nozzles specified on technical data sheet:

- Applications** The nozzles are tailored to atomize water in high pressure water mist systems. The nozzles are very suitable for applications within e.g.:
- Humidification
 - Lumber drying
 - Fire fighting
- The stainless steel design allows operating the nozzle with ordinary tap water.
- For even and far-reaching atomization of the water, relatively many nozzles with smaller capacity are superior to few nozzles with large capacity.
- Benefits**
- Suitable for ordinary tap water
 - Long service life
 - Excellent spray pattern
- Filtration** The stainless steel nozzles have a built-in strainer.
- It is a general rule that the better the filtration of the water, the higher the expected service life of the nozzles, and the less risk of clogging.
- Drop size by various pressure**
- The drop size is depending on the pressure. The distribution of droplets shown below is based on average measurements from different nozzle inserts:

100 bar / 1450 psi:

Drop size diameter	Distribution of droplets
0 - 25 micron meter	13%
25 - 50 micron meter	85%
50 - 80 micron meter	2%

80 bar / 1160 psi:

Drop size diameter	Distribution of droplets
0 - 25 micron meter	5%
25 - 50 micron meter	80%
50 - 80 micron meter	15%

Nozzle and adaptor connection

To avoid corrosion, high pressure stainless steel pipes and fittings must be used.

Recommended high pressure pipe:

Seamless stainless steel pipe according to standard ASTM 269 TP 316L / DIN2391 – C.
 12 × 1.5 mm
 Working pressure: 381 bar / 5525 psi
 Burst pressure: 1514 bar / 21950 psi

Recommended fittings:

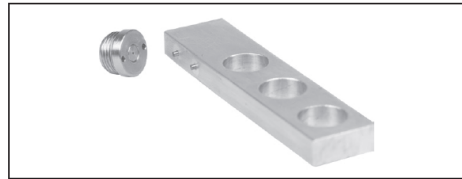
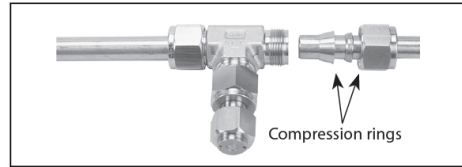
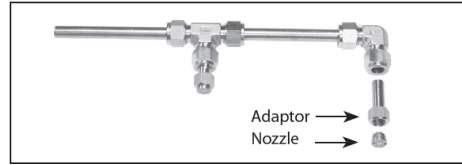
Stainless steel twin ferrule compression ring fittings.

Recommended Tight gel:

Tight gel must be used between the nozzle and the adaptor.
 Danfoss recommends Loctite 542 hydraulic thread tight gel.

To prevent particles from entering into the system and clogging the nozzles the following procedure must be followed:

- Deburr and clean pipes and fittings prior to the installation.
- Flush the system with water after assembling and before the nozzles are mounted.

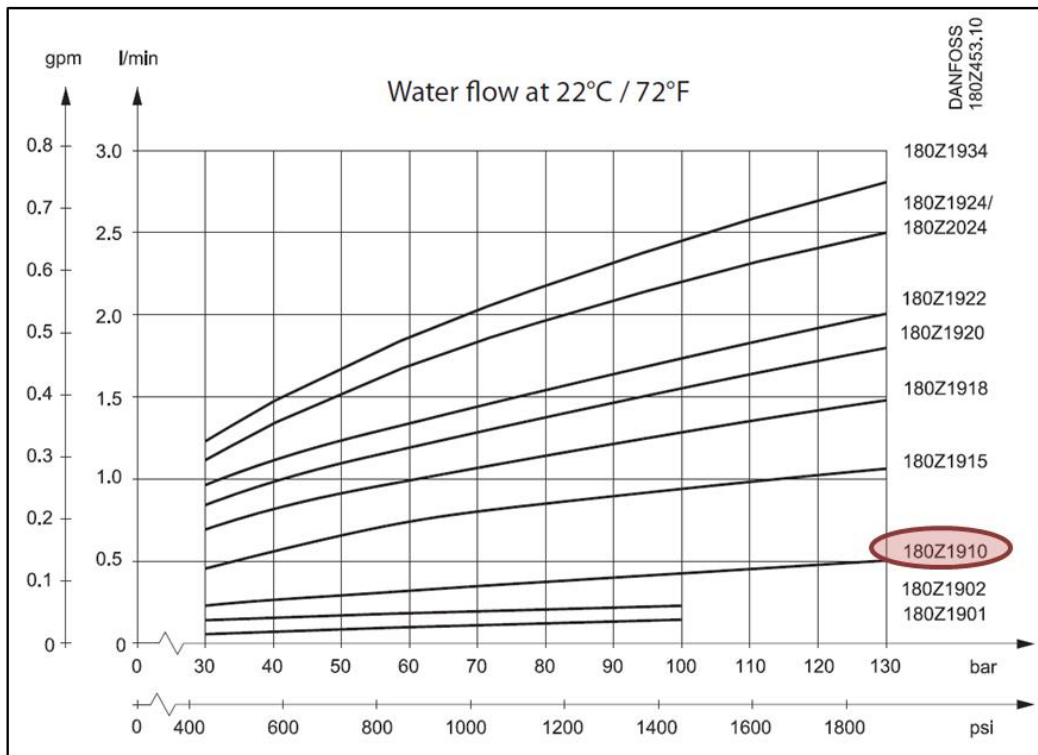


Tool

For easy mounting and dismounting of the stainless steel nozzles, Danfoss offers a handy tool: Code number 180Z0021.

Specific data on the Danfoss 1910 water mist nozzle:

Litre per hour	Litre per min.	US Gallon per hour	US Gallon per min.	Operating pressure / Max. pressure bar (psi)	Nozzle / house Material	Nozzle thread	Code number
25.2	0.42	6.6	0.1	100 / 130 (1450 / 1900)	AISI316 / 430	M13 × 1 mm	180Z1910



C. Water Mist Flow Rate Test

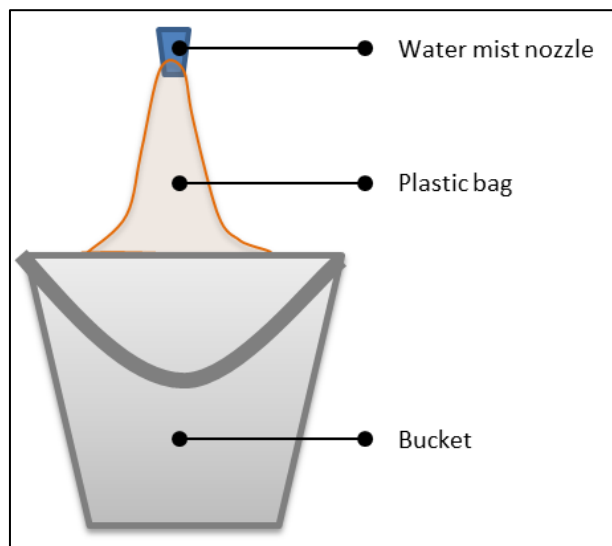
A test was done to quantify the actual mass flow rate of water of the Danfoss 1910 water mist nozzle used.

Equipment

- Danfoss 1910 Water mist system
- Plastic bag
- Bucket
- Weighing scale

Test Setup

A hole to fit the water mist nozzle was made at the base of the plastic bag and the test setup is as shown in the figure below.



Procedure Sequence

1. Weigh and record the combined weight of bucket and plastic bag (dry)
2. Prepare test setup
3. Run water mist system for 5 minutes
4. Weight and record the combined weight of bucket and plastic bag (wet)
5. Calculate the weight difference

Results

There was a weight difference of 2.09kg which translate to $\frac{2.09}{5} = 0.418 \frac{l}{min}$.

D. Sample FDS Script File (Scenario 5)

&HEAD CHID= 'EXP5_Extinguish_25kw', TITLE= 'EXP5_Extinguish_25kw'/

computational domain

&MESH IJK= 30,45,30, XB= 0,0.6, 0.2,1.1, 0,0.6 /

&MESH IJK= 60,20,60, XB= 0,0.6, 0,0.2, 0,0.6 /

end time

&TIME T_END=360 /

if not specified, surfaces aka obstacles have constant temperature

&MISC SURF_DEFAULT = 'INERT'
ALLOW_UNDERSIDE_PARTICLES = .TRUE. /

define wall material

&SURF ID = 'wall'
MATL_ID = 'PROMATECT-H'
COLOR = 'KHAKI'
THICKNESS = 0.01 /

define ceiling material

&SURF ID = 'ceiling'
MATL_ID = 'PROMATECT-H'
COLOR = 'KHAKI'
THICKNESS = 0.02 /

define material (info from <http://www.nu-techresources.com/datasheet/PROMATECTH-eng.pdf>)

&MATL ID = 'PROMATECT-H'
EMISSIVITY = 0.5
DENSITY = 870.
CONDUCTIVITY = 0.242
SPECIFIC_HEAT = 1.09 /

creating floor, ceiling and walls respectively

&OBST XB=0,0.6, 0.2,1.1, 0,0, SURF_ID='wall'/
&OBST XB=0,0.6, 0.2,1.1, 0.6,0.6, SURF_ID='ceiling'/
&OBST XB=0,0, 0.2,1.1, 0,0.6, SURF_ID='wall'/
&OBST XB=0.6,0.6, 0.2,1.1, 0,0.6, SURF_ID='wall'/
&OBST XB=0,0.6, 0.2,0.2, 0,0.6, SURF_ID='wall'/
&OBST XB=0,0.6, 1.1,1.1, 0,0.6, SURF_ID='wall'/

creating hole

&HOLE XB=0.2,0.4, 0.19,0.3, 0,0.5 /

creating vents

&VENT MB='XMIN', SURF_ID='OPEN' /
&VENT MB='XMAX', SURF_ID='OPEN' /
&VENT MB='YMIN', SURF_ID='OPEN' /
&VENT MB='YMAX', SURF_ID='OPEN' /
&VENT MB='ZMIN', SURF_ID='OPEN' /
&VENT MB='ZMAX', SURF_ID='OPEN' /

define fuel, heat of combustion in KJ/kg, soot yield is fraction of fuel converted into soot (info from http://www.branz.co.nz/cms_show_download.php?id=6502dc9e0bcd36a863218fc6039fef7e1a2b13f8)

&REAC ID = 'PROPANE'
SOOT_YIELD = 0.01
C = 3.
H = 8.
HEAT_OF_COMBUSTION = 46450
IDEAL = .TRUE.
CRITICAL_FLAME_TEMPERATURE = 1267 /

(configured to achieve 17kW)

define burner surface

&SURF ID = 'BURNER'
COLOR = 'RED'
HRRPUA = 1736 /

define burner coordinate and geometry (square pan of 10cm dimensions)

```
&OBST XB=0.20,0.28, 0.56,0.74, 0,0.1, SURF_IDS='BURNER','INERT','INERT' /
```

to call for water vapor (liquid) properties

```
&SPEC ID = 'SPRINKLER WATER VAPOR'
SPEC_ID = 'WATER VAPOR' /
```

define particle properties (assuming initial temperature is ambient and 'rosin rammler lognormal' distribution)

```
&PART ID = 'waterdroplets'
SPEC_ID = 'SPRINKLER WATER VAPOR'
DIAMETER = 46.03
GAMMA_D = 3.96
CHECK_DISTRIBUTION = .TRUE. /
```

define nozzle properties (offset, k_factor, operating_pressure and droplet_velocity from bjarne reference)

```
&PROP ID = 'waternozzle'
PART_ID = 'waterdroplets'
OFFSET = 0.1
K_FACTOR = 0.0418
OPERATING_PRESSURE = 100
PARTICLE_VELOCITY = 39
SPRAY_ANGLE = 0,12
PARTICLES_PER_SECOND = 15000 /
```

define device location, orientation and activation delay

```
&DEVC ID = 'only_waternozzle'
XYZ = 0.36,0.2,0.3
PROP_ID = 'waternozzle'
ORIENTATION = 0,1,0
QUANTITY = 'TIME'
SETPOINT = 60. /
```

introducing air inlet 100mm behind nozzle to increase flow velocity to match past experiments (as flowrate should already be the same)

```
&SURF ID = 'air_inlet'
VOLUME_FLOW = -0.045 /
```

positioning air inlet

```
&OBST XB=0.32,0.4, 0.09,0.1, 0.26,0.34,
&VENT XB=0.32,0.4, 0.1,0.1, 0.26,0.34,
COLOR='GREEN'
SURF_ID = 'air_inlet'
CTRL_ID = 'inlet delay' /
```

setting activation delay of air inlet

```
&CTRL ID = 'inlet delay'
FUNCTION_TYPE = 'CUSTOM'
INPUT_ID = 'TIMER'
RAMP_ID = 'inlet time ramp' /
```

```
&DEVC ID = 'TIMER'
XYZ = 0,0,0,
QUANTITY = 'TIME' /
```

```
&RAMP ID='inlet time ramp', T=0, F=-1 /
```

```
&RAMP ID='inlet time ramp', T=59, F=-1 /
```

```
&RAMP ID='inlet time ramp', T=61, F=1 /
```

creating obstruction 1st mesh layer below air inlet to promote turbulence

```
&OBST XB=0.32,0.33, 0.15,0.16, 0.26,0.27 /
&OBST XB=0.34,0.35, 0.15,0.16, 0.26,0.27 /
&OBST XB=0.36,0.37, 0.15,0.16, 0.26,0.27 /
&OBST XB=0.38,0.39, 0.15,0.16, 0.26,0.27 /
&OBST XB=0.32,0.33, 0.15,0.16, 0.28,0.29 /
&OBST XB=0.34,0.35, 0.15,0.16, 0.28,0.29 /
&OBST XB=0.36,0.37, 0.15,0.16, 0.28,0.29 /
&OBST XB=0.38,0.39, 0.15,0.16, 0.28,0.29 /
&OBST XB=0.32,0.33, 0.15,0.16, 0.30,0.31 /
&OBST XB=0.34,0.35, 0.15,0.16, 0.30,0.31 /
```

```

&OBST XB=0.36,0.37,      0.15,0.16,      0.30,0.31 /
&OBST XB=0.38,0.39,      0.15,0.16,      0.30,0.31 /
&OBST XB=0.32,0.33,      0.15,0.16,      0.32,0.33 /
&OBST XB=0.34,0.35,      0.15,0.16,      0.32,0.33 /
&OBST XB=0.36,0.37,      0.15,0.16,      0.32,0.33 /
&OBST XB=0.38,0.39,      0.15,0.16,      0.32,0.33 /
creating obstruction 2nd mesh layer below air inlet to promote turbulence
&OBST XB=0.33,0.34,      0.17,0.18,      0.27,0.28 /
&OBST XB=0.35,0.36,      0.17,0.18,      0.27,0.28 /
&OBST XB=0.37,0.38,      0.17,0.18,      0.27,0.28 /
&OBST XB=0.39,0.40,      0.17,0.18,      0.27,0.28 /
&OBST XB=0.33,0.34,      0.17,0.18,      0.29,0.30 /
&OBST XB=0.35,0.36,      0.17,0.18,      0.29,0.30 /
&OBST XB=0.37,0.38,      0.17,0.18,      0.29,0.30 /
&OBST XB=0.39,0.40,      0.17,0.18,      0.29,0.30 /
&OBST XB=0.33,0.34,      0.17,0.18,      0.31,0.32 /
&OBST XB=0.35,0.36,      0.17,0.18,      0.31,0.32 /
&OBST XB=0.37,0.38,      0.17,0.18,      0.31,0.32 /
&OBST XB=0.39,0.40,      0.17,0.18,      0.31,0.32 /
&OBST XB=0.33,0.34,      0.17,0.18,      0.33,0.34 /
&OBST XB=0.35,0.36,      0.17,0.18,      0.33,0.34 /
&OBST XB=0.37,0.38,      0.17,0.18,      0.33,0.34 /
&OBST XB=0.39,0.40,      0.17,0.18,      0.33,0.34 /
slice for generic velocity
&SLCF PBx=0.3,          VECTOR=.TRUE.,          QUANTITY='VELOCITY' /
slice for horizontal velocity
&SLCF PBx=0.36,         VECTOR=.TRUE.,          QUANTITY='V-VELOCITY' /
&SLCF PBz=0.3,          VECTOR=.TRUE.,          QUANTITY='V-VELOCITY' /
slice for turbulence resolution (aka how much of the turbulence energy is being resolved)
&SLCF PBX=0.36,         QUANTITY='TURBULENCE RESOLUTION' /
&SLCF PBz=0.3,          QUANTITY='TURBULENCE RESOLUTION' /
slice for water vapour, oxygen and propane densities respectively
&SLCF PBX=0.3,          QUANTITY='DENSITY',     SPEC_ID='WATER VAPOR' /
&SLCF PBX=0.3,          QUANTITY='DENSITY',     SPEC_ID='OXYGEN' /
&SLCF PBX=0.3,          QUANTITY='DENSITY',     SPEC_ID='PROPANE' /
slice for water vapour, oxygen and propane mass fractions respectively
&SLCF PBX=0.3,          QUANTITY='VOLUME FRACTION', SPEC_ID='WATER VAPOR' /
&SLCF PBX=0.3,          QUANTITY='VOLUME FRACTION', SPEC_ID='OXYGEN' /
&SLCF PBX=0.3,          QUANTITY='VOLUME FRACTION', SPEC_ID='PROPANE' /
slice for temperature
&SLCF PBx=0.3,          QUANTITY='TEMPERATURE' /
&SLCF PBx=0.5225,       QUANTITY='TEMPERATURE' /
devices to measure temperature (Thermocouples)
&DEVC ID='TEMP1',       XYZ=0.5225,0.3275,0.56, QUANTITY='THERMOCOUPLE' /
&DEVC ID='TEMP2',       XYZ=0.5225,0.3275,0.52, QUANTITY='THERMOCOUPLE' /
&DEVC ID='TEMP3',       XYZ=0.5225,0.3275,0.475, QUANTITY='THERMOCOUPLE' /
&DEVC ID='TEMP4',       XYZ=0.5225,0.3275,0.42,  QUANTITY='THERMOCOUPLE' /
&DEVC ID='TEMP5',       XYZ=0.5225,0.3275,0.36,  QUANTITY='THERMOCOUPLE' /
&DEVC ID='TEMP6',       XYZ=0.5225,0.3275,0.305, QUANTITY='THERMOCOUPLE' /
&DEVC ID='TEMP7',       XYZ=0.5225,0.3275,0.25,  QUANTITY='THERMOCOUPLE' /
&DEVC ID='TEMP8',       XYZ=0.5225,0.3275,0.19,  QUANTITY='THERMOCOUPLE' /
&DEVC ID='TEMP9',       XYZ=0.5225,0.3275,0.135, QUANTITY='THERMOCOUPLE' /
&DEVC ID='TEMP10',     XYZ=0.5225,0.3275,0.08,  QUANTITY='THERMOCOUPLE' /
end fds script
&TAIL /

```

E. Experimental (1-5) Procedure

Introduction

This document serves as an explicit guide for the experiments to be carried out in accordance with the thesis topic at hand, where the focus is on the effect of water concentration on a controlled fire.

There will be a total of three experiments each structured for comparison against parallel Computational Fluid Dynamic (CFD) simulations performed with Fire Dynamics Simulator (FDS). The experiments are designed for progressive validation where the components of fire and water are looked at individually initially. This promotes the ease of identifying potential discrepancies before proceeding to the final combined experiment.

Equipment

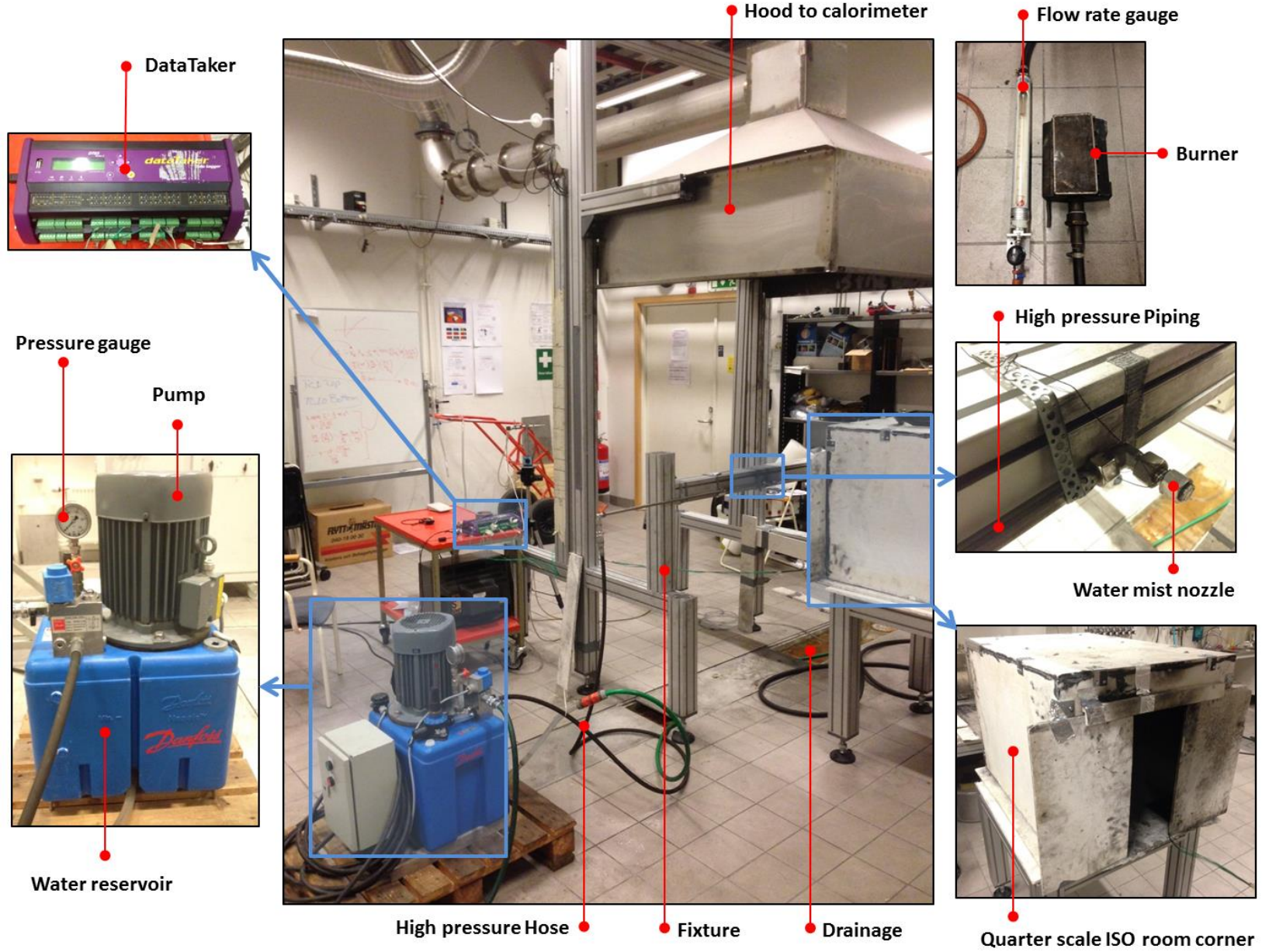
A list of equipment required for the experiments is given below.

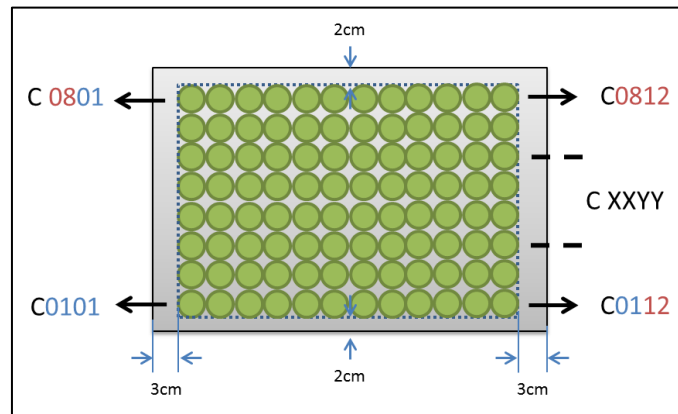
- Quarter scale ISO room corner/Enclosure
 - (Material: PROMATECT-H)
- Water mist system
 - Nozzle
 - (Danfoss hollow cone 1910: $0.42 \frac{L}{min}$, 100bar)
 - Pump
 - Piping
 - Water reservoir
- Fixture (to position water mist nozzle)
- Plastic cups (x96) of 7cm diameter
- Drainage system for water run off
- Gas distribution head (Burner) and piping

Measuring Equipment

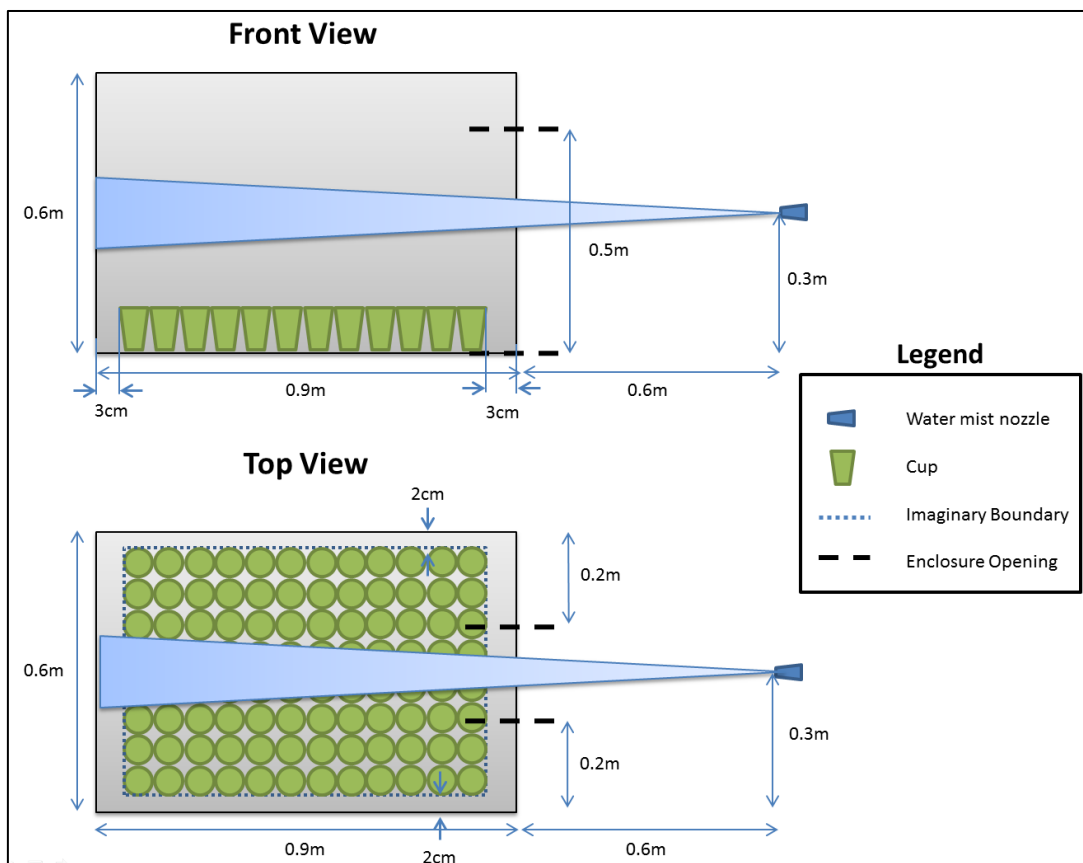
- Flow rate gauge (for propane supply)
- Pressure gauge (at water pump)
 - (to ensure pressure is 100bar)
- DataTaker (Laptop)
 - 10 Thermocouples
- Weighing scale
- Stopwatch
- Hood Calorimeter
- LSHR data acquisition (Desktop)
 - (Measures HRR)

ANNEX



Experiment 1: Water**Experiment Set-up:**

The cups are to be labelled in the following manner; “XXYY”, where “0101” is the first left most cup at the back row and “1015” is the right most cup at the front row.

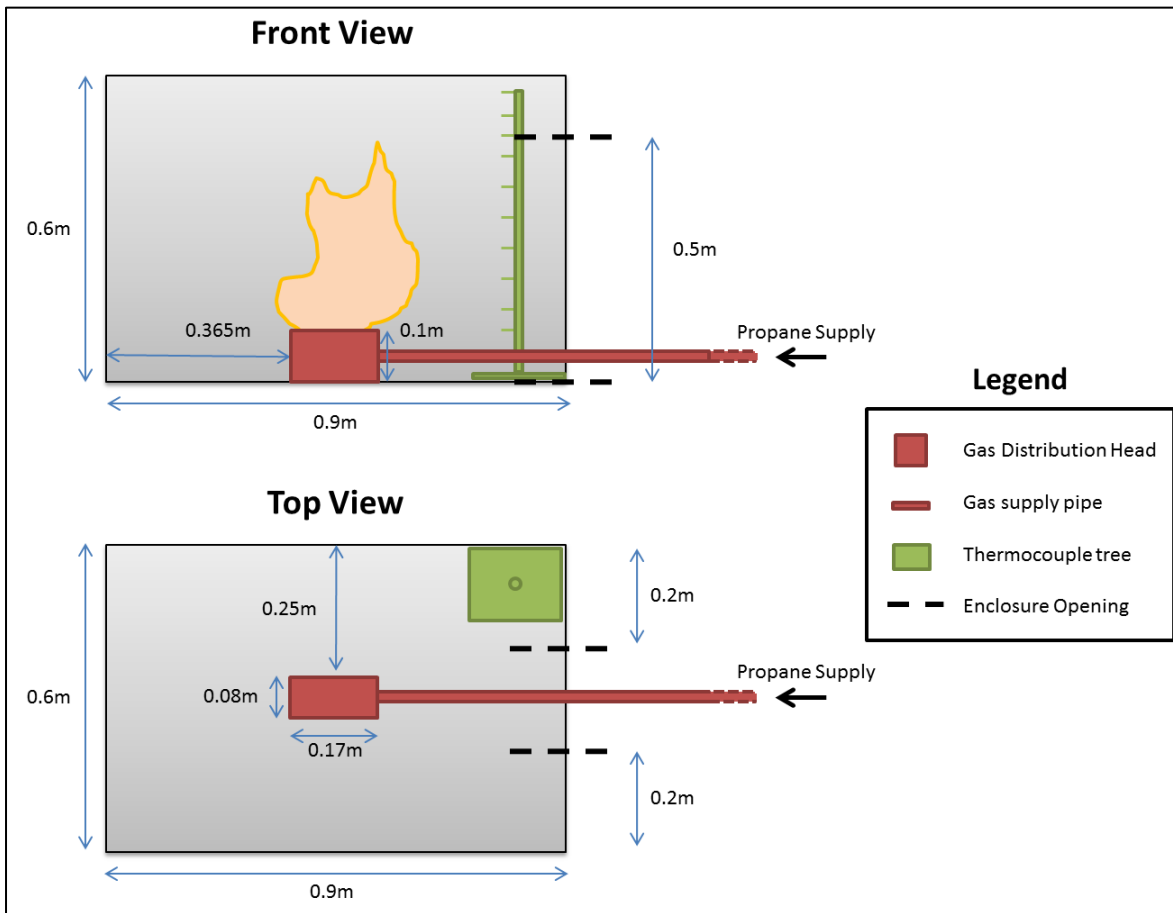


96 Plastic cups (of 6cm diameter) and the water mist nozzle are to be positioned as shown in the figure above on the floor of the enclosure and on the fixture respectively.

The experiment will be **run for 5 minutes** to ensure results are representative of steady state conditions.

Procedure Sequence:

1. Don personal protective equipment (PPE)
2. Display experiment procedure and risk assessment report at door
3. Turn on ventilation
4. Label cups
5. Weigh and record all empty cups
6. Prepare experiment setup
7. Turn on water mist system (water pump) and *Start stopwatch*
8. *(Once 5 mins elapses)* turn off water mist system (water pump)
9. Weigh and record all cups
10. Return laboratory to initial conditions
11. Turn off ventilation
12. Leave and lock up Laboratory
13. Remove experiment procedure and risk assessment from door
14. Return personal protective equipment (PPE)
15. Return Laboratory key to in-charge

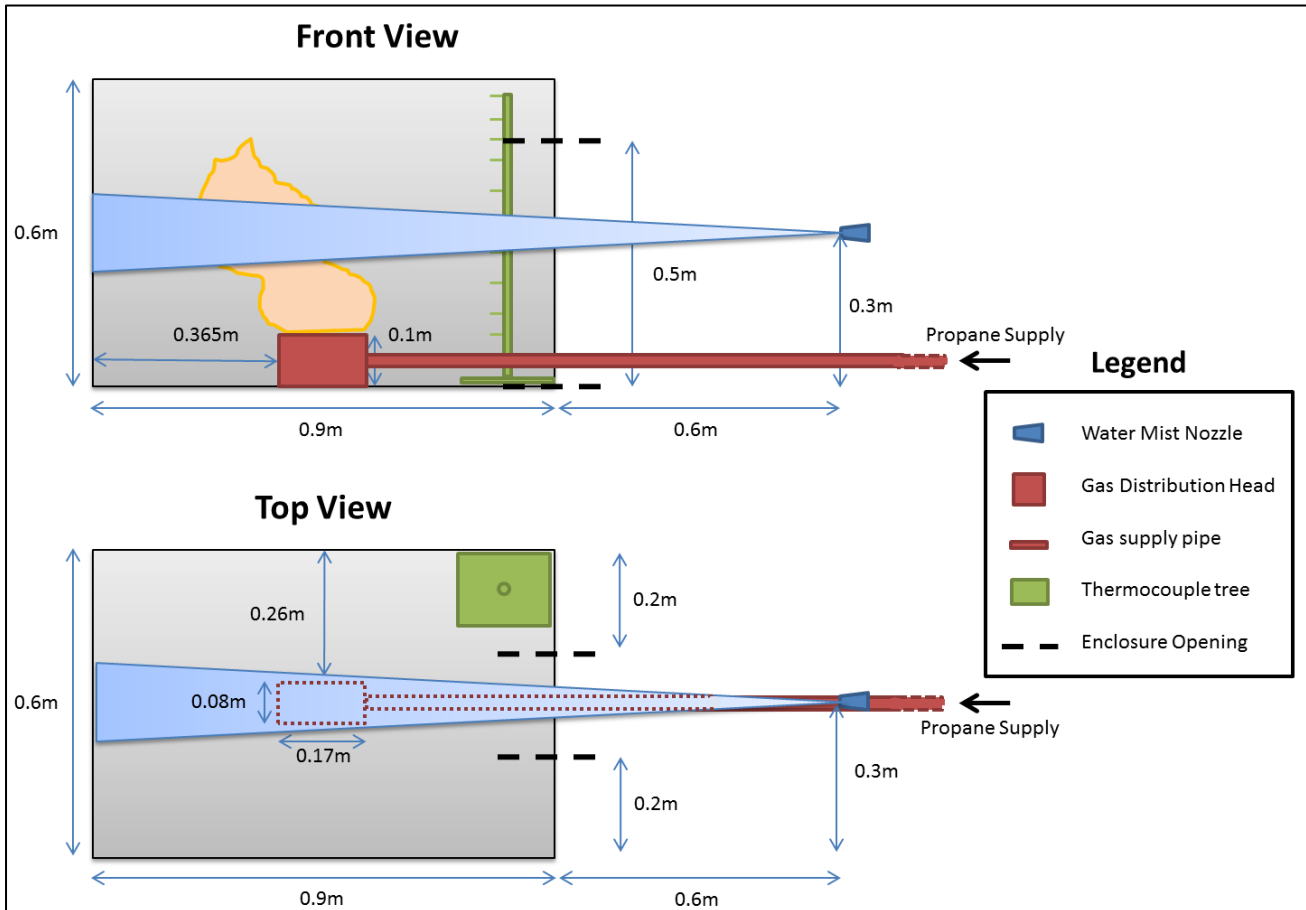
Experiment 2: Fire**Experiment Set-up:**

Gas distribution head (Dimensions: 0.18m*0.08m*0.08m) is to be positioned in the center of the enclosure as shown in the figure above. A propane flow rate to achieve 10kW is used.

The experiment will be run for 8 minutes to allow values close to steady state to be reached.

Procedure Sequence:

- Don personal protective equipment (PPE)
- Display experiment procedure and risk assessment report at door
- Turn on ventilation
- Prepare experiment setup
- Setup (link Thermocouples) on DataTaker (laptop and software)
- Calibrate the Gas analyser (Calorimeter)
- Record ambient air's composition (O₂, CO₂, CO)
- Setup LSHR (Desktop) data acquisition
- Perform prior test to attain correct fuel flow rate for 10kW to be achieved
- Start HRR measurements (Desktop) and start DataTaker measurements (Laptop) *Start Stopwatch*
- Turn on propane gas supply
- Ignite gas burner
- Record Ignition time on DataTaker
- *(Once 8 mins elapses) Turn off gas supply.*
- Stop HRR measurements (Desktop) and stop DataTaker measurements (Laptop)
- Record Ignition time on LSHR
- Export data as ".RAW" extension and retrieve data (Thumbdrive)
- Retrieve DataTaker data (Thumbdrive)
- Return laboratory to initial conditions
- Turn off ventilation
- Leave and lock up Laboratory
- Remove experiment procedure and risk assessment from door
- Return personal protective equipment (PPE)

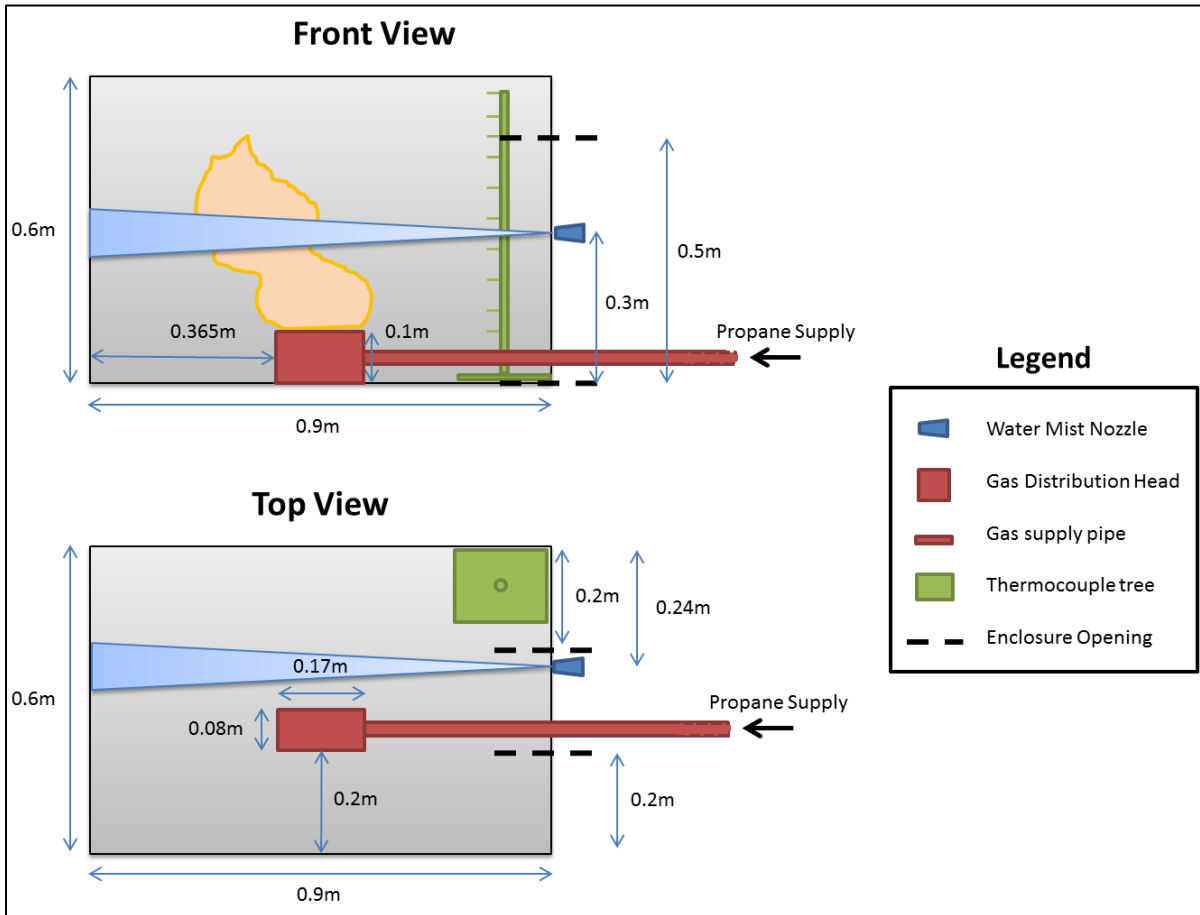
Experiment 3: Combination**Experiment Set-up:**

Gas distribution head (Dimensions: 0.18m*0.08m*0.08m) is to be positioned in the center of the enclosure as shown in the figure above. A propane flow rate to achieve 10kW is used.

The experiment will be **run for 8 minutes** to coincide for data comparison with experiment 2 with a **3 minute delay on the water mist activation**.

Procedure Sequence:

- Don personal protective equipment (PPE)
- Display experiment procedure and risk assessment report at door
- Turn on ventilation
- Prepare experiment setup
- Setup (link Thermocouples) on DataTaker (laptop and software)
- Calibrate the Gas analyser (Calorimeter)
- Record ambient air's composition (O₂, CO₂, CO)
- Setup LSHR (Desktop) data acquisition
- Perform prior test to attain correct fuel flow rate for 10kW to be achieved
- Start HRR measurements (Desktop) and Start DataTaker measurements (Laptop) *Start Stopwatch*
- Turn on propane gas supply
- Ignite gas burner
- Record Ignition time on DataTaker
- *(Once 3 mins elapses)*
- Turn on water mist system (water pump)
- **If flame extinguishes, turn off fuel supply immediately! Record time (and set event on LSHR)*
- *(Once 8 mins elapses)*
- Turn off water mist system (water pump)
- Turn off gas supply
- Stop DataTaker (Laptop) and HRR measurements (Desktop)
- Record Ignition time on LSHR
- Export data as ".RAW" extension
- Retrieve data from both DataTaker, (Laptop) and LSHR, (Desktop) on thumbdrive
- Return laboratory to initial conditions
- Turn off ventilation
- Leave and lock up Laboratory
- Remove experiment procedure and risk assessment from door
- Return personal protective equipment (PPE)

Experiment 4 & 5: Extinguishment test A & B**Experiment Set-up**

Gas distribution head (Dimensions: 0.18m*0.08m*0.08m) is to be positioned slightly off-centered in the enclosure as shown in the figure above. A propane flow rates to achieve 17kW and 25kW are used for experiments 4 and 5 respectively.

The experiments will be run for 6 minutes and a minute delay on the water mist activation.

Procedure Sequence

- Don personal protective equipment (PPE)
- Display experiment procedure and risk assessment report at door
- Turn on ventilation
- Prepare experiment setup
- Setup (link Thermocouples) on DataTaker (laptop and software)
- Calibrate the Gas analyser (Calorimeter)
- Record ambient air's composition (O₂, CO₂, CO)
- Setup LSHR (Desktop) data acquisition
- Perform prior test to attain correct fuel flow rate for 17kW /25kW to be achieved
- Start HRR measurements (Desktop) and Start DataTaker measurements (Laptop) *Start Stopwatch*
- Turn on propane gas supply
- Ignite gas burner
- Record Ignition time on DataTaker
- *(Once 1 min elapses)*
- Turn on water mist system (water pump)
- **If flame extinguishes, turn off fuel supply immediately! Record time (and set event on LSHR)*
- *(Once 6 mins elapses)*
- Turn off water mist system (water pump)
- Turn off gas supply (Use appropriate fuel flowrate)
- Stop DataTaker (Laptop) and HRR measurements (Desktop)
- Record Ignition time on LSHR
- Export data as ".RAW" extension
- Retrieve data from both DataTaker,(Laptop) and LSHR,(Desktop) on thumbdrive
- Return laboratory to initial conditions
- Turn off ventilation
- Leave and lock up Laboratory
- Remove experiment procedure and risk assessment from door
- Return personal protective equipment (PPE)

F. Experimental Risk Assessment

Introduction

The following document is intended to be used as a risk assessment for the experiments needed to complete the master's thesis entitled "Effect of Water Mist System on Controlled Fire".

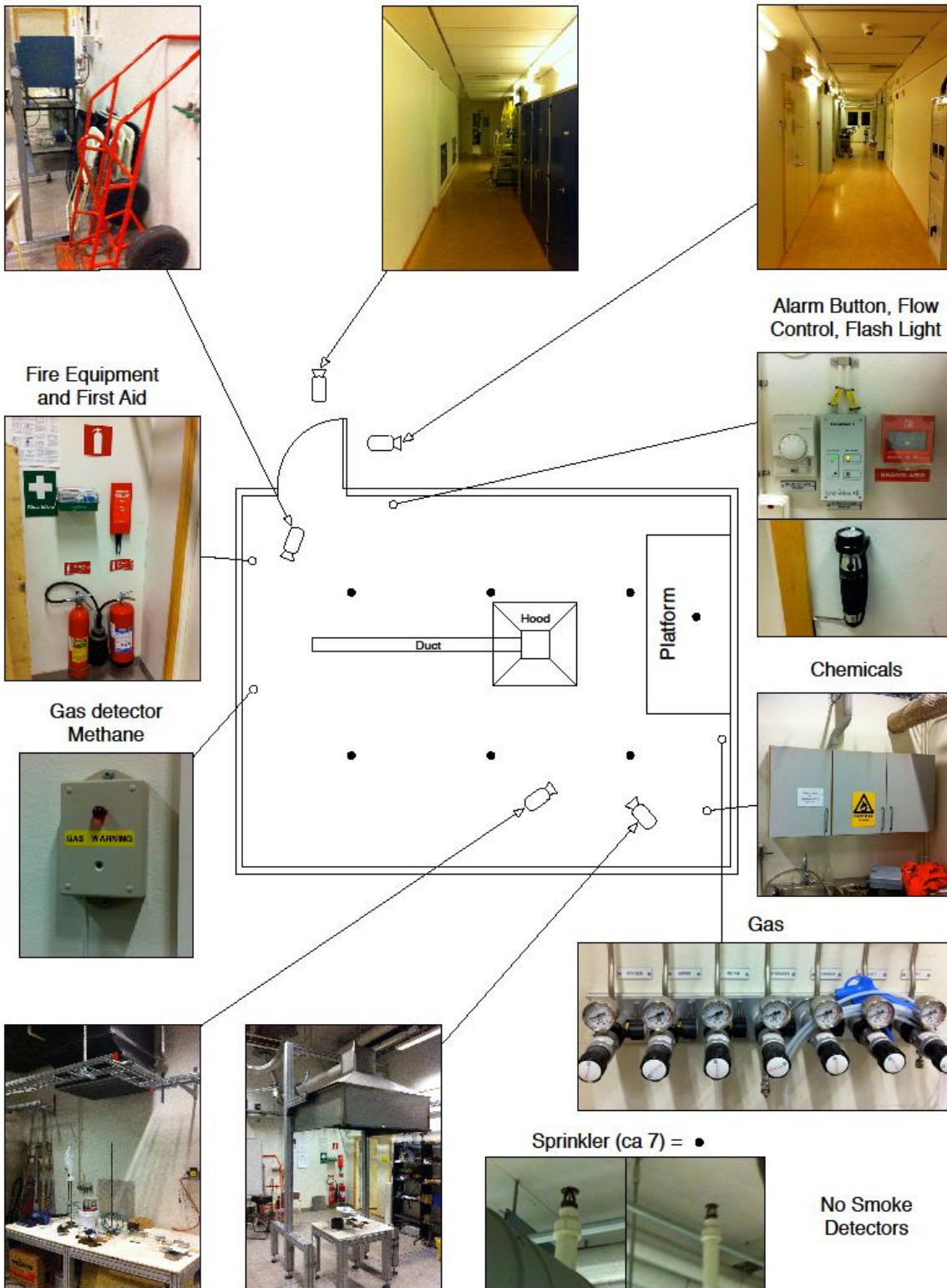
Value and Objectives

- Safety/Health
- Property and Equipment
- Results

Static Model

Testing Equipment Available

- Thermocouples (K type)
- Hood calorimeter
- High pressure electric water pump
- PROMATECT quarter ISO scale enclosure



by
Daniel Nilsson
2014-01-20

Dynamic Model

1	Check if the Lab/building is unlocked
2	Put on protective gear
3	Place experimental procedure and risk analysis sheets on the door
4	Check Ventilation
5	Ensure safety detection systems are in place/operational
6	Turn on/Calibrate/check for appropriate data transfer of the test equipment
7	Install experimental equipment
8	Check fuel source
9	Connect fuel source to the burner
10	Check mist system functionality
11	Check for fuel leaks at the connections
12	Ignite burner
13	Set mass flow rate and document value
14	Experimental procedure
15	Save data and export
16	Cool down the test room to a set value (30mins)
17	Check calibration of equipment
18	Repeat steps 7-17 two additional times
19	Remove test equipment
20	Transfer test data to backups
21	Shut down equipment
22	Clean up lab/return to starting conditions
23	Shut down ventilation
24	Lock up/leave lab with supervisor
25	Remove experimental procedure and risk assessment from the door
26	Remove/put away protective equipment

What If Analysis

Assumption: only values/objectives that could be affected are addressed

	Event	Causes	Consequences	Present Protection	Preventive Measures
1	<i>Check if the building/lab is unlocked</i>				
	Results	Door is locked to the lab/building	Not able to run the experiment	knock on the door	Have contact information for lab manager/professor
2	<i>Put on protective gear</i>				
	Safety/health	no available protective gear	Personal injury	more protective gear available compared to the number of students	Have contact information for lab manager/professor
	Results	cannot enter lab	Not able to run the experiment	more protective gear available compared to the number of students	Have contact information for lab manager/professor
3	<i>Place experimental procedure and risk analysis sheets on the door</i>				
	Safety/health	team forgot the documentation	potential injury to other occupants in the building	documentation must be present and approved	each team member has a copy
	Property and Equipment	team forgot the documentation	will not be able to use the facilities	documentation must be present and approved	each team member has a copy
	Results	team forgot the documentation	will not be able to run the experiments	documentation must be present and approved	each team member has a copy
4	<i>Check Ventilation</i>				

	Safety/health	ventilation not working/ utilised	possible risk for human safety in case of uncontrolled experiment	check that they are working at the present moment	Have contact information for lab manager/professor
	Property and Equipment	ventilation not working/ utilised	possible risk for equipment due to smoke	check that they are working at the present moment	Have contact information for lab manager/professor
	Results	ventilation not working/ utilised	Not able to run the experiment	check that they are working at the present moment	Have contact information for lab manager/professor
5	<i>Ensure safety detection systems are in place/operational</i>				
	Safety/health	they are not in proper conditions	possible risk for human safety in case of uncontrolled experiment	check that they are working at the present moment	Have contact information for lab manager/professor
	Property and Equipment	they are not in proper conditions	possible risk for property in case of uncontrolled experiment	check that they are working at the present moment	Have contact information for lab manager/professor
	Results	they are not in proper conditions	Not able to run the experiment	check that they are working at the present moment	Have contact information for lab manager/professor
6	<i>Turn on/Calibrate/check for appropriate data transfer of the test equipment</i>				
	Property and Equipment	Improper calibration	Damage to testing equipment	Calibration training with the lab manager	Follow the same procedure as the calibration lab session
	Results	something is not working	Not able to run the experiment	check that they are working at the present moment	Have contact information for lab manager/professor
7	<i>Install experimental equipment</i>				

	Safety/health	something breaks	possible injuries	ensure everyone knows how to deal with the equipment	Work in pairs at minimum to reduce probability of mistake(s) being made
	Property and Equipment	something breaks	loss of needed material	ensure everyone knows how to deal with the equipment	Work in pairs at minimum to reduce probability of mistake(s) being made
	Results	something breaks	Not able to run the experiment	ensure everyone knows how to deal with the equipment	Work in pairs at minimum to reduce probability of mistake(s) being made
8	<i>Check drainage system</i>				
	Safety/health	Excess water not drained effectively	Slips on excess water	Existing draining system but cables run in certain portion	Ensure draining system works as intended (Prior tests)
	Property and Equipment	Water gets into contact with sensitive equipment	Equipment gets damaged	Existing draining system but cables run in certain portion	Introduce 'dam' at appropriate drainage junction to direct flow
9	<i>Check fuel source</i>				
	Safety/health	the container has a gap	excessive exposure to fuel	check present stage	Have contact information for lab manager/professor
	Property and Equipment	the container has a gap	possible risk for property/explosion	check present stage	Have contact information for lab manager/professor
	Results	the container has a gap /run out of fuel source	Not able to run the experiment	check the stock the week before	Have contact information for lab manager/professor
10	<i>Connect fuel source to the burner</i>				
	Safety/health	there are leaks at the connections	possible risk for human heath/possible explosion	check that there are no leaks at the present moment	ensure that there are refills to change them

	Property and Equipment	there are leaks at the connections	possible risk for equipment/explosion	check that there are no leaks at the present moment	ensure that there are refills to change them
	Results	there are leaks at the connections	Not able to run the experiment	check that there are no leaks at the present moment	ensure that there are refills to change them
11	<i>Check for fuel leaks at the connections</i>				
	Safety/health	there are leaks at the connections	possible risk for human health/possible explosion	check that there are no leaks at the present moment	ensure that there are refills to change them
	Property and Equipment	there are leaks at the connections	possible risk for equipment/explosion	check that there are no leaks at the present moment	ensure that there are refills to change them
	Results	there are leaks at the connections	Not able to run the experiment	check that there are no leaks at the present moment	ensure that there are refills to change them
	<i>Insert burner</i>				
12	Safety/health	ignites suddenly	possible injuries	learn about its use	ensure it's turned off before installation
	Property and Equipment	ignites suddenly	loss of equipment	learn about its use	ensure it's turned off before installation
	Results	ignites suddenly	Not able to run the experiment	learn about its use	ensure it's turned off before installation
13	<i>Precaution if flame is extinguished</i>				
	Safety/health	Flame is extinguished by water mist system	Unburnt Propane gas would accumulate	None	Have personnel observing flame presence and at the gas supply. Gas supply to be turned off immediately

					if flame is extinguished
14	<i>Set mass flow rate and document</i>				
	Property and Equipment	Equipment do not work properly	Not able to measure mass flow rate	Calibration before lab	calibration after each experiment
	Results	Equipment do not work properly	Not able to measure mass flow rate	Calibration before lab	calibration after each experiment
15	<i>Ensure each team member knows their task</i>				
	Safety/health	Misunderstanding, members of the team not aware of the lab procedure.	someone might get injured	Team discussion prior to experiment	Each member to know and look out for tasks of other member(s)
	Property and Equipment	Misunderstanding, members of the team not aware of the lab procedure.	damage of the equipment	Team discussion prior to experiment	Each member to know and look out for tasks of other member(s)
	Results	Lab manager does not allow the experiment to proceed	not able to get results, or unreliable results	Team discussion prior to experiment	Each member to know and look out for tasks of other member(s)
16	<i>Experimental procedure</i>				
	Safety/health	part of the procedure is dangerous for people (gases, high temp)	someone might get injured	risk analysis	risk analysis, ensure each team member knows his/her task
	Property and Equipment	Due to experiment conditions, equipment might be damage	Cannot continue with the lab	procedure will be checked by lab supervisor	Ensure equipment is suitable for the lab conditions (temp, time, etc.)
17	<i>Save data and export</i>				

	Property and Equipment	Equipment might be damaged	can't get data	Calibrations	take some data before experiments in order to check the equipment
	Results	Equipment might be damaged	no results for conclusions	Calibrations	take some data before experiments in order to check the equipment
18	<i>Cool down the test room to a set value</i>				
	Results	not enough time for experiments	we might get different results with different initial conditions	Calculate the time that takes the room to cool down to a certain initial conditions	Take cooldown time into consideration during planning
19	<i>Check calibration of equipment</i>				
	Results	Due to past experiments equipment might not be calibrated	not actual results	Calibrations	Check equipment
20	<i>Repeat steps 7-19 as many times as experiments</i>				
21	<i>Remove test equipment</i>				
	Safety/health	due to high temperatures or smoke, someone might get injured	someone might get burnt, or inhale harmful gases	follow procedure for cooling down equipment	measure temp and smoke level before remove test
	Property and Equipment	malfunction during removal stage	some equipment broken	follow procedure for disassemble equipment	Work in pairs at minimum to reduce probability of mistake(s) being made
22	<i>Transfer test data to backups</i>				
	Results	Malfunctioning Data Acquisition	Data unable to be transferred	Online backup with the DAQ system	Backup data into thumbdrive after every experiment
23	<i>Shutdown equipment</i>				
	Property and Equipment	Improper shut down procedure	Damage to testing equipment	Lab equipment training for students	Lab manager present during testing

	<i>Clean up lab/return to starting conditions</i>				
24	Safety/health	Slip/trip/falls, and not wearing proper protective equipment	Personal Injury	wearing protective equipment provided	Ensure spill/ obstruction is remedied at earliest opportunity
	<i>Shut down ventilation</i>				
25	Property and Equipment	ventilation system not shut down	Other lab experiments might be affected by the change in air flow	Lab manager present to assist with lab protocol	Place this step in the experimental procedure
	<i>Lock up/leave lab with supervisor</i>				
26	Property and Equipment	Equipment stolen/broken	University must pay to replace or pay for repairs	Lab manager present to assist with lab protocol	Place this step in the experimental procedure
27	<i>Remove experimental procedure and risk assessment from the door</i>				
	<i>Remove/put away protective equipment</i>				
28	Safety/health	Slip/trip/falls	personal injury	none	take off protective gear slowly and while seated